CHANGING HYDROCLIMATIC CONDITIONS AND EXCESSIVE NITROGEN DEPOSITION AFFECT ECOSYSTEM FUNCTIONING OF A BOTTOMLAND HARDWOOD FOREST

A Dissertation

by

AJINKYA GIRISH DESHPANDE

Submitted to the Office of Graduate and Professional Studies of
Texas A&M University
in partial fulfillment of the requirements for the degree of

DOCTOR OF PHILOSOPHY

Chair of Committee,	Georgianne W. Moore
Committee Members,	Thomas W. Boutton
	Asko Noormets
	Charles W. Lafon
Head of Department,	Kirk O. Winemiller

December 2020

Major Subject: Ecosystem Science and Management

ABSTRACT

Bottomland hardwood forests (BHFs) along the Gulf coast of Texas have been experiencing a combination of disturbances in the form of hydroclimate changes and excessive anthropogenic nitrogen (N) deposition, both of which are connected through linkages between the regional hydrologic and N cycles. BHFs, which are dependent on optimally wet conditions, have received little attention amid rapidly changing climate and pollution scenarios, which are expected to become more irregular over the 21st century. This dissertation aimed to understand the integrated effects of these disturbances on BHFs by: 1) examining signals of physiological stress in response to climatic conditions in the past; 2) assessing tree water-use in flooded and non-flooded native as well as invasive species as a result of seasonal environmental changes; 3) investigating if persistent elevated deposition from pollution sources has led to N saturation and affected primary productivity, N transformations in the soil and accelerated N loss from these forests; and 4) determining the relative control of hydroclimate and N inputs on ecosystem productivity. A range of techniques such as dendrochronology, sap flow, atmospheric deposition monitoring, plant and soil isotopic analyses and biogeochemical modelling were used to address each objective.

Vegetation in the drier portions of the study area experienced growth inhibition and showed signals of stress during drought periods, and was more sensitive to wetter hydroclimatic conditions. Although trees growing in the wetter patches had suppressed water-use during early-growing season flooding, their recovery indicated resistance to

flooding stress. They were less sensitive to drier hydroclimate and were able to sustain their water-use during summer conditions. The younger and smaller invasive Chinese tallows had only slightly lower water-use than the mature native oaks, suggesting their potential to compete with the oaks for soil water on approaching maturity in the near future. Interestingly, despite exposure to excessive N deposition for decades, these forests did not show signs of N saturation as tree growth and N absorption continued to increase even at high deposition levels. However, despite excessive N inputs, signs of N loss were negligible, soil N concentrations were low and vegetation continued to absorb mineralized N, indicating rapid N retention and cycling through plants and soils.

Persistence of these bottomland hardwood forests is contingent upon frequent flooding, optimum wetting and maintenance of hydrologic connectivity over a large spatial extent within this patchy landscape. The drying of these wetland forests, which is already underway, induces stressful conditions and reduces productivity, while rendering the vegetation to be more sensitive to precipitation inputs. As strong sinks of anthropogenic N, these forests need to be conserved as sinks and filters for air and water pollutants. This dissertation provides vital baseline ecological, hydrological and biogeochemical information about this ecosystem that can aid cohesive conservation action and inform pollutant emission standards by integrating knowledge of distinct processes within the water, carbon and nitrogen cycles, that are strongly interconnected but usually studied and applied disjointedly.

DEDICATION

This dissertation is dedicated to all those who strive relentlessly to protect our vulnerable ecosystems against all odds.

ACKNOWLEDGEMENTS

I would like to thank my advisor, Dr. Georgianne W. Moore, and my committee members, Dr. Thomas W. Boutton, Dr. Asko Noormets and Dr. Charles W. Lafon for their guidance and support throughout the course of this dissertation. I am very grateful to Dr. Moore for her close support, both at professional and personal levels. Through her guidance and support, she made sure that I excelled at every aspect of my grad life at Texas A&M and I am sure she will continue to support me in the same way in future. Dr. Moore and the Moore lab group have been my family during my four years in College Station.

I am grateful to have had the continued support of my committee members who have closely followed my progress over the course of my Ph.D. I would like to thank Dr. Boutton, with whom I took two courses and co-authored several conference abstracts and a publication. He took very keen interest in my work right from my first semester and gave extremely valuable inputs on my research and my understanding of biogeochemistry. Thank you to Dr. Lafon for familiarizing me with the world of dendrochronology and making me perceive biogeography in ways that I had not imagined before. I would like to thank Dr. Noormets for his critical inputs on my proposal and research plan, that gave me significant clarity about the course of my research and made the execution of my project much smoother.

Thanks to my lab mates, fellow graduate students and colleagues for making these four years memorable. Special thanks to Dr. Luiza Aparecido, Dr. Caitlyn Cooper, Dr.

Paul Klockow and Dr. Aline Jaimes for embracing me when I first moved to the US and being available for me at every stage of my Ph.D. The second half of my Ph.D. would have been impossible without the support of Christopher Adkison, Aaron Trimble, Miriam Catalan, Ashley Cross, Manuel Flores and Austin Zen. I am sure our friendship has only just begun. I would like to thank Deanroy Mbabazi, Amir Sedaghatdoost, Kathryn Benson and Kathie Guerra for helping me with my field work and lab analyses. I am grateful to Dr. Parveen Chhetri for training me on dendrochronology, which ended up becoming a critical part of my dissertation. I am extremely thankful to Dr. Ayumi Hyodo for training me to conduct stable isotope analyses, sharing her immense technical knowledge with me, helping me write conference abstracts and research papers and ensuring the best possible outcomes of my work in the SIBS lab. I would like to thank my friend and seminar co-chair, Shishir Basant, for his counsel throughout my Ph.D. and for sharing his wide-ranging knowledge with me.

I would like to thank the entire Texas Water Observatory team for providing me with amazing research opportunities. I am grateful to the faculty and staff in the Department of Ecology and Conservation Biology at Texas A&M University for their efforts and time spent helping me through my program. I would like to thank Jennifer Sanchez and Curtis Jones of the US Fish and Wildlife Service, San Bernard National Wildlife Refuge for allowing me access to the study sites and for their unmatched cooperation. Special thanks to Dr. David Briske, with whom I worked as a teaching assistant and later as seminar co-chair for being a great mentor and for giving me new perspectives on ecology. I would also like to thank my previous advisors, Dr. Mallika

Shrivastav, Dr. Pratyush Patankar and Dr. Mridula Negi for preparing me for the rigors of a Ph.D.

I would like to thank my friends back home in India and in the US for keeping my spirits up during these years and for always being there for me. I am grateful to my best friend, Vertika Singh, for sharing my joys and lifting me up whenever I felt low. Despite being 8000 miles away, she has been one of my strongest support systems by being there for me regardless of the time and situation. I would like to thank my roommates, Dr. Ayush Jain and Ankur Kumar for all the celebrations, trips and fun and for taking care of me whenever I could not do so myself.

Finally, I would like to thank my parents, sister, brother-in-law and the rest of my family for encouraging me to pursue my ambitions, even if that meant getting to see me only once every year. Their unwavering support throughout my academic career ensured that I never felt pressured and it kept me away from all worries so that I could focus on my academics. While I write this, I cannot be happier thinking about being with them in less than two months! I would not have been able to make it this far without their love and support.

CONTRIBUTORS AND FUNDING SOURCES

Contributors

This work was supervised by a dissertation committee consisting of Dr. Georgianne W. Moore (advisor), Dr. Thomas W. Boutton, Dr. Asko Noormets of the Department of Ecology and Conservation Biology, and Dr. Charles W. Lafon of the Department of Geography.

All work was designed in part by Ajinkya Deshpande, Dr. Georgianne W. Moore, Dr. Thomas W. Boutton, Dr. Asko Noormets and Dr. Charles W. Lafon. Ajinkya Deshpande conducted field work, aided by Christopher Adkison, Aaron Trimble, Miriam Catalan, Ashley Cross, Dr. Luiza Aparecido, Kathryn Benson, Deanroy Mbabazi, Dr. Aline Jaimes, Austin Zen, Kathie Guerra and Shishir Basant. The dendrochronology work in this dissertation was conducted by Ajinkya Deshpande with training and equipment provided by Dr. Charles W. Lafon and Dr. Parveen Chhetri at the Department of Geography, Texas A&M University. Isotope analyses were conducted by Ajinkya Deshpande and supervised by Dr. Ayumi Hyodo at the Stable Isotopes for Biosphere Sciences Lab, Texas A&M University. Atmospheric deposition and soil nitrogen samples were analyzed by Ajinkya Deshpande and Amir Sedaghatdoost at the Department of Biological and Agricultural Engineering, Texas A&M University. Ajinkya Deshpande conducted the data analyses, data interpretation and the writing of this dissertation while being supported by Dr. Georgianne Moore, Dr. Thomas W. Boutton, Dr. Asko Noormets, Dr. Charles W. Lafon, Dr. Ayumi Hyodo and Dr. Luiza Aparecido. Eddy covariance

measurements used in Chapter IV were obtained from the Texas Water Observatory, led by Dr. Binayak Mohanty and a team of co-PIs. Access to the study sites was permitted by Jennifer Sanchez and Curtis Jones of the US Fish and Wildlife Service, San Bernard National Wildlife Refuge.

Funding Sources

Ajinkya Deshpande was supported in part by the James M. Carder Graduate Assistantship (2016-2019) and the Harry Wayne Springfield Graduate Merit Fellowship (2019-2020) from the Department of Ecology and Conservation Biology at Texas A&M University and the Mills Scholarship from the Texas Water Resources Institute at Texas A&M University.

Field work, lab analyses and purchase of research materials were funded by the Texas A&M Research Development Fund. Field equipment and travel was funded in part by the Texas Water Observatory. Funding for conferences and purchase of research materials were made possible in part by the departmental Graduate Student Research Mini-Grant, departmental Graduate Student Travel Grant and the Office of Graduate and Professional Studies Travel Award. The contents of this study are solely the responsibility of the authors and do not necessarily represent the official views of the funding parties.

TABLE OF CONTENTS

Page

LIST OF FIGURES

Page

LIST OF TABLES

Page

CHAPTER I

INTRODUCTION

Bottomland hardwood forests (BHFs) are a type of deciduous wetland forest that occur in major floodplains and river deltas in the southeastern and south-central United States. Like most other forested wetlands, BHFs are flooded or saturated intermittently and often seasonally (Ober, 2019). The frequency, timing, spatial extent and flooding depth in these forests determine the plant community composition and productivity, which ultimately drive the regional hydrologic and biogeochemical cycles (Simmons et al., 2007). Vegetation in bottomland hardwood forests is tolerant of intermittent and moderate flooding or saturated conditions (McKnight et al., 1980; Gardiner, 2001; King and Keim, 2019), making them effective sinks of floodwaters post storm events, especially in exurban locations, where they can reduce urban flooding risk (Simmons et al., 2007). These forests also provide other benefits such as recharging groundwater table, sequestering large amounts of carbon, retaining excess nutrients and pollutants and providing habitat for wildlife (Jenkins et al., 2010; Capon et al., 2013). However, the threats to these wetland forests are increasing at an alarming rate due to agricultural conversion, removal and conversion for timber production, construction of dams and river regulation, urban expansion and air and water pollution from various point and non-point sources (Tockner and Stanford, 2002; Naiman et al., 2005). Moreover, in addition to these disturbances, changing climatic conditions with increasing temperatures, varying precipitation patterns and increasingly frequent and severe drought and flood events have reduced the

distribution of bottomland hardwood forests in the southern US to only about 40% of their 121,000 km^2 expanse in the 1800s (USEPA, 2016).

In Texas, bottomland hardwood forests occur along the Gulf of Mexico coastline where major rivers like the Colorado, Brazos, Sabine, Neches, Trinity and smaller rivers like San Bernard and San Jacinto form their drainage basins. Bottomland hardwood forests in the Brazos-Colorado basin are known as Columbia bottomlands, which are partially protected and conserved within the San Bernard National Wildlife Refuge. Columbia bottomlands not only face the threats as other BHFs, but are also threatened by urban expansion from the city of Houston, pollution sources such as petroleum refineries located along the Gulf coast and frequent hurricane landfalls. As a result, the >2800 km^2 pre-settlement distribution of these forested wetlands has been reduced by over 70% to less than 810 km^2 (USFWS, 1997; Barrow and Renne, 2001; Barrow et al., 2005). Over the next century, Columbia BHFs are expected to experience even more unfavorable hydroclimatic conditions as temperatures are predicted to rise and precipitation patterns become more variable (Jiang and Yang, 2012; Awal et al., 2016). Columbia BHFs occur at the extreme southwestern edge of the bottomland hardwood forest type (Bray, 1906; Putnam et al., 1960). Edges of distribution ranges usually experience environmental conditions that are less favorable to the species as compared to the range interior (Rehm et al., 2015), which makes them more resilient and better adapted to survive in stressful conditions relative to core populations (Gutschick and Hormoz, 2003). In addition to the natural and human-induced threats, the biogeographic location of the Columbia BHFs makes them even more ecologically critical.

Rapidly transitioning hydroclimatic conditions can alter the hydrology of forest ecosystems and affect productivity (Boisvenue and Running, 2006). Vegetation in BHFs such as hardwood species and bottomland oaks are often tolerant of intermittent flooding but may not sustain prolonged waterlogging (McKnight et al., 1980; Gardiner, 2001; King and Keim, 2019). Additionally, their general adaptation to wetter soils renders them less tolerant to drought conditions (Silvertown et al., 1999; Sorrell et al., 2000). As a result, BHFs are sensitive to extreme hydroclimatic conditions. To understand how vegetation responds to a range of climatic and hydrologic conditions and to predict their future response, it is critical to investigate the retrospective response of forest growth and functioning to past environmental conditions.

Dendrochronology, the study of tree-rings, offers an effective way to understand these past responses. Narrower tree-rings correspond to lower productivity during a specific growing season in response to stressful environmental conditions, usually droughts but also other stressors such as waterlogged soils as commonly found in wetlands (Fang et al., 2011; Au and Tardif, 2012; Wang et al., 2017; Gao et al., 2018; Mikac et al., 2018; Szejner et al., 2020). On the other hand, wider tree-rings correspond to optimal growth in response to favorable growing conditions. By precisely dating tree-rings using dendrochronological techniques and removing the age-related growth signal by using detrending methods, the response of forest productivity to a range of climatic conditions can be assessed (Speer, 2012). These relationships can also be extrapolated to future climatic conditions projected by climate models and the future state of forest ecosystems can be projected (Williams et al., 2010).

Tree-rings not only provide information on past growth trends, but stable isotopic analyses of tree-ring wood can help reconstruct historic trends of ecophysiological responses to environmental conditions and provide insights on historic nutrient, biogeochemical and hydrologic cycling rates (McCarroll and Loader, 2004). Stable carbon isotopic composition ($\delta^{13}C$) of tree-rings is an effective indicator of the ecophysiological response of vegetation to environmental conditions primarily driven by climate (Farquhar et al., 1989; Robertson et al., 1997; Leavitt et al., 2002; McCarroll and Loader, 2004; Gessler et al., 2014). Under favorable growing conditions such as sufficient soil moisture availability and moderate vapor pressure deficit (VPD), stomatal conductance and leaf internal pCO_2 are relatively high, which maximizes isotopic discrimination against $^{13}CO_2$ by the primary carbon fixing enzyme RUBISCO. As a result, relatively more $^{12}CO_2$ is fixed by the plant during photosynthesis, yielding lower $\delta^{13}C$ values in plant tissues. Under stressful environmental conditions such as water limitation, plants reduce stomatal aperture to minimize water loss, the internal leaf pCO_2 concentration declines, discrimination against $^{13}CO_2$ by the RUBISCO enzyme declines, and $\delta^{13}C$ values in plant tissues increases (Farquhar et al., 1982; Farquhar and Sharkey, 1982; Farquhar et al., 1989; Ehleringer et al., 1993; Gessler et al., 2009; Gessler et al., 2014). Thus, plant tissues synthesized during stressful environmental conditions have higher $\delta^{13}C$ values. Narrower tree-rings and higher tree-ring $\delta^{13}C$ values are usually observed in response to moisture deficit conditions across most ecosystems (Liu et al., 2008; Au and Tardif, 2012; Timofeeva et al., 2017). However, in excessively wet ecosystems such as wetland forests, higher $\delta^{13}C$ values as result of stomatal closure in response to waterlogging have also been

observed (Stuiver et al., 1984; Anderson et al., 2005; Buhay et al., 2008; Voelker et al., 2014). Although debatable, a number of possible mechanisms have been suggested with significant evidence to support this relationship. These include disruption of water and nutrient uptake due to anoxic conditions in the root zone (Jackson and Drew, 1984), lowered root hydraulic conductivity (Davies and Flore, 1986), increased abscisic acid concentrations (Kozlowski and Pallardy, 1984) and accumulation of metabolic toxins from flooding (Jackson and Drew, 1984).

Total terrestrial evapotranspiration (66,000-69,000 km^3 water $year^{-1}$) is among the largest fluxes in the global water cycle (Oki and Kanae, 2006; Abbott et al., 2019), and approximately 80-90% of this flux is derived from plant transpiration (Jasechko et al., 2013). As the climate changes, there is potential for transpiration to be greatly altered as plant water use gets accelerated or suppressed in response to changes in atmospheric and soil moisture (Kirschbaum and McMillan, 2018). However, plant water-use in wetter ecosystems such as BHFs is rarely investigated and the knowledge of wetland tree response to hydrologic conditions with respect to water-use remains sparse. In wetland forests, the spatial variability in edaphic conditions is becoming increasingly contrasting due to forest removal, agricultural diversions, construction of dams, etc., causing some forest patches to remain unusually waterlogged for prolonged periods, while rendering some patches to be moisture deficient (Bruland and Richardson, 2005). As wetland plants are adapted to grow in moderately wetter soil conditions, anomalously dry or flooded conditions can perturb water-use and productivity.

Moreover, changing community composition and structure and proliferation of invasive species as a result of anthropogenic and natural disturbance also alters transpiration rates at a regional scale (Ewers et al., 2005; Cavaleri and Sack, 2010; Harrison et al., 2020). In Columbia bottomlands, rapid invasion by the Chinese tallow (*Triadica sebifera* (L.) Small) is an added concern. Invasive species are known to aggressively compete against native vegetation for water and deplete groundwater reserves (Cavaleri and Sack, 2010). Tallows are known to achieve remarkable flood tolerance at a very young age, which is comparable to or even more than some wetland tree species (Jones and Sharitz, 1990; Gabler and Siemann, 2013); however, its direct effect on the ecosystem water budget through transpiration is yet to be determined. Therefore, it is critical to measure tree water-use in native as well as invasive species growing under contrasting soil moisture conditions in such understudied, threatened ecosystems to aid conservation and management decisions. Sap flow measurements have been effectively used as a direct indicator of plant water stress across ecosystems, including wetlands. This technique not only provides a real-time estimate of variation in tree water-use, but also provides insights on the type, magnitude and timing of water-use response to corresponding climatic and environmental conditions. Sap flow measurements can be coupled with forest biometric measurements and scaled up to obtain stand transpiration estimates.

Apart from changing hydrologic conditions due to natural and anthropogenic pressures, BHFs along the Gulf coast of Texas are threatened by pollution impacts (USFWS, 1997; Barrow et al., 2005). Several small and major petroleum refineries are

located in the upwind direction of these forests, that not only emit sulphur dioxide, nitrogen oxide, carbon dioxide, carbon monoxide, methane, etc., but are also capable of depositing large amounts reactive nitrogen (N_r) and sulphur (S) in soluble as well as particulate forms on proximal ecosystems. Deposition of N_r increases plant productivity, soil microbial activity and overall nutrient cycling under initial low N availability conditions (Aber et al., 1989; 1998). However, elevated levels of deposition can have damaging effects on ecosystem functioning by causing biogeochemical imbalance in plants and soils and alter community structure by aiding species that prefer high-N environments (Aber et al., 1989; Stevens et al., 2004; De Vries et al., 2006). Other negative impacts of N deposition on forest ecosystems include decline in productivity (Aber et al., 1998; Bai et al., 2010), deceleration of mineralization and nitrification rates (Lovett and Rueth, 1999; Carreiro et al., 2000; Frey et al., 2004), increased leaching (Fang et al., 2009; Gundersen et al., 2011) , gaseous N loss through denitrification (Gundersen et al., 1998; van Groenigen et al., 2015), soil acidification (Wallace et al., 2007) and tree mortality in extreme situations (Aber et al., 1998; Magill et al., 2000; Lovett and Goodale, 2011).

To investigate the effects of N deposition on forest ecosystems, estimating N fluxes and pools is critical. However, as N gets stored and processed within the ecosystem in several different forms simultaneously, measuring absolute N fluxes and pools is a complex process (Amundson et al., 2003; Craine et al., 2009). Estimation of the isotopic composition of N in soils and plant tissues provides an effective alternative to this issue. Isotopic analysis also helps identify the source of N by distinguishing between anthropogenic and natural N incorporated by the ecosystem. The heavier stable isotope,

^{15}N, which makes up less than 0.4% of naturally occurring N, is usually discriminated against when N gets transformed from one form to another. Isotopically lighter N is more readily fixed and mineralized by microbes, absorbed by plants, dissolved in water and is easily lost in the form of leaching and gaseous emissions (Chapin et al., 2012). Therefore, the ratio of $^{15}N/^{14}N$ (denoted as $\delta^{15}N$ with respect to atmospheric N_2), which indicates isotopic fractionation of N in soil profiles and plant tissues indicates the rate at which N is retained, cycled and lost from the system (Högberg, 1997). Comparing $\delta^{15}N$ values and N concentration in soil profiles and plant tissues such as wood (tree-rings), leaves, roots and litter can facilitate our understanding of N transformation through an ecosystem. Tree-ring $\delta^{15}N$ values are effective indicators of historic N cycling rates and can be compared to past growth rates and climatic conditions (Gerhart and McLauchlan, 2014). The difference between soil and plant $\delta^{15}N$ can be used to assess the degree of isotopic fractionation of N and identify major fractionation pathways in soils, roots, aboveground plant parts and at the soil-water-plant interface (Högberg, 1997; Martinelli et al., 1999; Amundson et al., 2003) such as during plant N uptake aided by mycorrhizal fungi (Craine et al., 2009; Hobbie and Högberg, 2012), gaseous N loss during denitrification (Houlton et al., 2006), conversion of NH_4^+ to NO_3^- through nitrification (Högberg, 1997; Spoelstra et al., 2007), N fixation (Sra et al., 2004), preferential plant uptake of NH_4^+ (Yoneyama et al., 1991; Pennock et al., 1996; Yoneyama et al., 2001), transportation of absorbed N between plant tissues (Pardo et al., 2013), etc.

Measurement of plant and soil $\delta^{15}N$ values can provide insights regarding ecosystem and landscape-scale N dynamics. However, there is a critical need and lack of

knowledge on ecosystem- and landscape-scale understanding of plant and soil responses to elevated N deposition and their future projections. Biogeochemical models aided by accurate field measurements as input parameters provide a more holistic understanding of forest ecosystem functioning in response to elevated N deposition and the underlying mechanisms. A number of modeling studies have been conducted across different ecosystems to simulate forest productivity, plant physiological processes and soil nutrient dynamics under different N pollution or climate change scenarios (Hole and Engardt, 2008; Gaudio et al., 2015; Dirnböck et al., 2017; Tharammal et al., 2019; Van Houtven et al., 2019). However, one of the major shortcomings observed after reviewing these studies is the lack of investigation of integrated effects of N pollution and changes in precipitation patterns on ecosystems. A number of biogeochemical models have been developed over the last three decades to simulate ecosystem productivity, gas exchange, hydrologic fluxes, nutrient dynamics, C and N cycling, etc. under given climatic and deposition conditions. Some of the widely used models are Biome-BGC (Thornton et al., 2002), the PnET family (Aber and Federer, 1992), DNDC models (Li et al., 1992), NCAR CSEM (Gent et al., 2011), ForSAFE (Wallman et al., 2005), etc. Over the years, these models have been calibrated and parameterized for specific ecosystems and geographical locations.

The Forest-DNDC model is particularly applicable to wetland forests with N deposition and hydroclimate as primary drivers (Li et al., 2005). Forest-DNDC was created by integrating the PnET-N-DNDC model (improves estimates of aboveground processes) (Li et al., 2000; Stange et al., 2000) with Wetland-DNDC (improves soil biogeochemical and hydrological estimates) (Zhang et al., 2002), which enables the model

to switch between upland and wetland modes. The model has been validated with field measurements and applied across a variety of ecosystems across the globe such as cypress swamps, slash pine, spruce forests (Kurbatova et al., 2008), broad-leaf pine (Shu et al., 2019), fir (Lu et al., 2008), Eucalyptus plantation (Miehle et al., 2006), wetland forests (Cui et al., 2005), boreal forests (Kim et al., 2014; Kim et al., 2016), subtropical forests (Wang et al., 2011b), tropical dry forests (Dai et al., 2014), etc. with great efficiency.

This Columbia bottomlands present a unique opportunity to study the impacts of a changing hydroclimate and elevated N deposition on remnant bottomland hardwood forests that are rapidly declining owing to a variety of threats. This dissertation aims to understand the integrated effects of increasingly erratic climatic conditions along with excessive reactive N inputs on plant-soil-water relationships, plant physiological responses and primary productivity. A wide range of field-based and modelling techniques such as dendrochronology, plant and soil stable isotopic analyses, sap flow measurements, atmospheric deposition monitoring and biogeochemical modelling have been used in this dissertation.

The dissertation comprises of four chapters addressing overarching goals and specific objectives as follows:

1. Examine how BHFs respond to hydroclimatic variation in terms of growth and physiological stress using tree-ring widths and $\delta^{13}C$ values.

   Objectives:

   - understand the impact of hydroclimatic variation on growth rates using tree-ring width analysis.

- assess the magnitude of physiological stress inflicted by extreme hydroclimatic conditions using tree-ring $\delta^{13}C$ measurements.
- evaluate the relationship between physiological stress and growth inhibition.

2. Understand bottomland oak and invasive Chinese tallow tree water-use strategies under intermittently flooded and relatively drier growing conditions.

   Objectives:

   - estimate the relative difference in seasonal tree water-use under flooded and non-flooded conditions using sap flow measurements.
   - investigate if the invasive Chinese tallow has a different water-use strategy in response to varying environmental conditions as compared to native species.

3. Examine the effect of elevated N deposition on N cycling within the ecosystem using plant and soil $\delta^{15}N$ measurements.

   Objectives:

   - estimate the amount of atmospheric wet N deposition at three sites at increasing distances from a point source (petroleum refinery) and assess the chemical and isotopic composition of deposited N.
   - investigate the historic trend of N cycling in the forest under the effect of eight decades of anthropogenic N deposition using tree-ring $\delta^{15}N$ and N concentration chronologies.
   - understand the underlying processes by which N is fractionated through this ecosystem by comparing deposition, wood, leaf, litter and soil $\delta^{15}N$.

4. Model the integrated effects of anthropogenic N deposition and hydroclimatic change on forest productivity and investigate the potential for N saturation.

   Objectives:

   - validate the Forest-DNDC model for this ecosystem by comparing a set of modeled above- and belowground parameters to field measurements.
   - model and determine the major controls over forest productivity and heterotrophic respiration under different deposition and precipitation scenarios.
   - simulate soil N transformations to understand how precipitation and N deposition affect soil N cycling with its resultant impact on forest productivity.

CHAPTER II

BOTTOMLAND HARDWOOD FOREST GROWTH AND STRESS RESPONSE TO HYDROCLIMATIC VARIATION: EVIDENCE FROM DENDROCHRONOLOGY AND TREE-RING $\Delta^{13}C$ VALUES[*]

Synopsis

Wetland forests around the world have been reduced to a small proportion of their original expanse due to changing climatic conditions and intensification of human land use activities. As a case in point, the Columbia bottomland hardwood forests along the Brazos-Colorado Coastal Basin on the Gulf coast of Texas are currently threatened by an increasingly erratic hydroclimate in the form of both extreme floods as well as droughts, and by urban expansion. In this study, we use dendrochronology and tree-ring carbon isotopes to understand the effect of changing hydroclimatic conditions on the functional attributes of these forests. We examined tree-rings of *Quercus nigra* at four sites within the Columbia bottomlands, of which one site experiences frequent and prolonged flooding, while the other three are less flood-prone. The objectives of this study were to: (i) understand the impact of hydroclimatic variation on radial growth using tree-ring width analysis, (ii) assess the magnitude of physiological stress inflicted by extreme

[*] Reprinted with permission from "Bottomland hardwood forest growth and stress response to hydroclimatic variation: Evidence from dendrochronology and tree-ring $\Delta^{13}C$ values" Ajinkya G. Deshpande, Thomas W. Boutton, Ayumi Hyodo, Charles W. Lafon and Georgianne W. Moore, 2020. *Biogeosciences*, Accepted article.

hydroclimatic conditions using tree-ring $\Delta^{13}C$ measurements as a proxy, and (iii) evaluate the relationship between tree-ring width and $\Delta^{13}C$ values. Radial growth across the landscape was influenced most strongly by mid-growing season climate, while early-growing season climate had the strongest effect on $\Delta^{13}C$. Growth inhibition was minimal and tree-ring $\Delta^{13}C$ values were not affected in trees at the wetter site under extreme hydrological conditions such as droughts or floods. In addition, trees at the wet site were less sensitive to precipitation and showed no response to higher temperatures. In contrast, trees of the three drier sites experienced growth inhibition and had lower tree-ring $\Delta^{13}C$ values during dry periods. Our results indicate more favorable growing conditions and lower stress in trees growing under wetter hydrological conditions. Management and conservation strategies dependent on site-specific conditions are critical for the health of these wetland forests under a rapidly changing hydroclimate. This study provides the first dendrochronological baseline for this region and a better understanding of favorable conditions for the growth and health of these forests which can assist management decisions such as streamflow regulation and conservation plans.

Introduction

Wetland forests are subjected to drought and floods, both of which can alter productivity and cause physiological stress in plants (Miao et al., 2009; Vivian et al., 2014). These climate extremes and warming are predicted to increase in the 21st century across southern North America (Seager et al., 2007). Bottomland hardwood forests, a common wetland forest type, cover a significant proportion of the floodplains of the rivers

and bayous in coastal regions of the southeastern USA. Along the upper Texas Gulf coast, the lower basins of the Brazos River, San Bernard River and Colorado River combine to form the Columbia bottomland hardwood forests, an area of high biodiversity with a critical role in regional hydrology. Large portions of the Columbia basin forest have been cleared and land cover is now a mix of isolated forest patches, cropland, and pasture (Griffith, 2004), with only a few larger forest patches remaining (Fig. 1A). The pre-settlement distribution of these forests was >283,000 ha along a 150 km long corridor inland from the coast, but has since been reduced to about 72,000 ha (USFWS, 1997; Barrow and Renne, 2001; Barrow et al., 2005). In the last few decades, this ecosystem has been experiencing dramatic hydrologic variation caused by severe droughts (Schmidt and Garland, 2012; Hoerling et al., 2013; Moore et al., 2015) as well as floods (van Oldenborgh et al., 2017; Sebastian et al., 2019), altering hydrologic conditions over short temporal scales. Annual precipitation amounts have been highly variable with up to 61% more rainfall than average during some years, while up to 53% deficit during others, in addition to at least five major tropical storms and hurricanes. Rapid urbanization caused by the proximity to the city of Houston and increasing agricultural activity in the area have likely altered water cycling significantly in these forests (Kearns et al., 2015; TWDB, 2017). Similar forcing factors have altered the state of most wetland forest types in southeastern USA.

Dendrochronology, the study of tree-rings, has been extensively used to understand the response of forest growth to changing environmental conditions (Babst et al., 2013; Charney et al., 2016; Tei et al., 2017). Additionally, tree-ring carbon isotopic

composition is an indirect record of internal leaf CO_2 concentration, which is controlled by a balance between stomatal conductance and photosynthetic rate in response to environmental conditions (Farquhar et al., 1989; McCarroll and Loader, 2004; Gessler et al., 2014), such as temperature, vapor pressure and precipitation (Robertson et al., 1997; Leavitt et al., 2002). As tree rings are distinguished by their high temporal (annual or sub-annual) and spatial resolution, regional tree-ring chronologies and carbon isotopic values have the potential to identify a wide range of growth and stress response of vegetation to hydroclimatic variability. However, carbon isotopic composition of tree-rings ($\delta^{13}C$) is also influenced by the changing carbon isotopic composition of atmospheric CO_2. The increase in atmospheric CO_2 concentration mainly due to fossil fuel combustion has led to a significant decrease in $\delta^{13}C$ of atmospheric CO_2 over the last century (Graven et al., 2017). Although this change is relatively small over short temporal scales, this signal should be removed from tree-ring records when using tree-ring $\delta^{13}C$ to understand plant physiological responses to local conditions. Changes in carbon isotopic composition of atmospheric CO_2 can be accounted for by converting tree-ring carbon isotope ratio ($\delta^{13}C$) to carbon isotope discrimination ($\Delta^{13}C$) (Farquhar, 1983). Tree-ring $\delta^{13}C$ values are inversely related to $\Delta^{13}C$ values as higher discrimination results in a lower $\delta^{13}C$ ratio.

Studies conducted across the globe demonstrate growth inhibition signals in the form of narrow tree-rings in response to drought (Fang et al., 2011; Au and Tardif, 2012; Wang et al., 2017; Gao et al., 2018; Mikac et al., 2018; Szejner et al., 2020). Through these studies, a strong positive relationship between growth rates and precipitation has been well-established. However, tree growth is also known to be affected by waterlogging

and flooded soils (Astrade and Bégin, 1997; Kozlowski, 1997; St. George, 2014). These effects are more difficult to detect in tree-ring patterns and therefore very few studies have evaluated growth responses to flooding (Ballesteros-Canovas et al., 2015; Therrell and Bialecki, 2015; Meko and Therrell, 2020), particularly in southeastern USA (LeBlanc and Stahle, 2015).

Lower $\Delta^{13}C$ values of tree-ring cellulose usually reflect stress caused by low environmental moisture at the time of carbon fixation, while higher $\Delta^{13}C$ values are indicative of non-stressful growing conditions (Ehleringer et al., 1993; Saurer et al., 1995). Thus, dendroisotopic approaches combine the advantages of precisely dated and annually resolved tree rings with the sensitivity of carbon isotopic composition governed by ecophysiological responses to the environment (Gessler et al., 2009; Gessler et al., 2014). However, trees growing in wetland settings may not respond solely to moisture deficit. Excessive levels of precipitation and prolonged inundation or saturation in wetland ecosystems can also result in reduced stomatal conductance in trees, resulting in low discrimination values; however, this effect is highly variable across species (Stuiver et al., 1984; Ewe and Sternberg, 2002; Ewe and Sternberg, 2003; Anderson et al., 2005; Buhay et al., 2008; Voelker et al., 2014). These studies in wetlands attribute this positive relationship between tree-ring carbon isotopes and precipitation to excess water stress. Although debatable, a number of possible mechanisms have been suggested with significant evidence to support this relationship. These include disruption of water and nutrient uptake due to anoxic conditions in the root zone (Jackson and Drew, 1984), lowered root hydraulic conductivity (Davies and Flore, 1986), increased abscisic acid

concentrations (Kozlowski and Pallardy, 1984) and accumulation of metabolic toxins from flooding (Jackson and Drew, 1984). Additionally, higher evaporation rates at wetland sites where ponding is common can reduce vapor pressure deficit in the canopy, resulting in lower canopy conductance (Oren et al., 2001) and subsequently lower discrimination rates. Anaerobic conditions at waterlogged sites can also lead to isotopically depleted methane production from the soils and affect the ambient $\delta^{13}C$ in the canopy (Fisher et al., 2017). If these conditions that are specific to wetland ecosystems persist over a longer period during the growing season, carbon isotopic composition of tree-rings can be influenced.

In this study, we investigated how bottomland hardwood wetland forests of eastern Texas, USA respond to hydroclimatic variation and extremes under different edaphic conditions. The study was conducted at four sites, of which one was a frequently flooded wet site, while at the other three sites waterlogging and surface flooding were much less frequent and more ephemeral. Our first objective was to understand how radial growth is affected by hydroclimatic variation using tree-ring width analysis in water oak (*Quercus nigra* L.), a dominant species in the Columbia bottomland hardwood forest. We hypothesized that at relatively drier sites, trees have lower growth rates on average over long time scales compared to wetter sites. Periods of higher rainfall will be associated with increases in growth. However, in extremely wet conditions, at the frequently waterlogged site, trees will show a decline in growth caused by flooding and hypoxic conditions. Our second objective was to assess tree-ring $\Delta^{13}C$ as an indicator of physiological stress inflicted by hydroclimatic conditions on these forests. We hypothesized that tree-ring $\Delta^{13}C$

in trees growing under relatively drier soil conditions will increase during periods of higher rainfall. In contrast, the opposite trend is expected at the wetter site where increasing moisture would induce flooding stress. In addition, we hypothesized that trees growing where waterlogging is common are less stressed during dry periods than those at the drier sites because of slower depletion of soil water reserves. Our third objective was to evaluate the relationship between physiological stress and growth inhibition. Although a positive relationship between tree-ring $\Delta^{13}C$ and growth (tree-ring width) is expected in this study, the strength of this relationship could vary with site conditions. Given that water oaks are moderately tolerant of flooding, and dry conditions are also common in this ecosystem, we hypothesized that drought stress had a stronger effect on growth than flooding stress. Thus, we expected a stronger negative effect of physiological stress on growth at drier sites.

Methods

Study area

The study was conducted at four different sites located within the Brazos-Colorado Coastal Basin in the San Bernard National Wildlife Refuge, Brazoria and Fort Bend Counties, Texas. The four sites are Dance Bayou (DB), Big Pond (BP), Otto (OT) and Buffalo Creek (BC) (Fig. 1B; Table 1). Site DB was observed to be flooded most frequently after significant rain events from 2016 to 2019. This site also remained waterlogged, unlike the other three sites. Therefore, we refer to this site as the "wet site". The sites are located in Ecoregion III Western Gulf Coastal Plain and Ecoregion IV

Floodplain and Low Terraces, dominated by mixed bottomland hardwood forests (Griffith, 2004) at an elevation of about 16 m above MSL. Dominant tree species at these sites include *Quercus nigra* L. (water oak), *Quercus fusiformis* Small (live oak), *Celtis laevigata* Willd. (sugarberry) and *Triadica sebifera* (L.) Small (Chinese tallow). The climate of this region is classified as Humid Subtropical (Cfa) under the Köppen–Geiger climate classification system (Koppen, 1900). The average maximum monthly temperature is approximately 26 ^{o}C and the average minimum monthly temperature is approximately 15 ^{o}C. Mean annual rainfall is 1143 mm, with an average relative humidity of ~70% (NOAA, 2018a). The sites are located in the Linnville Bayou watershed of the San Bernard River Basin. As these forests are situated in the floodplain, sloughs are a common occurrence and inundate significant parts of the forest. Streamflow in Linnville Bayou and adjoining streams and sloughs that traverse the four sites is driven by at least 7 dams on the San Bernard River with heights ranging from 2.5-7.5 m (NID, 2020). Therefore, the presence of these dams and their varying discharge into Linnville Bayou adds significant complexity to the hydrology of Columbia Bottomlands in addition to an already fluctuating hydroclimate.

Soils are mainly vertisols and alfisols dominated by clay, loam and sandy loam texture (NRCS, 2020). The soils series include Aris fine sandy loam, Bacliff clay, Edna loam, Leton loam, Pledger Clay and Churnabog clay. In an Earth Resistivity Tomography study conducted by Guerra (2020) at sites DB, BP and OT, the wetter site DB had more conductive soil in the root zone as compared to the other two drier sites (Table 1). As all

three sites had similar soil salinity, the more conductive soils at site DB are attributed to higher soil moisture.

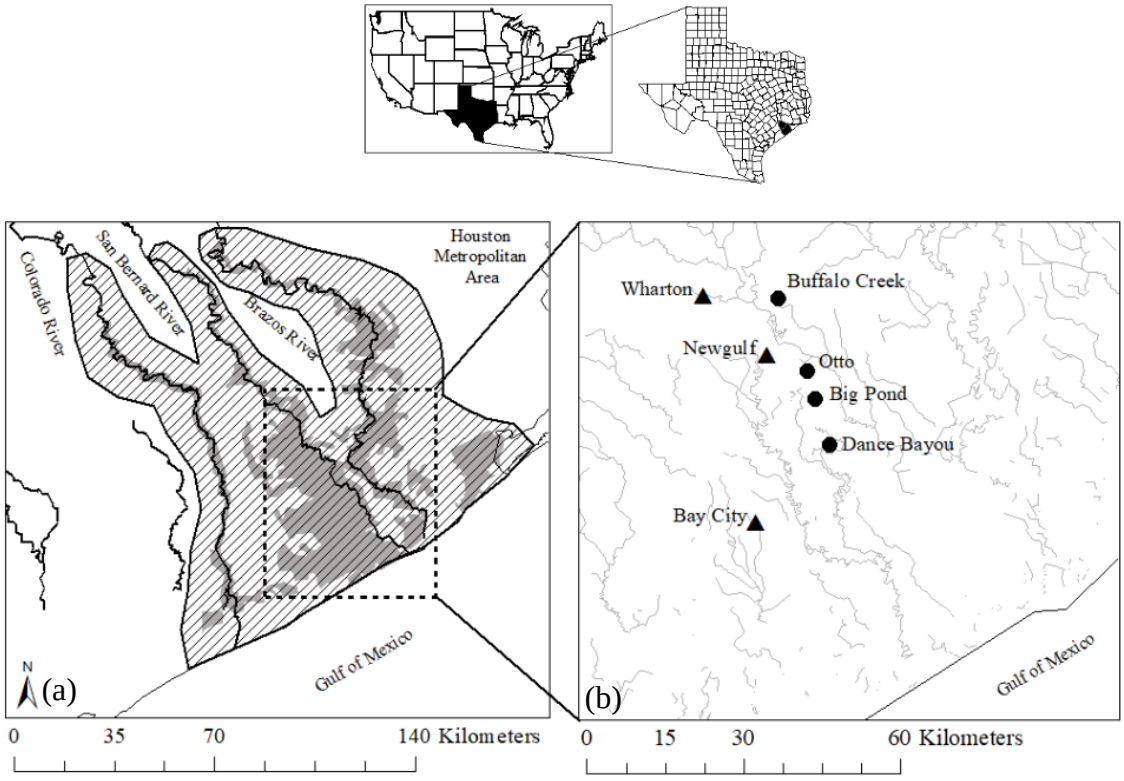

Figure 1. a) Current distribution of Columbia Bottomlands (grey) and historic extent shown by the slanted parallel lines (modified from USFWS, 1997; Houston Wilderness, 2007; Rosen et al., 2008). The area in which the study sites are located is shown by the dashed box. b) Locations of study sites (circles) and weather stations (triangles) in the Brazos-Colorado Coastal Basin.

Table 1. Site description with basic soil properties (adapted from NRCS, 2020) and resistivity measurements averaged over the top 100 cm depth (adapted from Guerra, 2020).

Site	Elevation (m)	Coordinates	Tree DBH (cm) (mean ± SE)	Clay %	Silt %	Sand %	Soil pH	Bulk Density (g/cm^3)	Organic Matter (%)	Resistivity (Ω•m) (mean)
DB	13	29°7'9.56" N 95°47'4.24" W	48.3 ± 5.6	33	58	9	7.4	1.37	1.7	9.9
BP	16	29°9'56.66"N 95°49'43.34"W	58.5 ± 3.2	71	28	1	7.1	1.12	4.8	16.2
OT	17	29°10'47.76"N 95°50'28.65"W	56.4 ± 4.7	71	28	1	7.1	1.12	4.8	12.2
BC	26	29°19'21.75"N 95°51'47.01"W	51.7 ± 3.8	55	34	11	7.8	1.20	2.2	N/A

Tree core sampling

We sampled eight mature *Q. nigra* trees at each site in May 2017. Healthy individuals with no obvious injuries like cavities, scars or diseases were selected. Preference was given to trees with larger diameters at breast height (>40 cm) and uniform girth (Stokes and Smiley, 1968). Three cores were extracted at breast height from every tree spaced equally around the circumference. Two cores were processed and used for ring-width measurements and the third core was used for $\delta^{13}C$ analysis after cellulose extraction.

Dendrochronology

Tree cores were dried to constant weight at 60 ^{o}C and mounted on 9.5 x 9.5 mm grooved core mounts. The mounted cores were sanded using a hand sander with progressively finer grades of sandpaper (60 to 400 grit) (Speer, 2012). Tree-ring widths were visually crossdated and then measured using MeasureJ2X linked to a sliding-stage microscope (2.5X). To verify and refine the crossdating, tree-ring widths were statistically assessed using the COFECHA program (Holmes, 1983). Site-level series intercorrelation between individual cores and mean sensitivity obtained from COFECHA were used to determine the quality of crossdating (Grissino-Mayer, 2001; Speer, 2012). Series intercorrelation indicates chronology-to-chronology variation in annual growth within a given chronology group, while mean sensitivity indicates if the variation in annual growth from year-to-year is sensitive enough for dendroclimatology analyses. As series intercorrelation can be a useful metric to interpret variations in growth between cores from the same tree, trees within a given site, cores across different sites and trees across different

sites, we calculated all four of these parameters separately (Bunn et al., 2020). To calculate series intercorrelation between trees within and across sites, we first averaged corresponding annual ring widths from multiple cores sampled from the same tree. The final standardized ARSTAN (A) chronology (ring-width index (RWI)) was generated for each site using the ARSTAN program, which mathematically standardizes tree-ring series by controlling the autocorrelation component in the time series and maximizes the climate signal (Cook and Holmes, 1984; Speer, 2012). Additionally, we also employed the Regional Curve Standardization (RCS) detrending method to generate site-level RWI using the RCS function (Biondi and Qeadan, 2008) in dplR R package (Dendrochronology Program Library in R) (Bunn et al., 2020). In the RCS detrending method, raw ring-width measurements of multiple trees from the same site are aligned by cambial age to calculate the average ring width for each annual ring. An age-related declining curve is then fit through the measurements and ratio of each measurement to the RCS curve value (expected growth) is then calculated to generate a RWI (Erlandsson, 1936; Briffa et al., 1992; Briffa and Melvin, 2011). Unlike in the ARSTAN method in which RWI is generated by aligning ring widths by calendar year, in the RCS detrending method, ring widths are aligned by cambial age. We also calculated basal area increment (BAI) for each tree using the inside-out method (Biondi, 1999) in dplR R package (Bunn et al., 2020). Site-level BAI was obtained by averaging BAI of all trees from the site for each year.

Climate data

Daily climate summaries for 1950-2016 from three weather stations (Bay City, Newgulf and Wharton, Texas, USA, Fig. 1B) were obtained from the NOAA NCEI

database (NOAA, 2018a) and Palmer Drought Severity Index (PDSI) measurement for the Texas Upper Coast Division was collected from the NOAA NESDIS database (NOAA, 2018b). Monthly and annual averages were used for analyses. As the three weather stations are located at equal distances from the sites (<25 km) and the measurements are highly correlated, an average of the three records was used for dendroclimatology analyses.

Tree-ring $\delta^{13}C$ analysis

Tree cores not utilized for ring-width analyses were hand-sanded using a sandpaper (220 grit) to enhance ring-visibility. Tree-rings were selected from years with a wide range of precipitation to cover the maximum breadth of the dry-wet hydroclimatic spectrum (235-1120 mm/year). Selected tree-rings were precisely excised using an X-Acto knife. For $\delta^{13}C$ analysis, α-cellulose was extracted from the tree-rings using a slightly modified version of the Jayme-Wise Method (Green, 1963), in which a Soxhlet extraction assembly is used (Leavitt and Danzer, 1993; Cullen and Macfarlane, 2005). $\delta^{13}C$ in tree-ring α-cellulose was analyzed using a Costech ECS 4010 elemental analyzer (Costech Analytical Technologies, Valencia, CA, USA) interfaced with a Delta V Advantage isotope ratio mass spectrometer (Delta V, ThermoFisher Scientific, Waltham, MA, USA) operating in continuous flow mode in the Stable Isotopes for Biosphere Science (SIBS) Lab, Texas A&M University (College Station, TX, USA). Tree-ring $\delta^{13}C$ was calculated in δ notation using the following equation:

$$\delta = \left[\frac{R_{SAMPLE} - R_{STD}}{R_{STD}}\right] * 10^3 \quad (1)$$

where R_{SAMPLE} is the $^{13}C/^{12}C$ ratio of the cellulose sample and R_{STD} is the $^{13}C/^{12}C$ ratio of

the V-PDB (Vienna Pee Dee Belemnite) standard (Coplen, 1995). Duplicate measurements taken after every 10 measurements yielded a precision of ±0.1‰.

Atmospheric $\delta^{13}C$ depletion trend over the study period was removed from the tree-ring carbon isotopic record by converting carbon isotope ratios ($\delta^{13}C$) to carbon isotope discrimination values ($\Delta^{13}C$) (Farquhar, 1983):

$$\Delta^{13}C = (\delta^{13}C_{atm} - \delta^{13}C_{plant})/(1 + \delta^{13}C_{plant}) \quad (2)$$

Average annual atmospheric $\delta^{13}C$ values from La Jolla Pier, CA, USA (Keeling and Keeling, 2017) were obtained to calculate $\Delta^{13}C$ (Table 2).

Table 2. Annual average atmospheric $\delta^{13}C$ values from La Jolla Pier, CA, USA.

Year	$\delta^{13}C$	Year	$\delta^{13}C$	Year	$\delta^{13}C$
1986	-7.70	1997	-8.02	2008	-8.34
1987	-7.77	1998	-8.11	2009	-8.32
1988	-7.87	1999	-8.13	2010	-8.36
1989	-7.87	2000	-8.10	2011	-8.38
1990	-7.89	2001	-8.11	2012	-8.43
1991	-7.92	2002	-8.14	2013	-8.47
1992	-7.91	2003	-8.23	2014	-8.51
1993	-7.89	2004	-8.24	2015	-8.51
1994	-7.95	2005	-8.26	2016	-8.59
1995	-8.01	2006	-8.33		
1996	-8.03	2007	-8.34		

Statistical analyses

To evaluate differences in mean $\Delta^{13}C$ values between sites, we used one-way ANOVA. Levene's test was used to check for equal variances, normality was tested using Shapiro-Wilk test and post-hoc analysis was conducted using Tukey HSD. Total monthly precipitation was calculated from daily summaries. Daily maximum temperatures for each day of the month were used to compute mean monthly maximum temperature. Monthly

PDSI values were used directly as obtained (NOAA, 2018b). To identify the portion of the growing season that has the strongest influence on growth and tree-ring $\Delta^{13}C$, we used simple linear regressions between site-wise annual ring-width index and $\Delta^{13}C$ against monthly precipitation, mean monthly maximum temperature and monthly PDSI for all months of the same year as well as the previous year. Additionally, to estimate the multi-month influence of early, late and overall growing season climate on growth and tree-ring $\Delta^{13}C$, we averaged monthly climate data over progressively longer periods of up to 8 months within the growing season. We conducted additional linear regression on these calculated means against annual ring-width index and $\Delta^{13}C$. The time interval during which climate was found to be most strongly influencing growth and tree-ring $\Delta^{13}C$ (maximum coefficient of determination) was used for dendroclimatology analyses. To understand the relationship between growth and stress, we also used linear regression between site-wise annual ring width index and $\Delta^{13}C$. All statistical analyses were conducted in R (R Core Team, 2012).

Results

Site chronologies

Site-level tree-ring width chronologies (ARSTAN and RCS) were closely related to precipitation trends. Patterns of RWI and BAI were similar between sites for much of the 40-year period, except a few wet years (1983, 1991, 1992, 1997, 2001, 2003 and 2007) (Fig. 2 a,b,c), whereas, tree-ring $\Delta^{13}C$ patterns were more variable, with values from site DB being higher in general (Fig. 2d). All site-level chronologies were found to be sensitive

enough for dendroclimatological analyses as mean sensitivity, which is a measurement of year-to-year variability in annual growth, fell within an acceptable range (Table 3). Forest stands at sites DB and OT were found to be younger (24 and 27 years, respectively) than the other two sites as indicated by the mean series lengths (Table 3). High series intercorrelations for the drier sites indicate lower within and between tree differences at these sites, as compared to the wettest site, DB (Table 4). Series intercorrelations across and within sites were slightly lower when calculated using tree-level means (Table 4). Ring-width indices calculated using the RCS and ARSTAN detrending methods were strongly correlated for all four sites (DB: $p<0.0001$; $R^2=0.71$; BP: $p<0.0001$; $R^2=0.93$; OT: $p<0.0001$; $R^2=0.82$; BC: $p<0.0001$; $R^2=0.92$) (Fig. 3). BAI at all four sites increased at a slow rate until the year 2000, after which an increasing shift was observed. At site DB, BAI increased more sharply possibly due to the stand being relatively younger, while at site BP, which had the most mature stand, change in BAI over time was less variable (Fig. 2c).

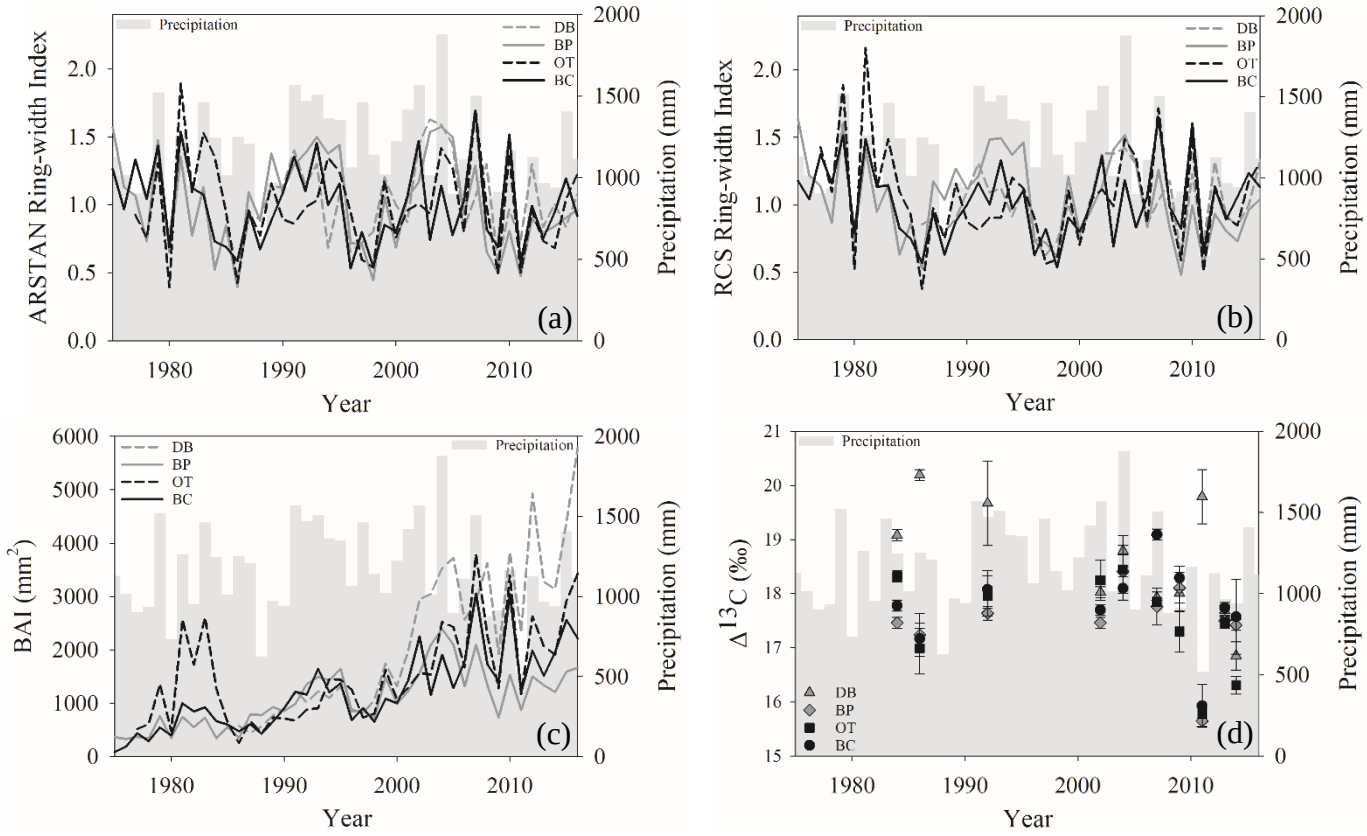

Figure 2. Temporal variation in a) ARSTAN ring-width index, b) RCS ring-width index, c) basal area increments and d) tree-ring Δ^{13}C values of *Quercus nigra* in the Brazos-Colorado Coastal Basin of Texas. Total annual precipitation is shown by grey shading.

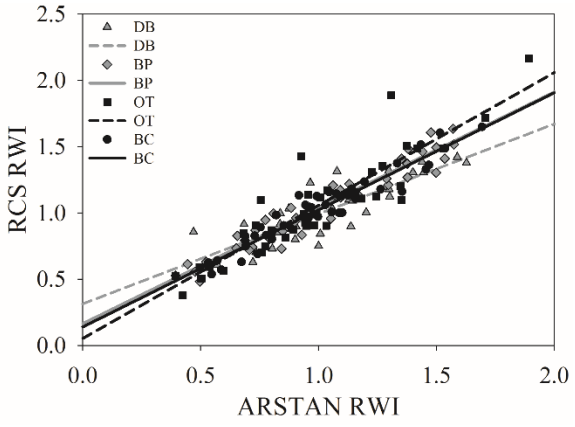

Figure 3. Relationship between site-level ring-width indices calculated using RCS detrending and using ARSTAN.

Table 3. Descriptive statistics of site-level as well as combined tree-ring chronologies generated using COFECHA.

Chronology	Number of trees	Number of dated series	Mean Sensitivity	Mean Series Length
All sites	32	64	0.37	32 years
DB	8	16	0.35	24 years
BP	8	16	0.36	40 years
OT	8	16	0.42	27 years
BC	8	16	0.37	38 years

Table 4. Series intercorrelation values calculated using chronologies from individual cores and tree-level means across all sites and within each site.

Chronology	Across all sites (individual cores)	Across all sites (tree means)	Within site (individual cores)	Within site (tree means)
All sites	0.64	0.59	-	-
DB	-	-	0.61	0.51
BP	-	-	0.70	0.65
OT	-	-	0.79	0.67
BC	-	-	0.68	0.66

Differences in site-level tree-ring $\Delta^{13}C$ values

Comparison between site-level mean tree-ring $\Delta^{13}C$ measurements averaged over the entire 40-year study period supports our second hypothesis. Tree-ring $\Delta^{13}C$ measurements were different between sites when averaged over the 40-year period [One-way ANOVA, F (3, 24) = 4.05, p = 0.01]. This indicates that at least one site has a significantly different mean $\Delta^{13}C$ signal over the 40-year period. Post hoc analysis indicates that the wet site, DB, had a higher mean tree-ring $\Delta^{13}C$ value as compared to two drier sites, BP (p=0.03) and OT (p=0.02) (Fig. 4).

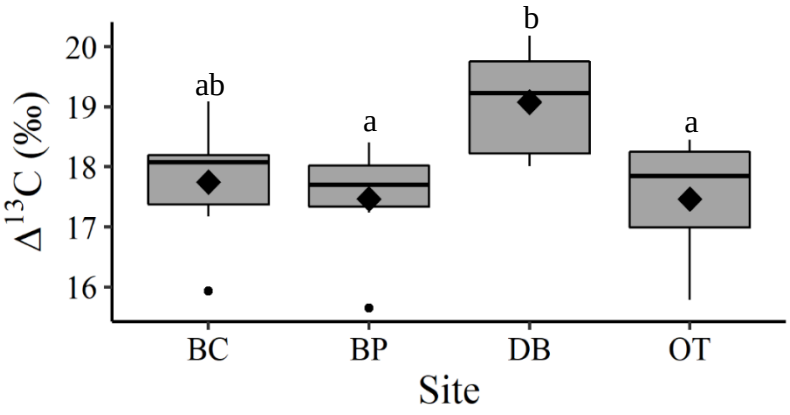

Figure 4. One-way ANOVA and Tukey post hoc analysis (denoted with letters) for mean difference in site-level tree-ring $\Delta^{13}C$ averaged over the 40-year period. Black diamonds indicate mean values, horizontal black lines indicate median values, black circles indicate outliers and grey boxes show values lying between the upper and lower quartiles.

Dendroclimatology analyses

Comparisons between ring-width indices and climate data reveal that growth rates are most strongly influenced by mid-growing season climate (May-July precipitation and maximum temperatures; July PDSI) (Appendix A: Table 13). Since a larger proportion of annual growth occurs during the mid-growing season, higher rainfall and lower maximum

temperatures during this period strongly drive annual growth rates. Similar comparisons between tree-ring $\Delta^{13}C$ measurements and climate data indicate that climatic conditions early in the growing season (April) are critical for causing physiological stress in these forests (Appendix A: Table 14).

As hypothesized, we observed a strong increase in RWI with mid-growing season precipitation. Although this positive relationship was expected for trees growing in drier conditions, we observed a similar but weaker positive relationship between RWI and precipitation even at the wet site (Table 5, 6; Fig. 5a). We had hypothesized that for the wettest site, radial growth would decline due to flood stress, however, no such decline was observed even during extremely wet phases (Fig. 5a). Drought conditions and maximum temperatures during the mid-growing season resulted in decreasing RWI at the drier sites, but not at the wet site, as expected (Table 5, 6; Fig. 5b, c). Climatic variables had similar relationships with ring-width indices calculated using both the ARSTAN and RCS detrending methods (Table 5, 6). BAI overall had a much weaker relationship with climatic variables. BAI at the drier sites had weak positive relationship with precipitation, while at the wetter site, BAI was independent of precipitation (Table 7). Maximum temperature and PDSI did not affect BAI at any of the sites (Table 7).

Table 5. Relationships between ARSTAN ring-width index and mid-growing season climatic conditions (α=0.05).

Site	Precipitation (May-July)		Temperature (May-July)		PDSI (July)	
	p value	R^2	p value	R^2	p value	R^2
DB	<0.05	0.13	ns	-	ns	-
BP	<0.001	0.39	<0.001	0.25	<0.001	0.49
OT	<0.001	0.42	<0.01	0.17	<0.001	0.31
BC	<0.001	0.44	<0.001	0.27	<0.001	0.47

Table 6. Relationships between RCS ring-width index and mid-growing season climatic conditions (α=0.05).

Site	Precipitation (May-July)		Temperature (May-July)		PDSI (July)	
	p value	R^2	p value	R^2	p value	R^2
DB	<0.05	0.19	ns	-	ns	-
BP	<0.001	0.43	<0.01	0.22	<0.001	0.50
OT	<0.001	0.35	<0.01	0.15	<0.001	0.27
BC	<0.001	0.39	<0.01	0.24	<0.001	0.39

Table 7. Relationships between basal area increment and mid-growing season climatic conditions (α=0.05).

Site	Precipitation (May-July)		Temperature (May-July)		PDSI (July)	
	p value	R^2	p value	R^2	p value	R^2
DB	ns	-	ns	-	ns	-
BP	<0.05	0.15	ns	-	ns	-
OT	<0.01	0.18	ns	-	ns	-
BC	<0.05	0.10	ns	-	ns	-

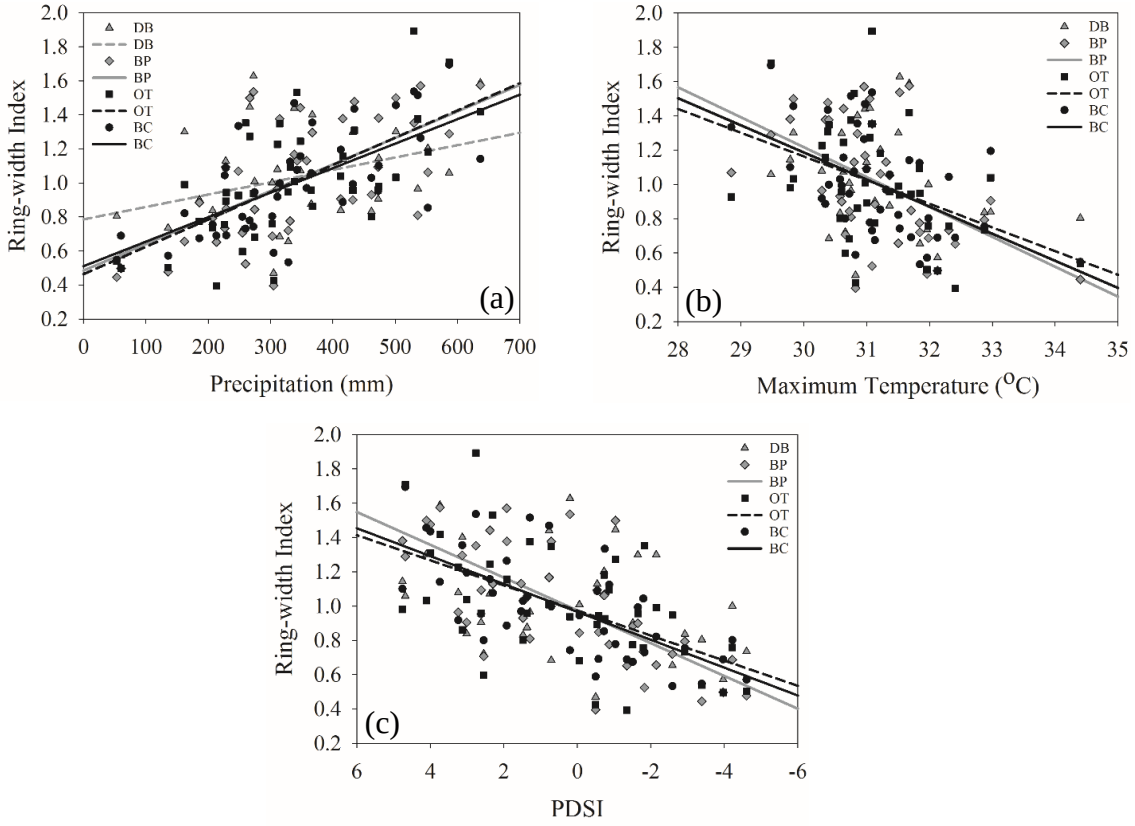

Figure 5. a) Relationship between ARSTAN ring-width index and mid-growing season precipitation (a), temperature (b) and PDSI (c). Site DB is represented by grey triangles, BP by grey diamonds, OT by black squares and BC by black circles. Regression lines are shown only for statistically significant relationships.

In line with our second hypothesis, we observed an increase in tree-ring $\Delta^{13}C$ values with increase in early-growing season precipitation at the drier sites (Table 8, Fig. 6a). We had hypothesized that high precipitation at the wet site will reduce carbon isotopic discrimination as a result of physiological stress caused by possible flooding stress. However, we found no relationship between tree-ring $\Delta^{13}C$ and precipitation at the wet site (Table 8). Higher maximum temperatures resulted in lower tree-ring $\Delta^{13}C$ values only at one of the drier sites (BC) (Table 8, Fig. 6b). PDSI did not have any effect on tree-ring $\Delta^{13}C$ values from all four sites (Table 8). Also, previous year's climate did not have any

statistically significant influence on either ring-width index or tree-ring $\Delta^{13}C$ measurements at any of the four sites.

Table 8. Relationships between tree-ring $\Delta^{13}C$ values and early-growing season climatic conditions (α=0.05).

Site	Precipitation (April)		Temperature (April)		PDSI
	p value	R^2	p value	R^2	p value
DB	ns	-	ns	-	ns
BP	<0.05	0.70	ns	-	ns
OT	<0.05	0.68	ns	-	ns
BC	<0.05	0.59	<0.001	0.94	ns

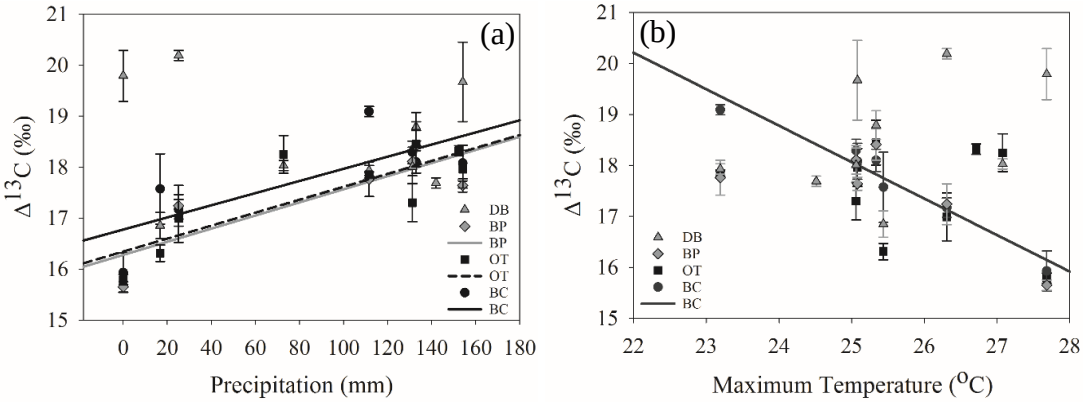

Figure 6. Relationship between tree-ring $\Delta^{13}C$ values and early-growing season (a) precipitation and (b) temperature. Site DB is represented by grey triangles, BP by grey diamonds, OT by black squares and BC by black circles. Regression lines are shown only for statistically significant relationships.

Relationship between RWI and tree-ring $\Delta^{13}C$

The comparison between tree-ring $\Delta^{13}C$ values and tree-ring width indices from corresponding years supports our third hypothesis only at the drier sites. ARSTAN as well as RCS ring-width indices were correlated with $\Delta^{13}C$ values only at sites OT (ARSTAN: $p<0.05$; $R^2=0.53$; RCS: $p<0.05$; $R^2=0.45$) and BC (ARSTAN: $p<0.05$; $R^2=0.58$; RCS: $p<0.05$; $R^2=0.62$). Tree-ring $\Delta^{13}C$ values were not correlated with annual growth at the

wet site DB, which indicates that trees at this site were able to minimize growth inhibition during stressful conditions as compared to trees at the drier sites (Fig. 7). Tree-ring $\Delta^{13}C$ values were not correlated with BAI at any of the sites.

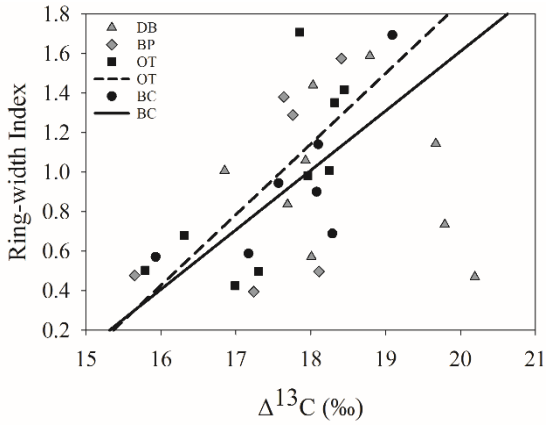

Figure 7. Relationship between ARSTAN ring-width index and tree-ring $\Delta^{13}C$. Site DB is represented by grey triangles, BP by grey diamonds, OT by black squares and BC by black circles. Regression lines are shown only for statistically significant relationships.

Discussion

Bottomland hardwood forests in the southeastern United States have been reduced to a small proportion of their original expanse. The hydrology of these wetland forests has been altered due to land use change and river regulation (Wear and Greis, 2002; Blann et al., 2009; Dahl, 2011) and the alteration is exacerbated by hydroclimatic anomalies such as droughts and floods (Ferrati et al., 2005; Erwin, 2008). These disturbances coupled with topographic heterogeneity cause some portions of these riverine wetland forests to be drier than others.

Contrary to our first hypothesis, similar annual radial growth of trees at the wetter site and the three drier sites during the past several decades suggests that trees at all sites

have access to moisture sufficient to sustain annual growth. Moreover, growth of trees at the wetter site was not inhibited by excessive moisture during wet years, which may reflect adaptation by *Quercus nigra* to the broad range of soil moisture conditions that occur in a floodplain forest (Gilman et al., 1994). Within the wetter site, we observed more heterogeneity in growth rates, which could be attributed to uneven waterlogging within the site. Although growth rates were correlated with rainfall across all sites, the wet site had a much weaker dependence on rainfall and showed no negative response to higher temperatures and drought severity. This suggests that wetland forests with high water tables are more independent of climatic conditions than their drier counterparts. It has been repeatedly observed across southeastern US that in wetter and hydrologically well-connected parts of wetland forests, vegetation experiences lower stress during non-favorable growing conditions (Clawson et al., 2001; Anderson et al., 2005; Gee et al., 2014; Allen et al., 2016).

Consistent with our second hypothesis, mean tree-ring $\Delta^{13}C$ values from the wetter site were significantly higher than those from the drier sites over a longer temporal scale, suggesting lower stomatal constraints on leaf gas exchange at the wet site as compared to those at the drier sites. Also supporting our second hypothesis, reduced stomatal conductance in trees from the drier site during drought years, clearly indicates prolonged stress caused by soil moisture deficit. This relationship between tree-ring $\Delta^{13}C$ and drought conditions (low precipitation and high temperatures) has been extensively observed across different ecosystems such as boreal forests (Brooks et al., 1998; Au and Tardif, 2012), wetlands (Anderson et al., 2005; Buhay et al., 2008), lowland rain forests

(Schollaen et al., 2013), deserts (Lipp et al., 1996), etc. Generally, forested wetlands are known are not known to be drought stressed because of ample soil moisture availability. However, it is important to note that in parts of Columbia Bottomlands, depending on site-level hydrologic conditions, vegetation does experience drought stress during some years when dry climatic conditions persist over a longer period.

Our third hypothesis that tree-ring $\Delta^{13}C$ would have a positive relationship with radial growth holds true under dry edaphic conditions, where drought stress restricts plant growth. Whereas in trees growing in wetter soils, tree-ring $\Delta^{13}C$ and radial growth were largely decoupled. Similar differences in the relationship between tree-ring $\Delta^{13}C$ and radial growth of the ring-porous bur oak (*Quercus macrocarpa* M.) have been observed across continental gradients where tree-ring $\Delta^{13}C$ correlates positively with radial growth at drier sites, while the relationship is negative under wetter conditions (Voelker et al., 2014). These differences have been attributed to indicators of site aridity (VPD, precipitation:evapotranspiration). A similar relationship has also been observed in pond cypress trees in the southeastern Everglades, Florida, USA (Anderson et al., 2005). While we did not observe a negative relationship between tree-ring $\Delta^{13}C$ and radial growth at the wet site, no correlation between the two highlights the beneficial effect of wetter hydrological conditions on vegetation at the flooded site. Consequently, the absence of drought-related stress signals at the wet site is possibly due to supplemental soil moisture availability from flooding. At the drier sites, drought-related lower tree-ring $\Delta^{13}C$ values are correlated with slower radial growth, which indicates that moisture deficit causes physiological stress in these trees, reducing stomatal conductance and eventually inhibits

growth. Additionally, tree-ring $\Delta^{13}C$ and radial growth at the wet site were highly uncorrelated especially during years when growing-season precipitation was more erratic (dry spring followed by a wet summer and vice versa). The drought effect of drier hydroclimatic conditions is ephemeral and less intense at the wet site due to slower depletion of soil water reserves. Therefore, seasonal dry spells slightly reduce tree-ring $\Delta^{13}C$ but do not always result in growth inhibition in wetter parts of this landscape due to sufficient moisture availability. We had expected to observe lower tree-ring $\Delta^{13}C$ values during extremely wet growing seasons due to flooding stress, but the absence of these signals indicates adaptation to excessive wetness. It has been suggested that wetland species that experience frequent flooding develop adaptive traits that enable rapid reopening of stomata with the recession of flood waters as oxygen availability in the root zone increases (Crawford, 1982; Kozlowski and Pallardy, 1984; Kozlowski, 2002). Consistent with this, our observations signify that trees growing in drier conditions do have a more distinct tree-ring $\Delta^{13}C$-growth relationship as compared to those growing in wet conditions.

We found that mid-growing season precipitation (from May to July) is most critical for growth in this landscape. Similarly, high temperatures during the same period were associated with suppressed growth. Therefore, adequate precipitation and moderate temperatures during this period are important controls over tree growth. However, due to changing climatic conditions and altered hydrology of this region, change in the seasonal moisture availability during this period can result in reduced productivity. Unlike the trees growing in drier conditions, the ones at the wet site are not affected by temperature and

drought severity throughout the growing season possibly because of residual soil moisture availability despite evaporation caused by higher temperatures. It is important to consider seasonal variation in precipitation because flood conditions in the dormant winter season do not necessarily help sustain growth throughout the summer in drier sites, especially if summers have below normal precipitation. On the other hand, trees at the wet site may benefit from access to soil moisture reserves from waterlogging caused by winter precipitation.

While the growth-climate relationship is more amplified during mid-growing season, tree-ring $\Delta^{13}C$ is more prominently dependent on early-growing season precipitation. Lack of precipitation early in the growing season (April) results in substantial physiological stress caused by reduced stomatal conductance in trees at the drier sites. This is an indication that although dry conditions early in the growing season cause stress in trees, most growth is attained during the mid-growing season. Therefore, trees can recover from the stress and attain normal growth rates if adequate precipitation occurs during the mid-growing season. The prominent dependence of physiological stress on spring precipitation could be the result of more energy and resource allocation during leaf out. However, this holds true only under dry edaphic conditions. Such seasonal variations have been observed across different biomes and have been attributed to formation of wood using previous or current growing season assimilates (Schollaen et al., 2013). It is apparent that if wood at the very beginning of the growing season is formed using assimilates from the previous growing season, earlywood tree-ring $\Delta^{13}C$ does not have a correlation with early-growing season precipitation from the current year (Helle

and Schleser, 2004; Porter et al., 2009; Schollaen et al., 2013). In our study, tree-ring $\Delta^{13}C$ is well-correlated with early-growing season precipitation from the current growing season. Although this indicates that majority of annual wood is formed using assimilates from the current growing season, it needs to be noted that earlywood portions of ring-porous oaks like those of *Q. nigra* have lower wood density (Gasson, 1987; Lei et al., 1996; Rao, 1997). Therefore, by using entire annual ring composites, the relatively small signal from the previous year could be present but not distinctly detected. Hence, comparing our ring-width indices and tree-ring $\Delta^{13}C$ values with previous years' climate yields no correlation ($p>0.05$) indicating its relatively weak effect.

Climate models have predicted a significant decrease in growing season precipitation and increase in temperature throughout Texas (Jiang and Yang, 2012) and especially in the Brazos River basin (Awal et al., 2016) where our study area is located. This region occurs at the extreme southwestern edge of the bottomland hardwood forest type (Bray, 1906; Putnam et al., 1960), which is also the southwestern edge of the distribution of *Q. nigra* and many other wetland tree species. Edges of distribution ranges usually experience environmental conditions that are less favorable (drier and warmer) to the species as compared to the range core (Rehm et al., 2015), which makes them more resilient and better adapted to survive in stressful conditions relative to core populations (Gutschick and Hormoz, 2003). Therefore, as climate changes, these native wetland tree populations will play key roles in helping the species maintain their geographic distributions.

Conclusion

This study provides insights on hydroclimatic conditions that can provide suitable conditions for better wetland forest productivity and health. Columbia bottomlands support a large diversity of plants, mammals, birds, reptiles and insects. The knowledge of optimum growing conditions for the vegetation in this region is critical for the survival and conservation of the biodiversity that is dependent on this ecosystem. We provide evidence that hydrologically wetter portions of this landscape experience less stress and subsequently lower growth inhibition in response to hydroclimatic changes as compared to drier areas. Trees in drier areas grew more slowly during dry and warm periods and were more sensitive to seasonal physiological stress. We observed variation in growth and stress responses to climatic conditions during different phases of the growing season. Our findings suggest that hydroclimatic changes to this ecosystem that alter the timing and frequency of wet conditions can negatively impact forest health. This study also provides the first tree-ring records from the Columbia bottomlands, which can act as a baseline for future ecological research in the region.

CHAPTER III

TREE WATER-USE STRATEGIES IN AN INTERMITTENTLY FLOODED BOTTOMLAND HARDWOOD FOREST

Synopsis

Quantifying plant water-use in wetland forests is critical as these ecosystems play critical roles in landscape and regional scale hydrologic cycles, and have become increasingly threatened by human and climatic disturbances. We measured sap flow in native and invasive tree species in an intermittently flooded slough and a drier upland patch in a bottomland hardwood forest in the Brazos-Colorado coastal basin, Texas, USA. Our objectives were to: (i) estimate the relative seasonal difference in tree water-use under contrasting hydrologic conditions using sap flow measurements, and (ii) determine if the invasive *Triadica sebifera* has a different water-use strategy compared to native species. Results indicate that trees growing under waterlogged conditions had lower but more consistent sap flow rates throughout the growing season with suppression during early-spring waterlogging. However, they rapidly recovered from flooding stress and were less sensitive to dry and warm summer conditions. In contrast, upland trees suppressed sap flow in the summer to prevent water loss. Sap flow in all trees responded positively to flooding up to a threshold. Lastly, *T. sebifera,* with overall smaller tree sizes and younger individuals, had only moderately lower sap flow rates as compared to mature native oaks. The invasive *T. sebifera* may have the potential to alter transpiration in the regional hydrologic cycle in the near future as their abundance is on the rise. This study provides a

better understanding of plant water-use in a rapidly shrinking wetland ecosystem, where invasion is an added concern.

Introduction

Prior to human settlement, extensive bottomland hardwood forests occurred along major lowland rivers throughout the southeastern United States. Removal of vegetation for agriculture and timber, dam construction, urban expansion and infestation by invasive plants, in addition to climate change, has greatly reduced the total area of these forests (Swift, 1984; Daryadel and Talaie, 2014). Furthermore, hydrology of wetlands that sustain riparian forests has been modified due to flow regulation, drainage ditches (Wear and Greis, 2002), impoundment from berms (Blann et al., 2009), and water table drawdowns (Dahl, 2011). Watersheds of the Brazos, San Bernard and Colorado Rivers form a floodplain on the Gulf coast of Texas. Bottomland hardwood forests known as the Columbia Bottomlands dominate the riparian zones in this floodplain. Over the past few decades, increasing anthropogenic pressure from the ever-expanding city of Houston coupled with a changing hydroclimate (Schmidt and Garland, 2012; Hoerling et al., 2013; Moore et al., 2015; van Oldenborgh et al., 2017; Sebastian et al., 2019) have reduced the expanse of these oak-dominated forests by more than 75% (USFWS, 1997; Barrow and Renne, 2001; Barrow et al., 2005) (Figure 1). These forests are dominated by wetland species, such as *Quercus nigra, Carya illinoinensis, Celtis laevigata*, that are largely intolerant of drought conditions (Luo et al., 2008; Laanisto and Niinemets, 2015).

Moreover, a changing climate is expected to significantly reduce precipitation in this region (Jiang and Yang, 2012), posing a threat to the native wetland vegetation.

Hydroclimate along the gulf coast of Texas has been inconsistent in the last five decades. Annual precipitation amounts have been highly variable with up to 61% more rainfall than average during some years, while up to 53% deficit during others. These fluctuations have resulted in numerous droughts (1988, 1999, 2005, 2011) and floods (1994, 2015, 2016). Additionally, the region is also prone to frequent tropical storms and hurricanes (1983, 2001, 2005, 2008, 2017), which can bring massive amounts of rainfall (up to 1000 mm) within 4-5 days, inundating large swaths of floodplain forests for prolonged periods.

Depending on whether bottomland hardwood forests are directly influenced by fluctuating river flows, flood conditions may readily transition into droughts, often multiple times in the same growing season (Vivian et al., 2014). Associated soil conditions can also transition rapidly from wet and hypoxic to dry and hyperoxic, and vice versa, which results in physiological stress on plants. Studies conducted to understand the effects of inundation on floodplain vegetation across the United States have yielded very contrasting results in terms of productivity (Mitsch et al., 1991), nutrient content (Saha et al., 2010), changes in anatomy (Hook and Scholtens, 1978), root functioning (Andersen et al., 1984), root growth (Baker et al., 2001), early senescence (Kozlowski, 1997), stomatal conductance (Ewe and Sternberg, 2003), among others. In some cases, flooding has been found to be beneficial to plant functioning, while it has proven to be detrimental in others (Odum et al., 1979). Additionally, wetland plants have been known to rapidly switch their physiological response to seasonal changes (Kozlowski and Pallardy, 1979; Crawford, 1982; Pezeshki and Chambers, 1985; Lande, 2009; Shannon et al., 2018). Although a wide range of physiological studies have been conducted in wetlands across

the US, a significant number of studies focus on effects of flooding on shrubs (Erickson, 1989), herbs (Jackson and Drew, 1984), seedlings (Zaerr, 1983) or plants grown in agricultural settings (Schaffer and Ploetz, 1989). While some studies have focused on tree physiology in forested wetlands, very few have attempted to quantify *in situ* tree water-use under flooded conditions (Krauss et al., 2015; Allen et al., 2016). Given that forested wetlands are expected to experience highly variable hydrologic conditions under future climatic scenarios, a better estimation of wetland tree water-use in response to floods and droughts is needed to understand the impacts on these sensitive ecosystems and the hydrological services they provide.

The timing and duration of wet and dry phases are also critical (Allen et al., 2016). Depending on species and site-specific edaphic conditions, some disturbances can promptly induce physiological stress, while in other cases, a lagged effect is observed, where stress is induced much later (Miao et al., 2009). This also holds true for the intensity of stress, which can vary according to the magnitude, nature and timing of the disturbance (Shafroth et al., 2002). Sap flow measurements have been effectively used as a direct indicator of plant water stress across ecosystems, including wetlands. In a study conducted on wetland trees by Allen et al. (2016), it was observed that at a hydrologically well-connected site, sap flow increased more sharply in *Quercus lyrata* as compared to *Celtis laevigata* during flooding events. Another study conducted in four coastal wetlands in South Carolina, USA demonstrated that same species can have variations in sap flow rates if site-level conditions are different even within the same landscape (Krauss et al., 2015).

Apart from hydroclimatic anomalies and human-induced disturbances, invasive species are a major threat to wetland forests (Zedler et al., 2004). Invasion by Chinese tallow (*Triadica sebifera* (L.) Small) has been on the rise in the southeastern US, including Columbia Bottomlands and other wetlands along the gulf coast (Bruce et al., 1995). This tree is known to aggressively displace native vegetation, threatening native oaks and other plant species (Bruce et al., 1997; Siemann and Rogers, 2003a). Chinese tallow has been found as the most abundant species in eight counties around Houston, Texas (Nowak et al., 2005). Tallow invasion has also been found to be aided by disturbance caused by wild hogs and canopy gaps created by extreme storm events, such as tornadoes and hurricanes (Siemann et al., 2009), which are common in this region. Moreover, tallow invasion is predicted to expand westward from the Gulf Coast of Texas and engulf several more wetlands along the coastal plains (Wang et al., 2011a). Tallows are known to achieve remarkable flood tolerance at a very young age, which is comparable to or even more than some wetland tree species (Jones and Sharitz, 1990; Gabler and Siemann, 2013). However, tallow seeds do not germinate under waterlogged conditions (Gabler and Siemann, 2013); therefore, invasion success is usually found to be higher in intermittently flooded soils rather than at locations that experience prolonged waterlogging (Cameron and Spencer, 1989). Although the tolerance of tallow to herbivory and range distribution has been studied extensively in this region, its direct effect on the ecosystem water budget through transpiration is yet to be determined. Invasive species are known to aggressively compete against native vegetation for water and deplete groundwater reserves. Thus, tallow

invasion adds even more complexity to the already fluctuating hydrology of the Columbia Bottomlands.

In this study, we investigated water-use strategies of trees growing under intermittently flooded and non-flooded conditions. Our objectives were to: (i) estimate the relative seasonal difference in water-use by trees growing in dry, upland conditions versus trees that experience intermittent waterlogging using sap flow measurements, and (ii) investigate if the invasive *Triadica sebifera* has a different water-use strategy as compared to other native wetland trees and the magnitude of this difference as the growing season progresses. The intermittently flooded patches in this forest have significantly wetter conditions as compared to the upland patches throughout the growing season. Therefore, we hypothesized that due to higher water availability, trees growing in these wetter patches will have higher sap flow rates over the entire growing season as compared to the drier patches. However, the relative difference in sap flow rates may vary seasonally. Sap flow in trees growing under drier soil conditions is expected to be more sensitive to wet periods caused by higher water use due to replenishment of soil water. However, we hypothesized that during periods of prolonged waterlogging, the inundated trees will have sustained sap flow rates due to better adaptation to flooded conditions. Based on the literature available on the behavior of *Triadica sebifera*, which is favored by flooded conditions, we hypothesized that it will consistently have higher water-use as it is known to be well-adapted to shaded and waterlogged conditions.

Methods

Site description

The study was conducted at the Big Pond unit (29°9'56.66"N 95°49'43.34"W) of San Bernard National Wildlife Refuge in Brazoria County, Texas, USA (Fig. 8). San Bernard National Wildlife Refuge is located in Ecoregion III Western Gulf Coastal Plain and Ecoregion IV Floodplain and Low Terraces, dominated by mixed bottomland hardwood forests (Griffith, 2004) and has a humid subtropical climate (Koppen, 1900). The area receives a mean annual rainfall of 1143 mm, with an average relative humidity of ~70% and the mean temperature is approximately 20 °C (NOAA, 2018a). The study site is located in a smaller basin of the San Bernard River within the Brazos-Colorado Coastal Basin. Numerous streams and bayous are a present in this floodplain, which create sloughs that inundate significant patches of the riparian hardwood forest. Soils are mainly vertisols and alfisols dominated by clay, loam and sandy loam texture (NRCS, 2020).

The Big Pond unit also includes upland areas that do not experience flooding as well as sloughs that are frequently waterlogged for prolonged periods. Flooding in these sloughs is mainly driven by upstream river flows. Sloughs are a critical feature in these floodplain forests and support substantial biodiversity, including wetland tree species like *Carya illinoinensis, Quercus virginiana and Quercus shumardii*, which account for 40%, 21% and 13% of basal area (BA), respectively. Although tallows constitute about 7% of basal area, nearly 20% of stand individuals are tallows, most of which are young individuals with smaller basal areas (mean 0.03 ± 0.01 m^2), indicating recent invasion. Vegetation in the upland areas is dominated by *Quercus nigra, Quercus virginiana and*

Celtis laevigata, which account for 32%, 15% and 15% of the basal area, respectively (Cross et al., in preparation).

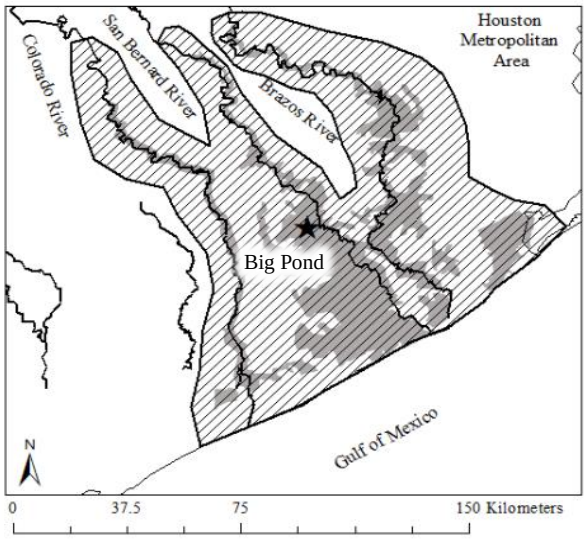

Figure 8. Current distribution of Columbia Bottomlands (grey), historic extent shown by the slanted lines (modified from USFWS, 1997; Houston Wilderness, 2007; Rosen et al., 2008) and location of the Big Pond study site.

Climate and flood data

A weather transmitter (WXT530, Vaisala, Vantaa, Finland) was installed in a clearing 60 m away from the study plots and was used to measure air temperature (°C), relative humidity (%), wind speed (m/s) and precipitation (mm) at 30 second intervals and 30-minute averages. Vapor pressure deficit (VPD, kPa) was calculated from air temperature and relative humidity as described by (Jones, 1992). Stage height (m) measurements were obtained from an online database supplied by USGS Station 08117500 on the San Bernard River in Boling, Texas (USGS, 2019). A flood pulse was

quantified when stage height exceeded a daily average of 2 m with at least 30 mm of rainfall recorded within a 24-h period.

Sap flow measurements

We established two 30-m diameter study plots, one of which was located in a frequently waterlogged slough, while the other was located in an upland area that seldom floods. In the upland plot, sap flow sensors were installed in three water oak trees (*Quercus nigra*), one live oak (*Quercus virginiana*) and one green ash (*Fraxinus pennsylvanica*); while in the slough plot, the sensors were installed in one Shumard oak and four Chinese tallows (*Triadica sebifera*). Selection and replication of species was restricted by the availability of a power source and spatial constraints due to limited access to viable trees. Sap flow was measured for a 6-month period from 9 March to 7 September, 2018, which encompasses a significant portion of the growing season from the beginning of spring to the end of summer. There was a gap in the measurement from 29 July to 13 August due to power failure. We used thermal dissipation probes (Granier, 1987), in which the reference and heated probes containing thermocouples were inserted in the outer 20 mm of the active xylem. We installed two sensors in each tree in radially opposite directions. The sensors were installed at a height of approximately 1.5 m. Healthy individual trees with no obvious injuries like cavities and scars or diseases were selected for the installation.

Temperature differences between the reference and heated probe were converted to sap flux density J_s (sap flow per unit sapwood area) (kg m^{-2} s^{-1}) using Granier's empirical calibration equation (Granier, 1987) (Equation 3). Sap flow measurements were

recorded every 30 seconds and averaged over 30-minute intervals and stored on a CR10X datalogger (Campbell Scientific Inc., Logan, UT).

$$J_s = 0.119 \left(\frac{\Delta T_M - \Delta T}{\Delta T}\right)^{1.231} = 0.119K^{1.231} \quad (3)$$

where, ΔT_M is the maximum temperature difference when sap flux is assumed to be 0, and ΔT is the actual temperature difference. Herein, J_s is expressed as hourly (kg m^{-2} h^{-1}) and daily (kg m^{-2} day^{-1}) totals, where daily total sap flux density was the sum of all J_s in a 24-h period.

Diameter-at-breast-height (DBH, cm) was measured for each tree and active sapwood area (SA, cm^2) was determined by visual examination of tree cores (Granier et al., 1994; Giothiomi and Dougal, 2002). Basal area (BA, cm^2) was calculated using DBH.

As environmental conditions vary significantly as the growing season progresses, to understand response of J_s to changing seasonal conditions, we divided the study period into three phases: 1) Early-spring (March 9 - April 30), 2) Late-spring (May 1 - June 30), and 3) Summer (July 1 – September 7).

Table 9. Individual description of sampled trees.

No.	Species	Plot	DBH (cm)	Basal Area (BA) (cm^2)	Sapwood Area (SA) (cm^2)
1	*Quercus virginiana*	Upland	48.4	1839	836
2	*Quercus nigra*	Upland	52.1	2131	871
3	*Quercus nigra*	Upland	67.1	3536	1697
4	*Quercus nigra*	Upland	65.0	3318	1075
5	*Fraxinus pennsylvanica*	Upland	66.3	3419	2906
6	*Quercus shumardi*	Slough	29.7	692	322
7	*Triadica sebifera*	Slough	41.2	1333	1055
8	*Triadica sebifera*	Slough	26.1	535	471
9	*Triadica sebifera*	Slough	24.5	475	389
10	*Triadica sebifera*	Slough	15.3	185	120

Statistical analyses

Simple linear regression was used to assess the relationship between precipitation and flood pulse, with stage height used as a proxy. The predictor variable was total daily precipitation with the mean stage height recorded on the following day as the response variable. To evaluate the difference in seasonal variation in J_s for the upland and inundated trees, we used two-way repeated measures ANOVA followed by post-hoc analysis using Tukey HSD. The same approach was used to investigate seasonal variation in J_s of Chinese tallow and native wetland tree species. Simple linear regression models were used to assess the response of J_s to changes in VPD. These regressions were conducted separately for the two plots during the three seasonal periods. To understand how sap flow responds

to inundation and changes in groundwater table depth during flood pulses, we used simple linear regression with J_s as the response variable and stage height as the predictor variable. When using regression between J_s and stage height, we filtered out days when daytime average VPD was less than 0.5 kPa to ensure that low J_s was a function of only stage height and not VPD. All statistical analyses were conducted in R (R Core Team, 2012).

Results

Precipitation and flood dynamics

A total of 421 mm of precipitation was recorded over the entire study period. Two storm events occurred in early-spring, one in March (37 mm) and the other in April (38 mm). These events resulted in two flood pulses with stage heights above 2.8 m after both storms (Figure 9). Another flood event occurred in mid-June as 110 mm rainfall was recorded in 4 days with 50 mm rainfall recorded in a single day. This precipitation resulted in a major flood pulse (stage height ~ 4.7 m, Figure 9). Total precipitation in June was 141 mm. During the flood pulses, when precipitation exceeded 10 mm in a 24-hour period, stage height responded with an increase on the following day (R^2=0.70; Figure 10). Other than the three flood pulses that occurred during the study period, two additional winter pulses also occurred in the month preceding the study period. June was the wettest month with 2 - 3 times the total monthly precipitation as previous months and July was the driest

month. The mean daily VPD throughout the study period was 1.2 kPa, with maximum rates observed in the month of August (VPD=1.6 kPa) (Figure 9).

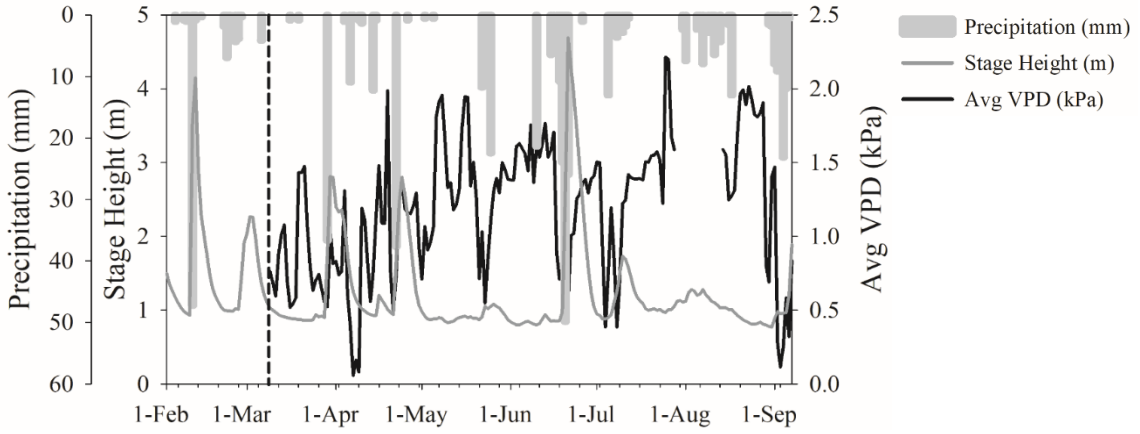

Figure 9. Daily total precipitation, daily average VPD and daily average stage height during the study period. Dashed line marks the beginning of the study.

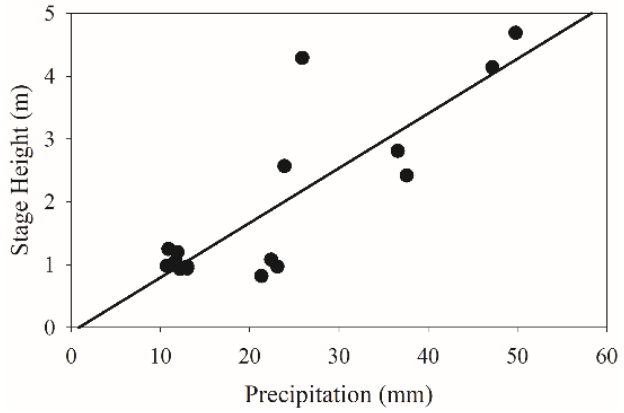

Figure 10. The relationship between precipitation and stage height recorded on the following day, when precipitation exceeded 10 mm/day (R^2=0.70; p < 0.001).

Sap flow across seasons

Sampled trees in the slough plot averaged 54% smaller in size as compared to the trees in the upland plot (Table 9). Consequently, daily tree water-use in the upland trees was much higher (100-400 kg day^{-1}) than in the slough trees (10-75 kg day^{-1}). Water-use

increased with DBH in the upland trees more strongly ($p<0.01$, $R^2=0.93$) as compared to that in the slough trees ($p<0.05$, $R^2=0.87$). Daily J_s was also higher in the upland trees (1200-2700 kg m^{-2} day^{-1}) as compared to the slough trees (700-1000 kg m^{-2} day^{-1}). However, DBH had no significant effect on daily J_s (Figure 11a). When daily total J_s was compared between individual trees, *Q. nigra* trees had the highest sap flux rates across seasons, followed by *F. pennsylvanica, Q. virginiana*, *Q. shumardi* and *T. sebifera*, respectively (Figure 11b). Overall, daily total J_s decreased in the summer for all individuals, except *Q. shumardi*, which suppressed J_s during early-spring.

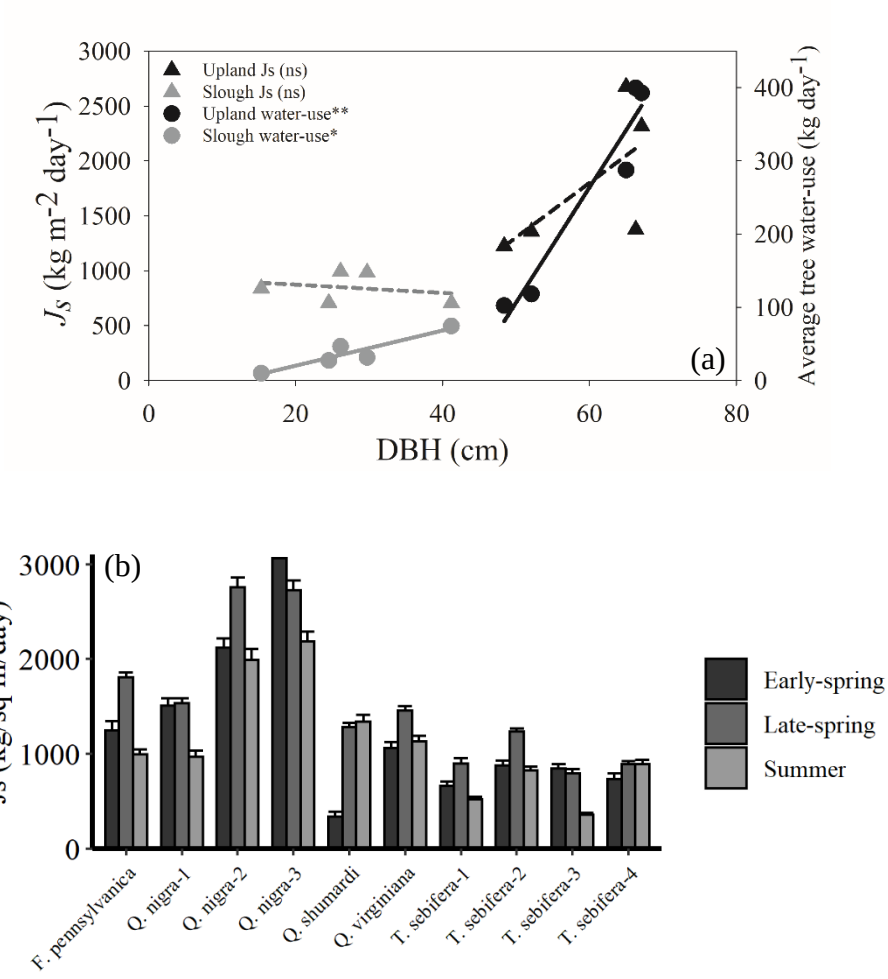

Figure 11. a) The relationship of tree DBH (cm) with daily total tree water-use (kg day^{-1}) and daily total J_s (kg m^{-2} day^{-1}) averaged over the entire study period. Upland tree water-use and J_s are represented by black circles and black triangles, respectively. Slough tree water-use and J_s are represented by grey circles and grey triangles, respectively. Significance levels labelled with **p<0.01, *p<0.05, and ns = non-significant (p>0.05). b) Seasonal daily total J_s of each individual tree.

Trees in the upland plot consistently had higher J_s per BA throughout the growing season (Figure 12,13). However, the difference in the estimated marginal mean daily J_s between the two plots declined as the growing season progressed, from 1107 ± 304 kg m^{-2} day^{-1} in early-spring (p > 0.05) to 1038 ± 304 kg m^{-2} day^{-1} in late-spring (p > 0.05) to

653 ± 305 kg m^{-2} day^{-1} in the summer ($p > 0.05$) (Figure 13). Daily J_s in the upland trees increased by 14% from early to late-spring ($p < 0.0001$) but declined by almost 27% in the summer ($p < 0.0001$) as soils dried out. Daily J_s in the slough plot was slightly more variable as it increased sharply by 43% in late-spring ($p < 0.0001$) with a smaller decline (17%) towards the summer ($p < 0.001$) (Figure 13).

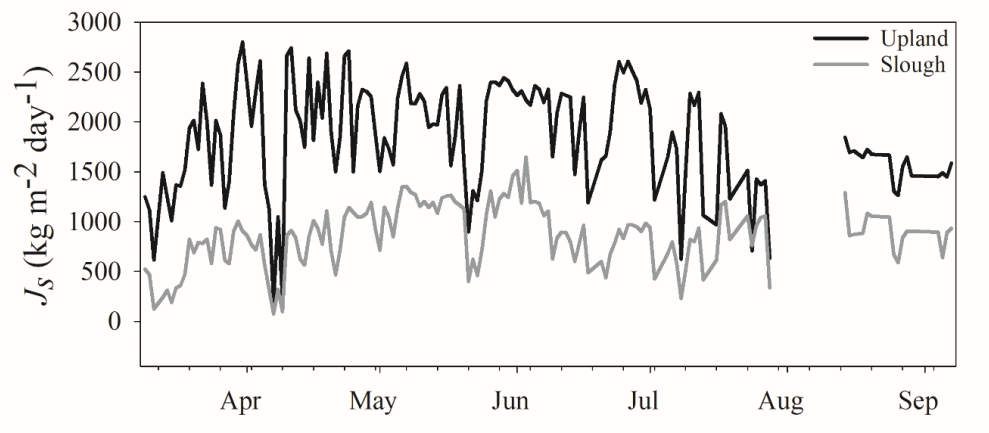

Figure 12. Variation in total daily J_s (kg m^{-2} day^{-1}) for the upland and slough plot for the entire study period.

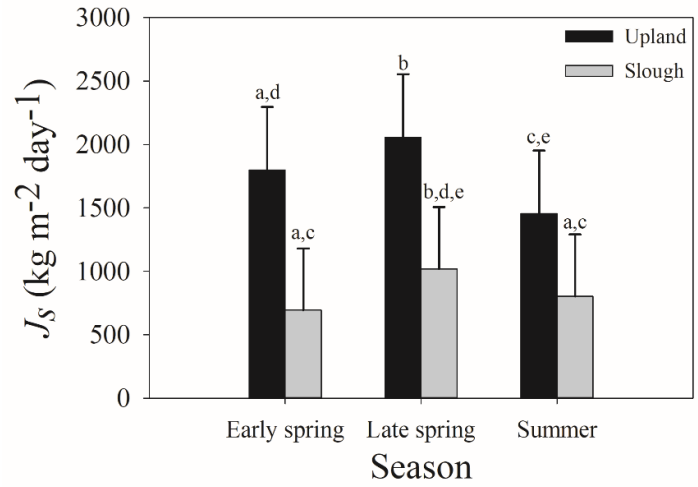

Figure 13. Comparison between estimated marginal mean daily J_s (kg m^{-2} day^{-1}) for the three seasonal periods (early-spring, late-spring and summer) and for the two plots calculated using two-way repeated measures ANOVA. Post-hoc analysis is denoted with letters and error bars indicate upper and lower limits at α=0.05.

Influence of vapor pressure deficit over J_s

As expected, throughout spring, sap flux rates in upland as well as slough trees increased strongly with VPD ($p < 0.0001$). VPD explained similar variability in J_s per BA in both the plots during this period (R^2=0.39-0.48; Figure 14a,b). However, in the summer, VPD had a much weaker effect on J_s as it explained only 12% variability in J_s in the slough trees ($p < 0.05$) (Figure 14b), while upland tree J_s showed no response to VPD (Figure 14a).

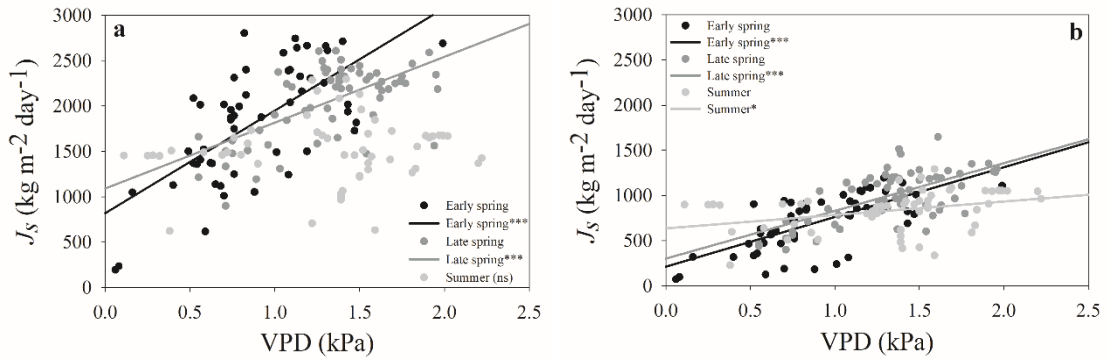

Figure 14. Relationship between total daily J_s (kg m^{-2} day^{-1}) and daily average VPD for the upland (a) and slough plot (b). Significance levels labelled with ***p<0.001, **p<0.01, *p<0.05, and ns = non-significant (p>0.05).

Combined effect of flooding and VPD on J_s

The three flood pulses that occurred during the study period caused waterlogging in the slough plot, but not in the upland plot. Although the upland plot was not directly waterlogged, the close proximity of the flooded patch to the upland plot can decrease the depth to groundwater. Therefore, although the upland trees are not usually inundated, these flood pulses can increase soil moisture availability in the root zone due to rising groundwater levels.

During the first two smaller flood pulses (i.e., stage height not exceeding 3 m), J_s increased with stage height. During the flood pulse in March, J_s increased with stage height in both plots, with stage height explaining more variability in J_s in the upland trees ($p < 0.01$; R^2=0.70) as compared to the inundated trees ($p < 0.05$; R^2=0.52) (Figure 15a). During the April flood pulse, the relationship between stage height and J_s weakened marginally in the upland trees as stage height explained 49% variability in J_s ($p < 0.05$), lower than that during the first flood pulse. In the slough trees, although the relationship remained positive, much less variability in J_s was explained by stage height ($p < 0.05$; R^2=0.38) (Figure 15b). During the larger flood pulse in June, in which stage height reached 4.7 m as compared to 2.8 m during the first two pulses, J_s in both the plots did not respond to changes in stage height. In both plots, J_s remained nearly constant until the stage height reached 3.5 m but indicated possible evidence of decline as stage height continued to rise up to 4.7 m (Figure 15c). Although stage height had a strong influence on J_s during the March flood pulse than VPD, VPD emerged as a stronger driver of J_s during the April and June flood pulses (Table 10).

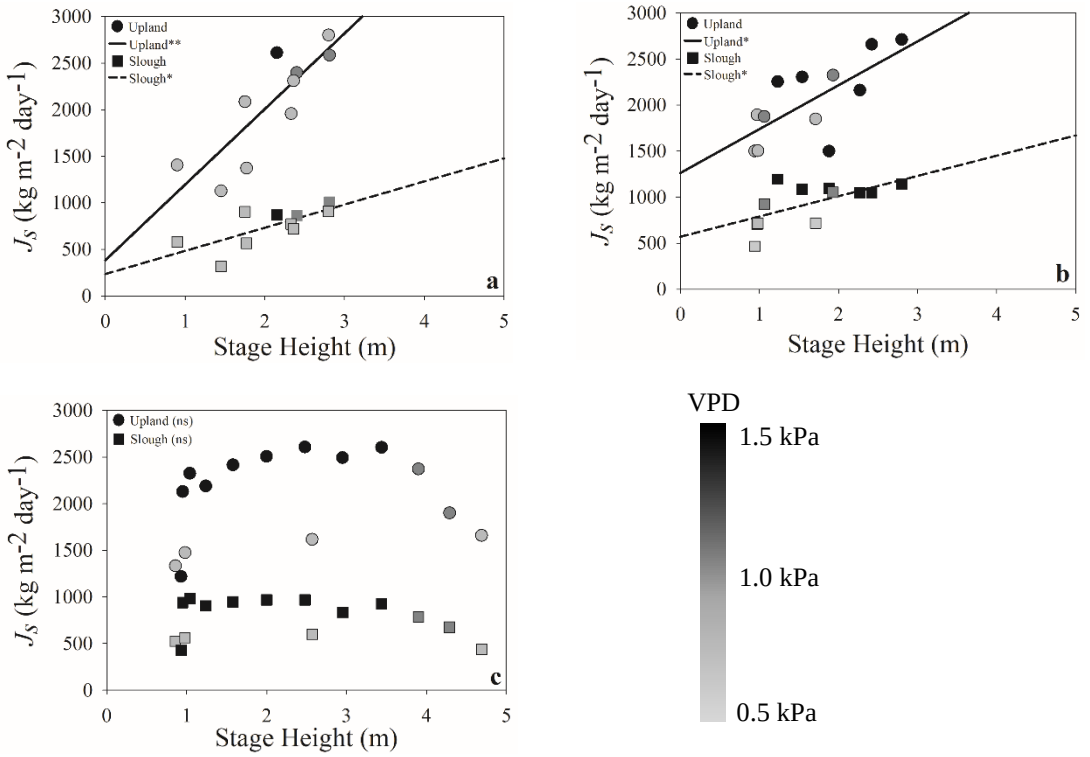

Figure 15. Relationship between total daily J_s (kg m^{-2} day^{-1}) and daily average stage height (m) during the March (a), April (b) and June (c) flood pulses. Upland plot is indicated by circles and slough plot by squares. Darker to lighter colored symbols indicate daily mean VPD (higher to lower, respectively). Significance levels labelled with **p<0.01, *p<0.05, and ns = non-significant (p>0.05).

Table 10. Pearson's correlation coefficients and regression results between daily total J_s and average daily VPD and average daily stage height during the three flood pulses.

Plot	Flood pulse	VPD			Stage Height		
		Pearson's r	p-value	R^2	Pearson's r	p-value	R^2
Upland	March	0.77	<0.01	0.59	0.84	<0.01	0.70
	April	0.78	<0.01	0.60	0.71	<0.05	0.49
	June	0.54	<0.05	0.29	0.23	ns	-
Slough	March	0.67	<0.05	0.45	0.72	<0.05	0.52
	April	0.97	<0.0001	0.95	0.62	<0.05	0.38
	June	0.68	<0.01	0.47	-0.12	ns	-

Comparison between native and invasive species

Over the entire study period, the J_s of Chinese tallow was only on average 23% less than that of the native wetland species ($p < 0.01$). The sap flux rates of native wetland species increased by 27% in late-spring ($p < 0.0001$) and declined by 27% in summer ($p < 0.0001$), eventually almost reaching their early-spring sap flux rates. Tallows displayed a similar trend but with a slightly more suppressed water-use later in the growing season as sap flux rates dropped by 31% in the summer as compared to late-spring ($p < 0.0001$) (Figure 16).

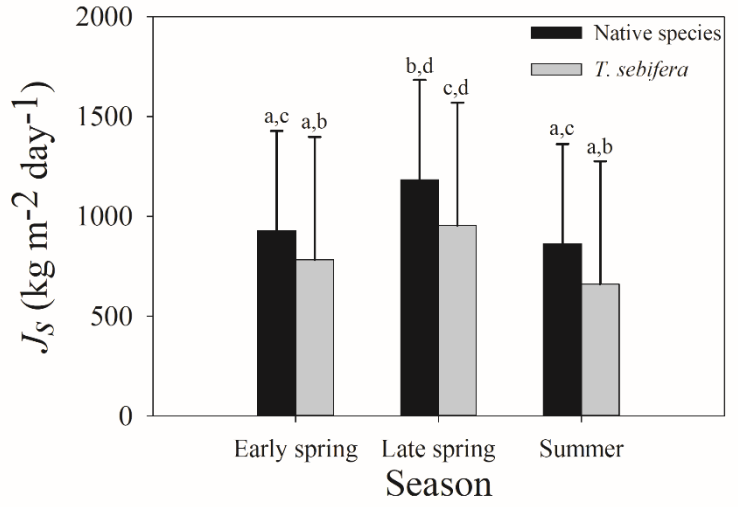

Figure 16. Comparison between estimated marginal mean daily J_s (kg m^{-2} day^{-1}) for the three seasonal periods (early-spring, late-spring and summer) and for different species (native wetland species and Chinese tallow) calculated using two-way repeated measures ANOVA. Post-hoc analysis is denoted with letters and error bars indicate upper and lower limits at α=0.05.

Discussion

Seasonal patterns of sap flow

We observed substantial differences between sap flux rates of trees growing in upland, non-flooded conditions and those growing with intermittent waterlogging throughout the growing season. At the onset of the growing season in early spring, contrary to our hypothesis, trees growing in the slough had a much lower J_s that was only about 40% of that in the upland trees. Two flood pulses occurred in the winter, right before the start of the growing season, supplying ample moisture to the upland trees while possibly waterlogging the slough trees. It has been commonly observed that lack of oxygen in the root zone and accumulation of phytotoxic compounds due to flooding can disrupt root functioning and water uptake (Kozlowski, 1997; Colmer and Greenway, 2005; Bailey-Serres and Colmer, 2014; Shabala et al., 2014). To counter these anaerobic conditions, flooded trees are known to delay their leaf-out (Broadfoot and Williston, 1973) and maintain low water-use (Pezeshki, 1993; Else et al., 2009) until conditions become favorable in the root zone. Root respiration and water uptake resume with the recession of flood waters as oxygen availability in the root zone and belowground tissues increases, and accumulated phytotoxic compounds dissipate, resulting in favorable conditions (Crawford, 1982; Kozlowski and Pallardy, 1984; Kozlowski, 2002). This is evident from our observations in late-spring as daily sap flux rates in the flooded trees increased by 326 kg m^{-2} on an average. By late-spring, two flood pulses had occurred, again saturating the soils in the slough. Despite, these saturated conditions, sap flux rates in the flooded trees continued to rise as days got warmer.

We observed a similar pronounced decline in sap flux rates in both plots in the summer. It is important to note that even in a wetland forest, soil moisture can become limiting as increasing temperatures and atmospheric dryness induce soil evaporation, resulting in suppression of plant water uptake, especially during the summer. This conflicts with prior studies showing water limitations only during extreme droughts (Middleton and Kleinebecker, 2012). However, it has been commonly observed in wetlands around the world that drought-like conditions can rapidly develop after dry spells or if hydrologic connectivity of the wetland is disrupted (Parolin, 2001; Dewey et al., 2006). Despite a major flood pulse in June, trees in both upland and slough areas were unable to sustain their sap flux rates in the summer, likely due to high VPD rates. This demonstrates the speed with which conditions can transition from waterlogged to moisture deficient even in wetland environments.

Sap flow response to flooding and atmospheric dryness

Wetland plants have been observed to respond to short-term flood pulses in different manners. In some cases, inundation caused by flooding is beneficial to vegetation (Mitsch et al., 1991), whereas, it is detrimental in others (Parolin and Wittmann, 2010). These effects are variable across species (Voesenek et al., 2004; Allen et al., 2016), environmental and topographic conditions (Megonigal et al., 1997; Allen et al., 2016), frequency and severity of flooding (Kreuzwieser and Rennenberg, 2014), among others. We observed a pronounced rise in sap flux rates following moderate early-spring flood pulses in both upland and slough trees. Sap flux continued to increase with stage height under early-spring conditions until a very large flood in late spring. This suggests a

threshold of flood tolerance in these trees, beyond which they exhibit stressful response to hypoxic conditions. Surprisingly, sap flux in the upland trees also declined during the flood pulse. Likely, the sensitivity of these trees to both atmospheric dryness and soil saturation explains this trend.

VPD is known to be a strong driver of sap flow (Ewers et al., 2002; Bovard et al., 2005; Adelman et al., 2008), especially when soil moisture is not limited (Oren and Pataki, 2001). Consequently, in the spring, we observed an increase in J_s with VPD in both the plots, with the relationship being almost equally strong. However, in the summer, with increasingly dry conditions, trees in the upland plot stopped responding to VPD, which possibly indicates stomatal closure to prevent excessive water loss. In the summer, slough trees had a weaker response to VPD than in spring. Such reductions in J_s could be due to the adaptation of these trees to prolonged saturated soil conditions, which results in reduced stomatal conductance in response to small decline in soil moisture. Decline in J_s in response to slightly reduced soil water reserves has been observed in old-growth temperate forests (Hölscher et al., 2005) but the relationship is largely unexplored in wetland forests.

Water-use strategy by the invasive Chinese tallow

Invasive species are usually known to aggressively outcompete native vegetation for water (Cavaleri and Sack, 2010). Chinese tallow is known to be extremely flood tolerant (Jones and Sharitz, 1990; Gabler and Siemann, 2013); therefore, we had hypothesized that tallows that occur in the slough at our study site will consistently have higher J_s than the native wetland species. However, despite having a larger sapwood area

to basal area ratio, tallow sap flux rates were marginally lower than the native species. It should also be noted that most invasive tallow trees in this patch were younger and smaller in size (7% of total basal area) as compared to the native trees. This relative size difference may explain lower J_s and water-use in tallows, but the potential for water use to surpass that of natives when tallow trees grow to maturity remains uncertain. Additionally, tallows grow densely in wetland forests and riparian zones, constituting nearly half of the stand density, relative frequency and basal area in some regions (Jubinsky, 1995). Therefore, as their abundance and basal area increases, tallow invasion may hold the potential to alter water balance in this region by significantly increasing the amount of transpired water in these already drying wetlands (Dahl and Allford, 1996). Tallow water-use declined more sharply in the summer than native species, indicating lower drought tolerance. This study provides the first estimates of Chinese tallow sap flux rates relative to native wetland trees.

Conclusion

This study provides a better understanding of the variability in plant water-use response to climatic as well as edaphic drying and wetting. Intermittent flooding in wetland forests is critical for ecosystem functioning; however, anthropogenic pressure and hydroclimatic changes are leading to severe alterations to the hydrology of these ecosystems, eventually resulting in shrinking habitats and drying of wetlands. Columbia Bottomlands represent the state of such disturbed wetlands across the southeastern United States. Our results provide evidence that intermittent flooding and waterlogging can put vegetation under short-term stress caused by hypoxic conditions, resulting in a lower

water-use when trees are flooded. The timing of this waterlogging is important as sap flux rates recover when flooding recedes. Although upland trees don't undergo this stress, they experience substantial drought-like stress in the summer as conditions get drier. The magnitude of flood pulses is critical, although VPD emerges as the dominant driver of sap flow. Lastly, we provide novel evidence that the invasive Chinese tallow tree could be a moderately conservative water-user as compared to native wetland species, although this may only be the case for smaller tree-sizes and lower density stands. The potential for this invasive species to alter the transpiration component in the water balance in wetland forests deserves further study. Our estimates can help understand plant-water relations better in this dynamic system and aid management and conservation decisions under changing hydroclimatic conditions and species invasions.

CHAPTER IV

NITROGEN CYCLING AND RETENTION IN A BOTTOMLAND HARDWOOD FOREST WITH ELEVATED N DEPOSITION

Synopsis

N deposition is a major concern in ecosystems across the globe, with potential impacts on biodiversity, primary production, and biogeochemical processes. Despite some progress in reducing N deposition in the US, many areas still receive high levels of deposition from anthropogenic sources. Bottomland hardwood forests (BHFs) along the Texas Gulf coast occur in close proximity to reactive N (N_r) emission sources such as petroleum refineries and croplands. We quantified total N deposition of nitrate and ammonium using ion exchange resin collectors, and soil and plant N pools and their $\delta^{15}N$ values to assess the effect of deposition from a refinery and other non-point sources on N cycling and retention in a BHF. We aimed to: (i) estimate the amount and chemical composition of atmospheric inorganic-N deposition at 3 sites increasingly distant from the refinery, (ii) investigate the historic trend of plant N uptake in response to 8 decades of elevated deposition using tree-ring N concentration and $\delta^{15}N$ values, and (iii) understand the underlying processes by which N is partitioned through this ecosystem by comparing $\delta^{15}N$ values of deposition, plant tissues, and soils. Overall, wet N deposition across the landscape was 3.2–3.6 times higher than the national average, highest near the refinery, and dominated by NH_4^+-N. The higher proportion of NH_4^+-N in deposition was strongly reflected in the soil inorganic N pool. Soil $\delta^{15}N$ values were affected by NH_4^+-N

concentration, suggesting the control of NH_4^+-N deposition over soil N cycling. Tree ring $\delta^{15}N$ values were distinctly lower in trees closest to the refinery, indicative of an anthropogenic source. Tree-ring N concentration and basal area increment trends were strongly correlated and both measurements increased dramatically with increase in refinery emissions, suggesting a fertilizing effect due to N deposition. Despite exposure to anthropogenic N deposition for several decades, trees in this region did not show signs of N saturation such as a decline in N absorption or growth over time, indicating N retention capacity of these BHFs. Although long-term input and uptake of inorganic N can accelerate N losses from the system and deteriorate environmental conditions, results suggest that these BHFs are currently strong sinks for N_r that remove large quantities of anthropogenic N emissions.

Introduction

Deposition of inorganic N from anthropogenic sources increases the input of reactive N in an ecosystem in addition to N fixation, which is the primary process through which atmospheric N_2 gets assimilated in ecosystems. Atmospheric deposition of N is a rising concern in the US, China, Brazil, India and Greece among others (Decina et al., 2020). Currently, about 94 Tg yr^{-1} inorganic N is deposited on terrestrial ecosystems (Ackerman et al., 2019), of which 60% is of anthropogenic origin (Kanakidou et al., 2016), which is estimated to be at least three times as compared to the pre-industrial era (Holland et al., 1999; Galloway et al., 2004; Fowler et al., 2013). Atmospheric N contains reactive compounds such as NH_x (NH_3 + NH_4^+), NO_y (NO_x + NO_z) and soluble and insoluble

organic N. However, the most commonly found compounds in anthropogenic N deposition are NO_3^-, HNO_3, NH_3 and NH_4^+ (Galloway et al., 2004). While the chemical composition of anthropogenic N deposition varies spatially by a large extent, it depends on the source such as agricultural activities, vehicular emissions, petrochemical refineries, coal-based power plants, etc. (Holland et al., 2005; Paulot et al., 2013; Du et al., 2014). Over much of the 20th century, oxidized N compounds were the dominant form of N deposition (Galloway et al., 2004; Kanakidou et al., 2016; Li et al., 2016). Therefore, the majority of our knowledge and understanding of ecosystem response to N deposition is based on how excessive oxidized N compounds get cycled through ecosystems. Using an atmospheric chemistry-transport model, Kanakidou et al. (2016) predicted that future amounts of oxidized N compounds in deposition will decrease relative to 20th century trends, but will be offset by an increase in deposition of reduced N compounds. This shift is already being observed in field measurements as Du et al. (2014) and Li et al. (2016) estimated the contribution of reduced N in deposition to be 60-65%. With reduced N compounds expected to dominate the composition of N deposition, a significant knowledge gap exists on the understanding of ecosystem response to this changing chemical composition of N deposition.

Natural ecosystems, especially forests, are known to retain N from atmospheric deposition and act as sinks for excessive anthropogenic N pollution (Nowak et al., 2006; Mayer et al., 2007). Forests can act as filters to combat N pollution through retention in soils as well as plants. Forest soils can rapidly transform N compounds into forms available for plant uptake or immobilize significant amounts of N depending on existing

nutrient and climatic conditions, while vegetation can absorb and metabolize inorganic and dissolved organic N (DON) through both root and foliar uptake. The most proven examples of air pollution removal by natural ecosystems originate from urban and riparian forests. Urban forest remnants have been documented to remove N air pollution removal across the globe (Nowak et al., 2006; Yin et al., 2011; Rao et al., 2014; García-Gómez et al., 2016). In these fragmented forest patches, two major mechanisms have been observed to effectively remove N-pollution from mainly dry deposition: interception of N deposition on canopy surfaces and stomatal absorption of gases such as NO and NO_2 (Smith, 1990; Nowak, 1994; Beckett et al., 1998). Peri-urban forests that occur in the transition zones between urban and rural areas receive larger proportions of N deposition from urban as well rural sources (mainly agriculture) and have been found to be even more effective sinks of excessive atmospheric N (García-Gómez et al., 2016). Riparian forests, on the other hand, remove N pollutants via different mechanisms such as retention in soils and plant uptake through roots, which enables them to retain dry as well as wet N deposition (Lowrance et al., 1997; Verhoeven et al., 2006; Mayer et al., 2007). Riparian buffers are also known to effectively trap N compounds (mainly NO_3^-) from run-off and leachate while acting as filters for vital water sources such as rivers, streams and groundwater (Lowrance, 1992; Haycock and Burt, 1993; Lowrance et al., 2000; 2005). Therefore, riparian forests located in exurban or peri-urban areas have an even greater potential of removing large quantities of N pollution through a combination of retention mechanisms.

Although N compounds such as NH_4^+, NO_3^- and DON are readily absorbed by vegetation (Chapin et al., 2002) and utilized to increase primary productivity as a result of a fertilizing effect (Thomas et al., 2010; De Vries et al., 2014), excessive amounts can cause nutrient imbalance in plants as well as soils (Aber et al., 1989; De Vries et al., 2006). Under initial low N conditions, deposition of most reactive N compounds has positive impacts on forest ecosystems, such as increase in plant growth and soil microbial biomass and activity (Aber et al., 1989; 1998). However, excessive amounts can alter species composition (Stevens et al., 2004; Bobbink et al., 2010), disrupt microbial functioning and reduce mineralization and nitrification rates (Lovett and Rueth, 1999; Carreiro et al., 2000; Frey et al., 2004), increase N loss through leaching (Fang et al., 2009; Gundersen et al., 2011), runoff and denitrification (Gundersen et al., 1998; Fenn et al., 2003a; van Groenigen et al., 2015), cause soil acidification (Wallace et al., 2007), eutrophication (Bouwman et al., 2002; Rhodes et al., 2017) and eventually lead to plant mortality in extreme cases (Aber et al., 1998; Magill et al., 2000; Lovett and Goodale, 2011).

The natural isotopic composition of N in soils and plant tissues can provide insights regarding their roles in the N cycle. The heavier stable isotope, ^{15}N, which makes up less than 0.4% of naturally occurring N, is usually discriminated against when N gets transformed from one form to another (Craine et al., 2015; Denk et al., 2017; Chalk et al., 2019). Isotopically lighter N is more readily fixed and mineralized by microbes, absorbed by plants, dissolved in water and is easily lost in the form of leaching and gaseous emissions (Chapin et al., 2012). This preferential transformation of isotopically lighter N is called fractionation. Therefore, the ratio of $^{15}N/^{14}N$ (denoted as $\delta^{15}N$ with respect to

atmospheric N_2) in soil profiles and plant tissues indicates the rate at which N is retained, cycled and lost from the system (Högberg, 1997).

In forest ecosystems, isotopic fractionation of N occurs through three major pathways simultaneously in soils, roots, plants and at the soil-water interface (Robinson, 2001; Kolb and Evans, 2002; Bustamante et al., 2004; Craine et al., 2015): denitrification, nitrification, and transfer during mycorrhizal absorption. Denitrification causes the highest fractionation of N is during gaseous N loss to the atmosphere in the form of NO, N_2O and N_2 but also as a by-product of nitrification (Houlton et al., 2006). Nitrification occurs when NH_4^+ is oxidized to NO_2^- and subsequently NO_3^-. As a result, NO_3^- formed at the end of this process has a substantially lower $\delta^{15}N$ and the $\delta^{15}N$ signature of residual NH_4^+ gets heavier in the soil (Högberg, 1997; Spoelstra et al., 2007). Both of these pathways are microbially driven. Therefore, conditions that favor microbial activity such as higher soil moisture and temperature, accelerate N fractionation in soil (Handley et al., 1999; Martinelli et al., 1999; Amundson et al., 2003; Bai et al., 2012). The third major fractionation pathway is the transfer of N from mycorrhizal fungi to plant roots, during which fungi transport isotopically lighter N to the roots (Craine et al., 2009; Hobbie and Högberg, 2012). Additionally, fixation, preferential uptake of NH_4^+, leaching, and runoff are known to influence fractionation to varying degrees in some ecosystems (Yoneyama et al., 1991; Pennock et al., 1996; Yoneyama et al., 2001; Sra et al., 2004; Craine et al., 2015).

Tree-rings indicate past annual or sub-annual incremental tree growth rates, and their isotopic composition provides a retrospective insight on past nutrient cycling rates in

the ecosystem. By analyzing $\delta^{15}N$ values of precisely dated tree-rings, the N status of an ecosystem can be tracked through time and future trends can be predicted. Studying tree-ring $\delta^{15}N$ provides a wide spatial coverage over a long temporal scale and this isotopic signal is a direct indication of plant N uptake and soil N status (Gerhart and McLauchlan, 2014). Tree-ring $\delta^{15}N$ chronologies can also be compared to past climatic conditions such as precipitation and temperature and proximal anthropogenic drivers like fertilizer application, vehicular emissions, emissions from refineries and power plants, non-point pollution sources, etc. However, $\delta^{15}N$ signatures of N emissions from these sources are not consistent and can vary significantly (>20 ‰) (Savard et al., 2017). Dry and wet deposition also have varying $\delta^{15}N$ values as atmospheric reactions of N with water and water vapor modify the isotopic composition of deposited N (Heaton et al., 1997; Elliott et al., 2009; Mara et al., 2009). Therefore, deposited and tree-ring N can sometimes have a significantly different $\delta^{15}N$ value relative to the pollution source. Usually, tree-ring $\delta^{15}N$ values range from -8 to 4 ‰, but in forests affected by anthropogenic N deposition, they have been found to range from -13 to 13 ‰ (Gerhart and McLauchlan, 2014).

Over the last two decades, numerous studies have been conducted to investigate the effect of reactive N pollution on forest ecosystems using tree-ring $\delta^{15}N$ (Saurer et al., 2004; Battipaglia et al., 2009; Guerrieri et al., 2009; Sun et al., 2010; Leonelli et al., 2012; Jung et al., 2013). The most pioneering study was conducted by Saurer et al. (2004) in which NO_x from vehicular emissions were detected for the first time in tree-rings and a mixing model was used to calculate the $\delta^{15}N$ of deposited reactive N using soil and tree-ring $\delta^{15}N$. Theoretically, in trees growing under the long-term effect of continual pollution,

tree-ring $\delta^{15}N$ is expected to indicate a consistent increase or decrease over time, depending on the chemical nature of the pollutants. However, this does not hold true in practice as tree-ring $\delta^{15}N$ studies focused on inferring pollution effects on forest N cycling have observed varying trends. Saurer et al. (2004) observed an increase in tree-ring $\delta^{15}N$ in response to vehicular emissions and Guerrieri et al. (2009) also observed an increase in response to emissions from a petroleum refinery. Contrastingly, tree-ring $\delta^{15}N$ chronologies indicated a decreasing trend under the effect of vehicular pollution (Leonelli et al., 2012) and ceramic industries (Sun et al., 2010), while emissions from vehicles (Battipaglia et al., 2009) and oil sands mining (Jung et al., 2013) had no effect on tree-ring $\delta^{15}N$.

In this study, we used plant and soil $\delta^{15}N$ along with deposition measurements to understand the effect of excessive anthropogenic N deposition on the N status of a bottomland hardwood forest in Texas, USA. Our objectives were to (i) estimate the amount of atmospheric N deposition at three sites at increasing distances from a point source (petroleum refinery) and assess the chemical and isotopic composition of deposited N, (ii) investigate the historic trend of N cycling in the forest under the effect of eight decades of anthropogenic N deposition using tree-ring $\delta^{15}N$ and N concentration chronologies, and (iii) understand the underlying processes by which N is fractionated through this ecosystem by comparing deposition, wood, leaf, litter and soil $\delta^{15}N$. We hypothesized that the amount of N deposition will be subsequently lower at sites farther from the refinery. Isotopically depleted NH_4^+-N was expected to be the major component of N deposition owing to the large NH_3 gas emissions from the refinery. As continual

long-term N deposition increases the amount of inorganic N in an ecosystem, which in turn accelerates soil N cycling and plant N uptake rates, we hypothesized that the tree-ring $\delta^{15}N$ chronologies will show a declining trend over time, however, the decline will be steeper at the site closest to the refinery. Tree-ring N concentration and basal area increment (BAI) were expected to increase over a few decades of deposition as initial low N conditions promote plant N uptake and growth but a flatter trend was expected later in the chronology as the forest would approach N saturation due to excessive inputs. We hypothesized that plant $\delta^{15}N$ will be lower as compared to soil $\delta^{15}N$ due to fractionation during uptake but expected the difference in plant and soil $\delta^{15}N$ to be higher at the site closest to the refinery. As soil moisture drives microbial N transformation, soil water content was expected to increase soil $\delta^{15}N$ values due to the loss of isotopically lighter N caused by nitrification and denitrification. Lastly, we expected foliar $\delta^{15}N$ to be slightly depleted as compared to wood $\delta^{15}N$ as has been documented previously (Pardo et al., 2013).

Methods

Study area

Columbia bottomland hardwood forests are a part of the San Bernard National Wildlife Refuge, Texas, USA. The refuge spans over Brazoria, Matagorda and Fort Bend counties on the Gulf coast of Texas, about 40 km southwest of the Houston Metropolitan Area. The 54,000-acre refuge extends 150 km from the coast to inland as the habitat transitions from salt water marshes to freshwater marshes and eventually into mixed

bottomland hardwood forests. This floodplain ecosystem is formed as the Colorado, San Bernard and Brazos Rivers flow into the Gulf of Mexico. The bottomland hardwood forests mainly occur along these rivers and their smaller streams and bayous. The climate is humid subtropical (Koppen, 1900) and the region receives a mean annual rainfall of 1143 mm, with an average relative humidity of ~70% and the mean temperature is approximately 20 °C (NOAA, 2018a).

The study was conducted at three sites located within the Columbia bottomlands. The sites are situated along a 25-km transect in the downwind direction (northwest) of the Phillips 66 Sweeny Refinery, which is the 18th largest petroleum refinery in the US and among the top 100 largest refineries in the world (OGJ, 2019). Established in 1942, the refinery processes about 256,000 barrels of crude oil per day and emits about 16,300 kg of ammonia annually (USEPA, 2020). The sites, namely Dance Bayou (DB), Big Pond (BP) and Buffalo Creek (BC) are located at distances of 5, 13 and 29 km from the refinery, respectively. Due to topographical differences and proximity to a major stream, site DB floods more frequently as compared to BP and BC. Soils in this region are mainly vertisols and alfisols dominated by clay, loam and sandy loam texture. The soils series include Aris fine sandy loam, Bacliff clay, Edna loam, Leton loam, Pledger Clay and Churnabog clay (NRCS, 2020). The most dominant vegetation in these forests include *Quercus nigra* L. (water oak), *Quercus virginiana* Mill. (live oak), *Celtis laevigata* Willd. (sugarberry) and *Triadica sebifera* (L.) Small (Chinese tallow) which account for 32%, 15%, 15% and 12% of the basal area, respectively (Cross et al., in preparation).

Nitrogen deposition

Total deposition of NH_4^+-N and NO_3^--N was measured using ion exchange resin (IER) columns (Fenn and Poth, 2004). Four IER columns were installed at each of the three sites on September 12, 2018 and replaced on March 20, 2019. The columns were installed in pairs with one column placed under the canopy and another one in the nearest clearing to capture throughfall and bulk deposition, respectively. Two pairs of columns (a total of 4 columns) were installed at each site to capture spatial variability. The column pairs were installed at a distance of at least 400 m from each other and were used as sampling locations for tree cores, leaf tissue, litter and soil. The IER columns were prepared by filling a 36 cm long and 1.27 cm diameter PVC tube with 35 g Amberlite IRN150 mixed-bed IER, which is a mixture of Amberlite IRN77 cation exchange resin and IRN78 anion exchange resin. Every PVC tube was sealed with polyester fiber on both ends, a drain cap was fitted at the bottom as an outlet for rainwater and a 10 cm diameter funnel was attached at the top to capture precipitation. The columns were exposed for six months and replaced once over a one-year period (November 2018-2019). After the exposure, the columns were extracted to recover NH_4^+-N and NO_3^--N using 400 ml 2M KCl solution. NO_3^--N concentrations were estimated using the Cd reduction method at 543 nm (American Society for Testing Materials, 1987) and NH_4^+-N concentrations were estimated using the phenate method at 640 nm (Parsons et al., 1984). Total deposition of NO_3^--N and NH_4^+-N per land area (kg/ha) as bulk deposition and throughfall were calculated by determining the amount of each ion collected in a column and the surface area of the funnel opening. The amount of N deposition intercepted by the canopy was

calculated as the difference between the amount of bulk deposition and throughfall. Site-level measurements were obtained by averaging deposition captured by multiple columns at each site.

Tree core sampling, $\delta^{15}N$ and N concentration analyses

Six *Q. nigra* trees were sampled at each site in October-November 2019. Healthy, mature individuals with no obvious injuries like cavities, scars or diseases were selected. Preference was given to trees with larger diameters at breast height (>40 cm) and uniform girth (Stokes and Smiley, 1968). We ensured that each core reached the pith of the tree. Dendrochronological analysis of these trees including dating, ring-width measurement and $\delta^{13}C$ estimation was already conducted during a previous study (Deshpande et al., 2020), and we sampled the same trees for $\delta^{15}N$ analysis. The inside-out method (Biondi, 1999) from the dplR dendrochronology program library in R (Bunn et al., 2020) was used to calculate basal area increment (BAI) from raw ring-width measurements from each tree (Deshpande et al., 2020) and site-level mean BAI was calculated. For tree-ring $\delta^{15}N$ and N concentration measurements, the cores were dried to constant weight at 60 ^{o}C and hand-sanded using a sandpaper (220 grit) to enhance ring-visibility. After visually crossdating each core, two-year ring composites were extracted from the outermost ring (2019) up to the pith. Each sample was ground and tree-ring $\delta^{15}N$ and N concentration was analyzed using a Costech ECS 4010 elemental analyzer (Costech Analytical Technologies, Valencia, CA, USA) interfaced with a Delta V Advantage isotope ratio mass spectrometer (Delta V, ThermoFisher Scientific, Waltham, MA, USA) operating in continuous flow mode in the Stable Isotopes for Biosphere Science (SIBS) Lab, Texas A&M University

(College Station, TX, USA). Tree-ring $\delta^{15}N$ was expressed in δ notation using the following equation:

$$\delta^{15}N\ (‰) = \left[\frac{R_{SAMPLE} - R_{STD}}{R_{STD}}\right] * 10^3 \quad (4)$$

Where, R_{SAMPLE} is the $^{15}N/^{14}N$ ratio of the tree-ring sample and R_{STD} is the $^{15}N/^{14}N$ ratio of the standard (atmospheric N_2) (Mariotti, 1983).

Leaf and litter sampling and $\delta^{15}N$ analyses

Leaf and litter samples were collected on October 26, 2019 from two sampling locations at each site from within a 10 m radius around the IER column pairs. At each location, four leaf samples from *Q. nigra* trees each weighing at least 200 g were collected from a height of 3-3.5 m using a pole pruner. Similar amount of eight pooled litter samples (bottomland oak species) were collected from under the same trees. All eight leaf and litter samples from each site were dried to constant weight at 60 ^oC and pulverized using a ball mill (Retsch Oscillating Mixer Mill MM400). $\delta^{15}N$ and N concentration were measured on these samples was conducted using the same procedure mentioned above.

Soil sampling

From each sampling location, four 50 cm deep soil cores were extracted on October 26, 2019 and sub-divided into five depth increments (0-10, 10-20, 20-30, 30-40 and 40-50 cm). Of the eight soil cores collected from each site, four cores were dried at 60 ^oC and used for $\delta^{15}N$ analysis, while the remaining four cores were used for NH_4^+-N and NO_3^--N estimation.

Soil $\delta^{15}N$, N concentration, NH_4^+-N/NO_3^--N estimation

Half of the total soil cores collected were dried, passed through a 2 mm sieve to remove coarse organic matter and were used for $\delta^{15}N$ and N concentration analysis conducted using the same procedure mentioned above. The other half were kept field moist and inorganic-N was extracted from each incremental sample within 36 hours of sampling. Inorganic-N was extracted by shaking 15 g of soil sample with 50 ml 2M KCl for 1 hour. The solution was then filtered over pre-leached (2M KCl) #40 Whatman filter paper. The extractant was used to estimate NO_3^--N concentrations using the Cd reduction method at 543 nm (American Society for Testing Materials, 1987) and NH_4^+-N concentrations were estimated using the phenate method at 640 nm (Parsons et al., 1984).

$\delta^{15}N$ of deposited N

A two-end member isotopic mixing model proposed by Saurer et al. (2004) was used to estimate the $\delta^{15}N$ value of deposited N at the three sites. In this mixing model, $\delta^{15}N$ value of deposited N is calculated using $\delta^{15}N$ values of tree-rings and soil. We used soil $\delta^{15}N$ values from all depth increments to get a range of $\delta^{15}N$ values of deposited N. The model assumes that tree-ring $\delta^{15}N$ is a reflection of two sources: background N from soil and N from deposition. The model is represented as:

$$\delta^{15}N_{tree-ring} = (\delta^{15}N_{background} - \delta^{15}N_{emission})N_{tree-ring}N_{background} + \delta^{15}N_{emission} \quad (5)$$

where, $\delta^{15}N_{tree\text{-}ring}$ = $\delta^{15}N$ value of tree-ring from the corresponding year; $\delta^{15}N_{background}$ = soil $\delta^{15}N$ value; $\delta^{15}N_{emission}$ = $\delta^{15}N$ value of deposited N; $N_{tree\text{-}ring}$ = N concentration in tree-ring; $N_{background}$ = N concentration in soil.

Statistical analyses

To evaluate differences in mean tree-ring $\delta^{15}N$ values between sites, we used one-way ANOVA. Levene's test was used to check for equal variances, normality was tested using Shapiro-Wilk test and post-hoc analysis was conducted using Tukey HSD. We used the same statistical approach to differences in mean $\delta^{15}N$ values of soil, wood, leaves and litter samples from 2019. $\delta^{15}N$ values were separated site-wise during this analysis.

Results

Nitrogen deposition

Total deposition of inorganic-N was marginally higher (~11%) at the site closest to the refinery as compared to the other two sites, but overall, 3.5 times higher than the national average. Total inorganic-N deposition at the closest site, DB, was 12.8 ± 0.02 kg/ha/yr, while 11.5 ± 0.4 kg/ha/yr and 11.4 ± 0.5 kg/ha/yr inorganic-N deposition was recorded at sites BP and BC, respectively (Fig. 17). NH_4^+-N was the major form of inorganic-N in deposition, irrespective of distance from the refinery. Total inorganic-N deposition composed of 87% NH_4^+-N at site DB and 95% at BP and BC. The modeled $\delta^{15}N$ signature of N in total deposition increased with distance from the refinery. Site DB had the lightest total deposition $\delta^{15}N$ signature (mean 2.01 ± 1.5 ‰), while sites BP (mean 3.56 ± 0.29 ‰) and BC (mean 5.51 ± 0.31 ‰) had higher $\delta^{15}N$ values (Fig. 17). Canopy interception of deposited N varied from 48–68% across sites, and NH_4^+-N and NO_3^--N were intercepted in similar proportions (~50% each).

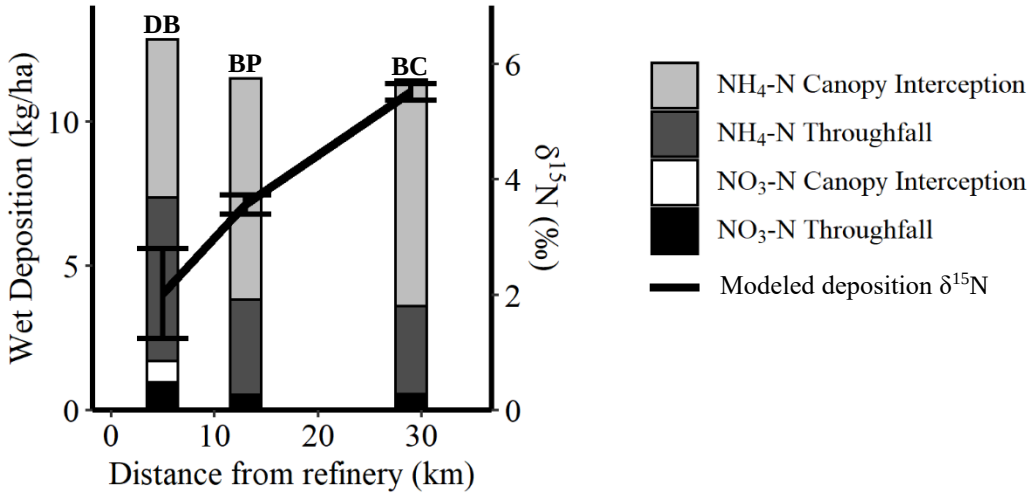

Figure 17. Total deposition of inorganic-N (NH_4^+-N and NO_3^--N) (kg/ha) at the three sites. Shaded bars indicate the amount of NH_4^+-N and NO_3^--N intercepted by the canopy and the amount reaching the forest floor via throughfall. Black line represents the mean modeled $\delta^{15}N$ of deposited N using the isotopic mixing model. Error bars on the black line represent the variation in modeled $\delta^{15}N$ of deposited N caused by varying $\delta^{15}N$ values and N concentration in tree-rings and soil depth intervals.

Soil N concentration, NH_4^+-N, NO_3^--N and $\delta^{15}N$

The concentration of soil NH_4^+-N with respect to NO_3^--N was about five times greater at all the three sites. Average concentrations of NH_4^+-N and NO_3^--N were similar across the three sites (Fig. 18). Across all the three sites, soil $\delta^{15}N$ values were lower in the top 10 cm soil, ranging from 4.5–6.3 ‰ (Fig. 19 a,b,c). Beyond 10 cm, $\delta^{15}N$ values increased by about 2–2.5 ‰ and remained consistent up to 50 cm depth within an average range of 6.8–7.9 ‰. N concentration had an opposite trend as N concentrations were highest in the top 10 cm soil (2-3 g N/kg soil) and decreased beyond 10 cm, while remaining constant up to 50 cm depth (Fig. 19 a,b,c). Soil NH_4^+-N and NO_3^--N

concentrations had similar declining trends with depth, except at site BC, where NO_3^--N remained constant throughout the 50 cm soil profile (Fig. 19 d,e,f).

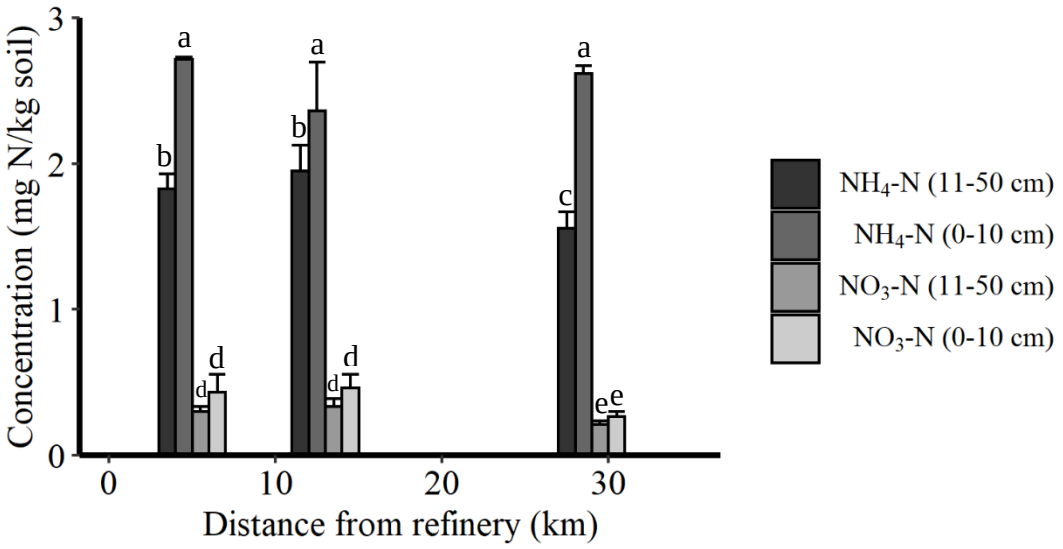

Figure 18. Average concentration of NH_4^+-N and NO_3^--N (mg N/kg soil) in soils at the three sites represented as their respective distances from the refinery (DB: 5 km, BP: 13 km, BC: 29 km). Tukey HSD is denoted with letters, and standard error bars indicate categories with significance differences, as indicated by ANOVA ($p<0.05$).

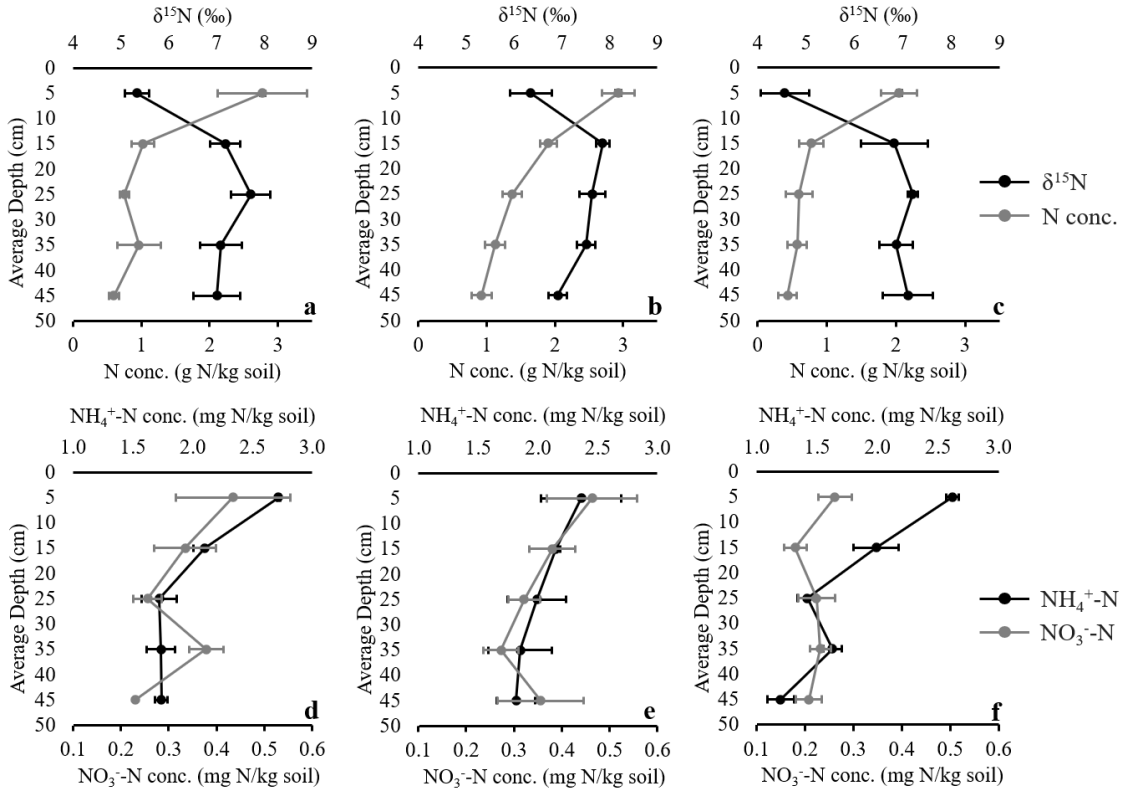

Figure 19. Soil $\delta^{15}N$ values (‰) and total N concentration (g N/kg soil) across the top 50 cm soil profile at the three sites DB (a), BP (b) and BC (c). Soil NH_4^+-N and NO_3^--N concentration (mg N/kg soil) across the top 50 cm soil profile at the three sites DB (d), BP (e) and BC (f).

Comparing deposition, soil and vegetation $\delta^{15}N$

Mean $\delta^{15}N$ values of the top 10 cm soil were on an average 2.1 ‰ lower as compared to the next 40 cm at all three sites ($p<0.01$). 0-10 cm and 10-40 cm soil $\delta^{15}N$ values were similar between sites, irrespective of their distance from the refinery ($p>0.05$) (Fig. 20). 0-10 cm soil $\delta^{15}N$ values were closer to wood, leaf and litter $\delta^{15}N$ relative to the deeper soil. Wood $\delta^{15}N$ values (from 2019 tree-rings) increased and became less variable with increasing distance from the refinery ($p<0.05$). Wood $\delta^{15}N$ values from DB were lower and more variable (mean 2.2 ± 1.43 ‰), while they were higher at site BP (mean

3.73 ± 0.27 ‰) as compared to DB, and tree-rings at site BC had the highest $\delta^{15}N$ values (mean 5.54 ± 0.18 ‰). As soil $\delta^{15}N$ values were similar across all three sites, fractionation between soil and wood decreased from DB (mean 4.6 ± 2.95 ‰; $p<0.001$) to BP (mean 3.05 ± 2.28 ‰; $p<0.01$) to BC (mean 0.97 ± 2.96 ‰; $p>0.05$). Leaf and litter $\delta^{15}N$ increased with distance from the refinery. Also, at each site, $\delta^{15}N$ values of leaves were similar to those of litter ($p>0.05$) (Fig. 20). Mean difference between leaf and litter $\delta^{15}N$ was 0.2 ‰ at DB and BC, and 0.3 ‰ at BP. Foliar $\delta^{15}N$ values represented wood $\delta^{15}N$ at site DB (mean difference 0.7 ‰; $p>0.05$), but wood $\delta^{15}N$ at sites BP (mean difference 1.7 ‰; $p>0.05$) and BC (mean difference 2.4 ‰; $p<0.05$) were heavier as compared to foliar $\delta^{15}N$ (Fig. 20). Overall, wood, leaf and litter $\delta^{15}N$ followed an increasing trend similar to that of modeled $\delta^{15}N$ of deposition with increasing distance from the refinery.

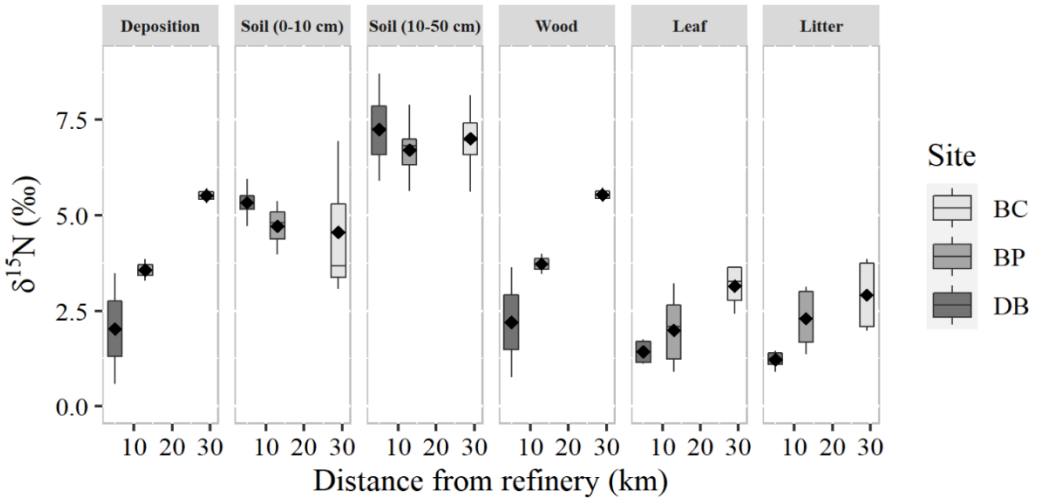

Figure 20. $\delta^{15}N$ values (‰) of deposition (modeled), soil (0-10 and 10-50 cm), wood, leaves and litter sampled in November 2019. Tree-rings corresponding to 2019 were analyzed to obtain wood $\delta^{15}N$. Black diamonds indicate mean values, horizontal black lines indicate median values and grey boxes show values lying between the upper and lower quartiles.

Tree-ring N concentration and $\delta^{15}N$ values

Annual air emission records of ammonia gas from the refinery were available from 1994-present (USEPA, 2020). Until 1999, ammonia was emitted only as fugitive air (gaseous emissions from equipment due to leaks and other unintended or irregular releases) at a rate of 4500 kg NH_3/year. Between 2000-2005, no air emissions of ammonia were recorded from the refinery, however, starting 2006, ammonia is being emitted through stack release (from smoke stacks) with a rapid increase in annual emissions, currently measuring at 16,300 kg NH_3/year. Tree-ring N concentration over the study period did not vary among sites, but a steep increase in tree-ring N concentration was observed at all three sites beginning approximately around 2006 (Fig. 21a), which coincides with the onset of stack emission of ammonia gas from the refinery. This abruptly increasing trend in tree-ring N concentration could be an indication of deposition and subsequent plant uptake of reactive N originating from the refinery. Moreover, tree-ring N concentration values from the two sites closer to the refinery were also positively correlated with annual refinery NH_3 emissions (DB: $p<0.05$, $R^2=0.31$; BP: $p<0.01$, $R^2=0.49$) (Fig. 21b). Site-level BAI increased over time with a trend similar to tree-ring N concentration (Fig. 21a). BAI and tree-ring N concentration were strongly correlated at all three sites (DB: $p<0.0001$, $R^2=0.92$; BP: $p<0.0001$, $R^2=0.88$; BC: $p<0.0001$, $R^2=0.76$) (Fig 21c). For each 5000 mm^2 increase in BAI, tree-ring N concentration increased by 0.8 g N/kg at DB, 1.5 g N/kg at BP and 1.8 g N/kg at BC.

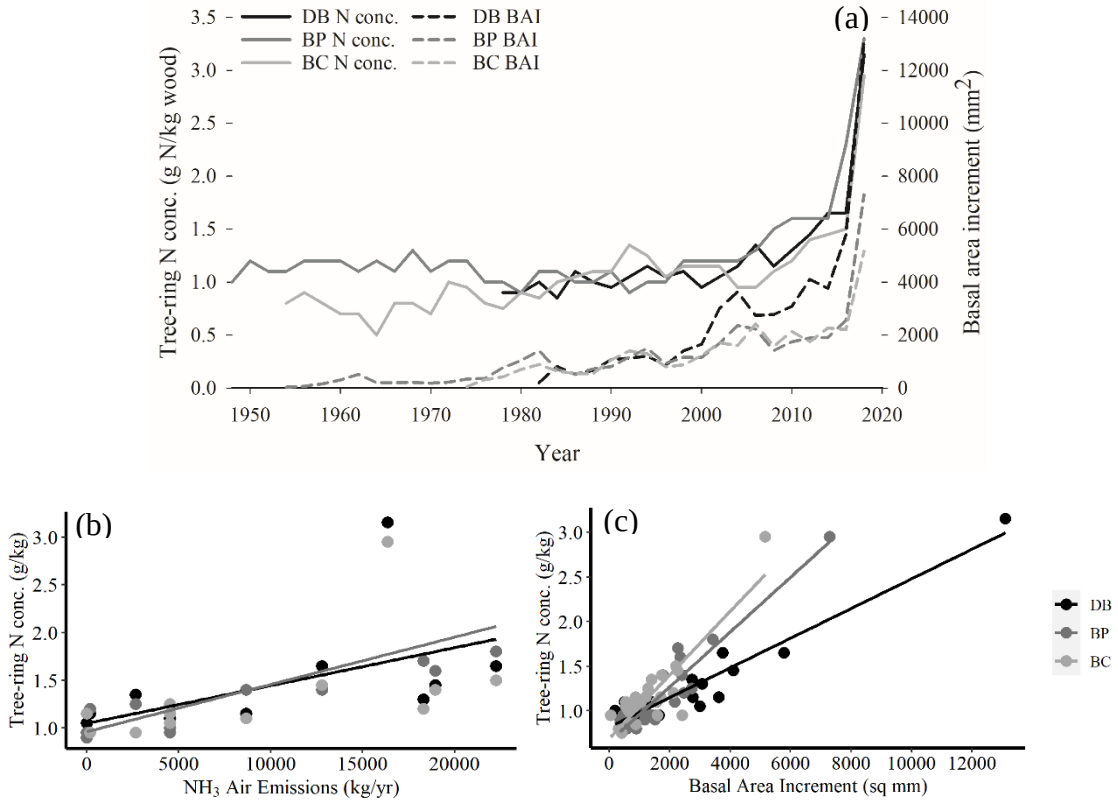

Figure 21. a) Tree-ring N concentration and BAI chronologies from the three sites from 1948-2019. b) Relationship between tree-ring N concentration and ammonia emission from the refinery (kg yr^{-1}) and c) Relationship between tree-ring N concentration and annual BAI (mm^2) ($\alpha = 0.05$). Regression lines are shown only for statistically significant relationships.

Tree-ring $\delta^{15}N$ values ranged from -5.1 to 3.4 ‰ at site DB, -5.6 to 4.8 ‰ at site BP and -3.8 to 5.5 ‰ at site BC (Fig. 22a). Overall, at the site farthest from the refinery (BC), the trend in tree-ring $\delta^{15}N$ indicated gradual enrichment over time (assimilation of isotopically heavier N). Because sampled trees at site DB were younger as compared to the more mature stands at sites BP and BC (mean tree ages of 37, 52, and 55 years, respectively), shorter tree-ring $\delta^{15}N$ and N concentration chronologies at site DB limited our ability to confirm temporal changes in enrichment at that site. During the period when

no ammonia emissions were recorded from the refinery (2000-05), tree-ring $\delta^{15}N$ from the site closest to the refinery increased from -4 ‰ to 2.9 ‰ on an average and then declined again to 4.2 ‰ with the resumption in emissions (Fig. 22b). However, tree-ring $\delta^{15}N$ and N concentration were positively correlated at only the farthest site from the refinery ($p<0.001$; $R^2 = 0.36$), while no correlation was observed at sites DB and BP. BAI had no correlation with tree- ring $\delta^{15}N$ values at any of the sites.

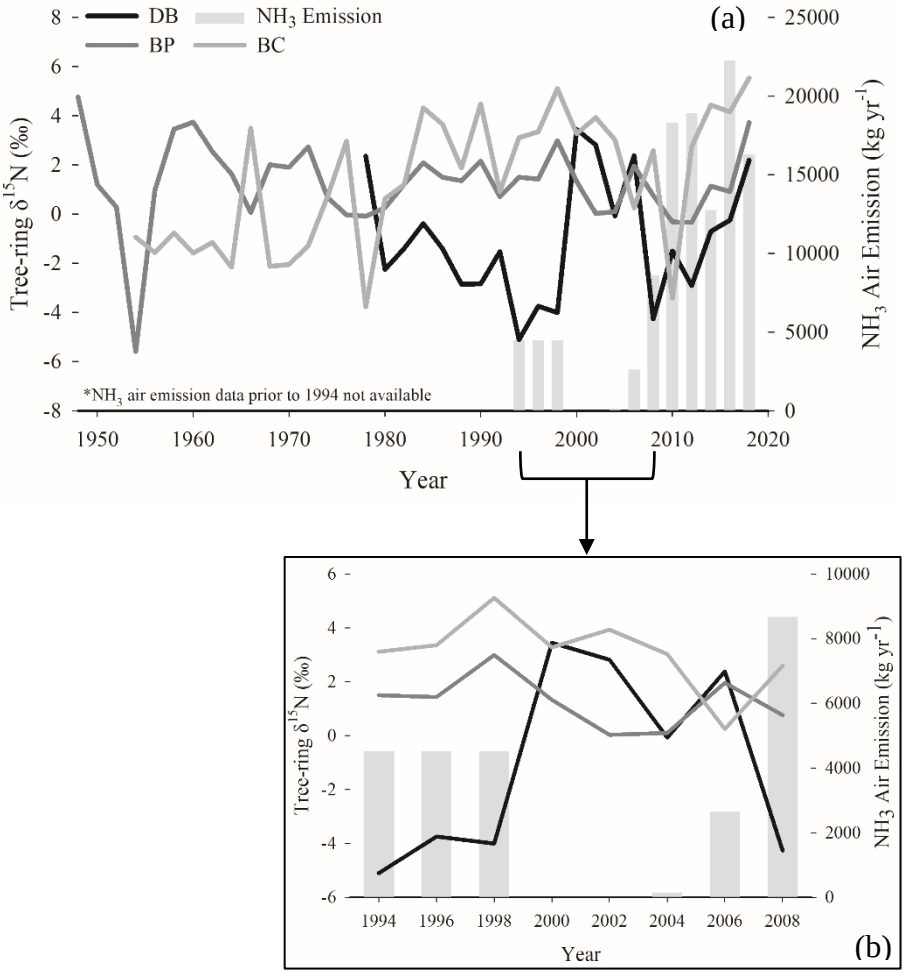

Figure 22. a) Tree-ring $\delta^{15}N$ chronology from the three sites from 1948-2019 and b) Variation in tree-ring $\delta^{15}N$ values (‰) from 1994-2008 in response to the fluctuation in ammonia emission from the refinery (kg yr^{-1}). Grey bars indicate total annual ammonia emission from the refinery.

Comparison between site-level mean tree-ring $\delta^{15}N$ values averaged over the 41-year period that covers all three chronologies indicates a significant difference between the three sites [One-way ANOVA, $F(2, 60) = 14.76$, $p < 0.0001$]. Post hoc analysis indicates that the site closest to the refinery (DB) had a lower mean tree-ring $\delta^{15}N$ value as compared to the other two sites BP ($p < 0.01$) and BC ($p < 0.0001$) (Fig. 23).

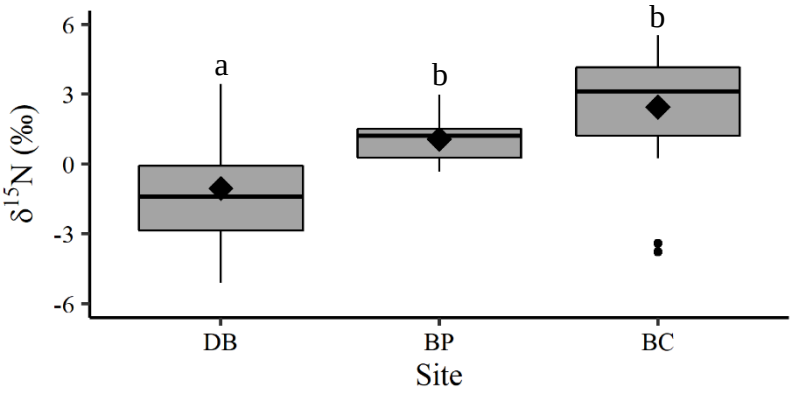

Figure 23. One-way ANOVA and Tukey post hoc analysis (denoted with letters) for mean difference in site-level tree-ring $\delta^{15}N$ (‰) averaged over the 41-year period covering all three chronologies. Black diamonds indicate mean values, horizontal black lines indicate median values, black circles indicate outliers and grey boxes show values lying between the upper and lower quartiles.

Discussion

Our estimates of total inorganic-N deposition in an industrialized region near Houston, TX indicate deposition rates ~3.5 times higher as compared to the national average (Du et al., 2014), and even well above that of the Midwest where fertilizer is the main anthropogenic source. Our measured deposition rates are in good agreement with total deposition estimated by (Zhang et al., 2012) and (Schwede and Lear, 2014) for this region in their continental-scale studies. However, total N deposition estimated in these studies not only include inorganic-N, but also other forms such as organic and gaseous-N.

This suggests that in ecosystems located in close proximity of pollution sources, the actual *in situ* deposition rates can be significantly higher than estimates from atmospheric transport models, satellite measurements and spatial interpolations from scattered monitoring sites. It is evident that wetland forests along the Brazos-Colorado River Basin experience elevated N deposition capable of perturbing the regional N cycle. Such elevated levels of deposition have been observed, but only in downwind areas in very close proximity to emission sources such as transportation, agriculture, and industry (Fenn et al., 2003b). Although our sites are located downwind from a major petroleum refinery, the distances from this point-source are considerable (~30 km). Additionally, since we did not observe a substantial decline in deposition at sites farther from the refinery, it is possible that the origin of the deposited inorganic N could be a combination of emissions from the refinery and other non-point sources. This suggests that the entire landscape is prone to elevated levels of N deposition on a larger spatial scale. In recent times, 60-65% of N deposition in the US has been estimated to be in the form of NH_4^+-N (Du et al., 2014; Li et al., 2016), but about 91% of inorganic N deposited in our study area was NH_4^+-N. This trend is concerning, since excessive concentrations of NH_4^+-N can eventually be toxic due to pH imbalance and anion/cation imbalance (Raven and Smith, 1976; Chaillou and Lamaze, 2001; Britto and Kronzucker, 2002; Miller and Cramer, 2005). Moreover, N emissions are not currently regulated under the National Ambient Air Quality Standards (NAAQS) in the US.

Observed $\delta^{15}N$ values provided useful insights into the nature, source and possible fate of deposited N in the Columbia bottomlands. However, due to the reactive nature of

N species, different emission sources can have highly variable $\delta^{15}N$ values, which can further get modified due to atmospheric reactions. $\delta^{15}N$ values of NH_x usually indicate a relatively lighter isotopic signal of NH_3 gas (-31 to -15 ‰), while heavier $\delta^{15}N$ of NH_4^+-N (-12 to 17 ‰), with particulate NH_4^+-N being heavier than NH_4^+-N in wet deposition (Savard et al., 2017). Our modeled $\delta^{15}N$ values of deposited N range from 2.0 to 5.5 ‰ (increasing with distance from the refinery), which indicate possible mixing of NH_x from different sources. Relatively heavier $\delta^{15}N$ suggests a lower proportion of NO_x in the deposition, which is reinforced by the low concentration of NO_3^--N in the captured deposition. Moreover, our sites are not located in the proximity of major roadways or power plants, reducing the possibility of NO_3^--N deposition. Overall, despite the evidence of mixing, modeled isotopic composition and high concentration of measured NH_4^+-N in deposited N along with high NH_x emissions from the refinery suggest a significant contribution of NH_4^+-N from the refinery and secondarily from agricultural activities (the only other possible source of NH_x in the region).

Our tree-ring $\delta^{15}N$ values averaged over a span of four decades indicated enrichment with distance from the refinery but the increase was smaller from 13 km to 29 km. The site closest to the refinery had a much lighter isotopic signature (mean -1.04 ± 0.5 ‰) over most of the study period, suggesting that NH_x deposition from the refinery possibly has a $\delta^{15}N$ signature close to 0 ‰. At the farther sites, the average signature was enriched possibly due to mixing from other sources. This observation is further reinforced by tree-ring $\delta^{15}N$ values from 2000-05, when NH_3 emissions from the refinery had temporarily ceased. During this period, we observed an abrupt increase in tree-ring $\delta^{15}N$

values from the site closest to the refinery. The heavier tree-ring $\delta^{15}N$ values recorded only during this period suggest a possible shift in the source of deposition for a brief interval. This change was not observed at the other two sites. We also did not observe a gradual increase or decrease in site-level tree-ring $\delta^{15}N$ over time. Such changes have been observed in studies where emission sources are absent during the initial time period covered by the tree-ring chronologies (Poulson et al., 1995; Saurer et al., 2004; Guerrieri et al., 2009; Savard et al., 2009; Leonelli et al., 2012; McLauchlan and Craine, 2012; Jung et al., 2013). Tree-ring $\delta^{15}N$ records at such sites indicate a shift (consistent enrichment or depletion) after the emergence of the emission source. The absence of such a trend from our sites indicates that the sources of emissions and deposition on these forests have been present throughout the period that our chronologies cover. The areas around our sites have been heavily cultivated and used for grazing for close to a century (USFWS, 1997; Barrow et al., 2005), while the refinery was established in 1942, which precedes our longest chronology. On an average, our overall tree-ring $\delta^{15}N$ values from all three sites were slightly heavier as compared to those observed in other studies that have mainly investigated NO_x pollution effects (Saurer et al., 2004; Battipaglia et al., 2009; Guerrieri et al., 2009). Unlike $\delta^{15}N$, our N% chronologies did not differ between sites possibly owing to similar overall background N deposition rates, although the sources of deposition seem to vary across sites. We had hypothesized that tree-ring N% would gradually increase, assuming low N conditions during the initial phase of our chronology. With accumulation of N in the ecosystem over time, the tree-ring N% chronology was expected to flatten with possible N saturation. However, no such trend was observed as tree-ring

N% values did not vary until about 2006, following which a rapid increase was observed at all three sites. This steep rise coincides with the emission rates from the refinery. Although this trend in tree-ring N concentration did not correlate with ring-width index from Deshpande et al. (2020), tree-ring N concentration had a strong positive effect on BAI at all three sites. BAI measurements do incorporate tree-age effects, due to which BAI usually increases rapidly during initial years after establishment before flattening out as the tree approaches maturity. However, at two out of our three sites, BAI remained stable during initial years after tree establishment and a rapid increase was observed with an increase in tree-ring N concentration. This suggests that N inputs have a fertilizing effect on these trees, causing increase in growth. It also indicates relatively low and consistent deposition rates until about late-1990s. This ecosystem seems to be a strong inorganic N sink with a large N retention capacity, barely indicating signs of saturation despite high N deposition levels over more than at least two decades. However, plants do have a threshold capacity of N absorption (~3.5% in wood) (Martius, 1992; Martin et al., 2015; Tang et al., 2018) beyond which, excessive N inputs can have deteriorating toxic effects not only on the vegetation, but also on soils (Aber et al., 1989; Frey et al., 2004; Campbell et al., 2009; Butterbach-Bahl et al., 2011; Lovett and Goodale, 2011). If similar deposition rates persist owing to increasing emissions, the ecosystem could eventually experience N saturation.

Foliar and wood $\delta^{15}N$ values were similar only at the site where atmospheric inputs and wood $\delta^{15}N$ was lighter. This suggests that fractionation within plant tissues is lower when the absorbed N is already isotopically depleted. At the other two sites where wood

and deposition $\delta^{15}N$ were relatively heavier, the absorbed N underwent further fractionation within the plant. Such fractionation of heavier absorbed N within the plant has been observed and attributed to the requirement of isotopically lighter N in the leaves, where it undergoes biochemical transformation for the formation of the photosynthetic enzyme, RuBisCo (Evans, 1989; Evans and Seemann, 1989; Takashima et al., 2004). Also for this purpose, a higher concentration of N is essential in the foliage as compared to other plant parts and fractionation into lighter isotopic forms enables more energy efficient N transport to the leaves (Pardo et al., 2013). This suggests that at sites which receive depleted $\delta^{15}N$ deposition or where significant fractionation in the soil makes more depleted $\delta^{15}N$ available for plant uptake, absorbed N undergoes minimal fractionation within the plant.

NH_4^+-N from wet deposition was apparently the main source of inorganic N in soils and for plant uptake and acts as a primary control over tree-ring $\delta^{15}N$ values. However, the presence of NO_3^--N in soils indicates the co-occurrence of nitrification but at a slower rate. As observed in many other studies in forest ecosystems (Garten, 1993; Emmett et al., 1998; Hobbie and Ouimette, 2009), at all the three sites, soil $\delta^{15}N$ values were depleted at the surface (0–10 cm) as compared to the next 40 cm, which can be attributed to a range of possible factors including soil moisture, microbial activity, and fractionation during root uptake. The higher moisture availability and possible aeration in the top 10 cm soil may have resulted in accelerated microbial activity, decomposition and N cycling (mainly ammonification), resulting in a higher concentration of NH_4^+ and depleted $\delta^{15}N$ values. Another possible mechanism that explains relatively enriched $\delta^{15}N$

values from 10–40 cm is the accumulation of heavier ^{15}N at these depths as a result of fractionation during N uptake by mycorrhizal fungi associated with tree roots. Mycorrhizal fungi discriminate against heavier ^{15}N and preferentially transfer isotopically lighter N to the roots, leaving behind an accumulation of heavier ^{15}N in the soil (Högberg et al., 1996; Hobbie et al., 2000). Bottomland oaks usually have shallow roots systems (Vozzo, 1990; Gilman et al., 1994; Burke and Chambers, 2003) associated with ectomycorrhizal fungi (Filer, 1975; Jurgensen et al., 1996), that can fractionate against isotopically heavier N by as much as 9.6 ‰ (Hobbie and Ouimette, 2009). Other less likely explanation is denitrification. Although wetland ecosystems are usually known to have higher denitrification rates (Ullah and Zinati, 2006; van Cleemput et al., 2007; Peralta et al., 2010; Batson et al., 2012), which can be a major fractionating pathway (Handley and Raven, 1992; Houlton et al., 2006), our soil was sampled during a relatively drier phase when denitrification is minor and $\delta^{15}N$ and soil θ_v were negatively corelated. Lastly, NO_3^- availability is a precursor for denitrification, therefore, if denitrification occurs, soil $\delta^{15}N$ should positively correlate with NO_3^--N concentration, which was not observed at any of the three sites.

Deciduous forests such as subtropical and temperate forested wetlands and hardwood forests are known to have high N retention rates and low N losses even at high deposition levels (Jacks et al., 1994; Aber et al., 1998; Magill et al., 2000). Our findings from the Columbia bottomlands reinforce these observations. These bottomland hardwood forests are important reservoirs for floodwaters during extreme events like hurricanes and tropical storms and help reduce flooding risk in the Houston metropolitan area. The

Columbia Bottomlands Mitigation Bank was also established in 2017, through which appropriate compensatory mitigation is provided for unavoidable impacts to wetlands and functioning of more than 320 acres of bottomland hardwood forests is sustained. The potential of these forested wetlands to retain and remove N pollution has not been explored before. Our results suggest that this ecosystem can provide this vital service without experiencing detrimental impacts of N saturation. As evident from our findings, large amounts of N retention in plants and transformation in soils can remove reactive N compounds from the atmosphere, prevent gaseous loss of greenhouse N gases, nitrate contamination of groundwater and stream pollution through surface and sub-surface run-off, which can eventually contaminate drinking water sources. In a study conducted by Sedaghatdoost et al. (2019) to assess the redox biogeochemistry of these soils, no evidence of soil acidification was observed as the pH ranged from 7.2-8.6, indicating effective N retention in soils. Less than 25% of the Columbia Bottomlands are protected within the San Bernard National Wildlife Refuge, leaving a significant area covered by these forests unprotected. Increasing agricultural incursion and removal for commercial activities are rapidly declining the remaining habitat, making the conservation and protective management of this ecologically critical ecosystem more vital than ever.

Conclusion

This study provides evidence of elevated background N deposition in bottomland hardwood forests of the Brazos-Colorado Basin originating mostly from a petrochemical refinery at rates 3.2-3.6 times higher than the national average. Currently, these bottomland hardwood forests are strong sinks of reactive N, retaining large quantities of

anthropogenic N from emissions. In the absence of this valuable ecosystem service of N retention in forest soil and plant pools, soil acidification and N contamination of water sources such as streams and groundwater would be in a much aggravated state.

NH_4^+-N dominated total wet N deposition, reflecting the emission source. Soil N pools and $\delta^{15}N$ were also affected by NH_4^+-N, suggesting the control of deposited NH_4^+-N over soil N cycling. However, long-term increasing trends of tree-ring N concentration and BAI indicate that deposited N is rapidly absorbed in plant N pools, resulting in increased plant growth and transfer of inorganic N from soils to plants, thus reducing the possibility of soil N saturation, leaching and run-off of excess N. Interestingly, despite exposure to anthropogenic N deposition for several decades, continued absorption of this N into vegetation without showing signs of N saturation is an important ecosystem service that has not been realized and applied in this region and other BHFs. In the US, BHFs occur in proximity of urban centers and these forested wetlands are also associated with freshwater sources. Consolidated conservation efforts among stakeholders and cohesive action between management agencies, river regulation authorities and pollution control agencies can lead to an effective use of these ecosystems to sequester and filter air and water pollutants in exurban and peri-urban areas in the southeastern US.

CHAPTER V

MODELLING THE EFFECTS OF ANTHROPOGENIC NITROGEN DEPOSITION ON FOREST PRODUCTIVITY AND NITROGEN CYCLING IN AN EXURBAN BOTTOMLAND HARDWOOD FOREST

Synopsis

Deposition of reactive nitrogen (N_r) from anthropogenic sources on terrestrial ecosystems has increased several fold since the pre-industrial era. Addition of N_r to forest ecosystems through dry and wet atmospheric deposition shows beneficial impacts on the ecosystem in the initial stages but excessive amounts can cause N saturation and have detrimental impacts. Forested wetlands along the Gulf coast of southeastern US are threatened by elevated N deposition emanating from refineries, urban areas and agriculture. Moreover, a highly variable hydroclimate aggravates the disturbance caused to these rapidly declining ecosystems. In this study, we used the process-based biogeochemical model, Forest-DNDC to understand the response of forest productivity and soil N cycling to a range of N deposition and hydroclimatic scenarios in a bottomland hardwood forest in close proximity of a major petrochemical refinery in Texas, USA. Our objectives were to (i) validate the Forest-DNDC model for this ecosystem by comparing a set of modeled above- and belowground parameters to field measurements, (ii) model and determine the major controls over forest productivity and heterotrophic respiration under different scenarios, and (iii) simulate soil N transformations to understand how precipitation and N deposition affect soil N cycling with its resultant impact on forest

productivity. Our results suggest that Forest-DNDC reasonably represents observed variation in forest productivity and N cycling in this intermittently flooded wetland forest. Application of the model indicated that excessive N deposition is a strong constraint on forest productivity in this ecosystem with indications that possible inhibition of microbial activity due to excessive N_r inputs resulting in decreasing mineralization and nitrification rates slows down productivity at high deposition levels. Moreover, the forest seems to be retaining N in large quantities with marginal N losses. The study provides a baseline of biogeochemical interactions in the region, which will help predict forest productivity under future emission and climate scenarios and aid the regulation of air emissions from refineries to ensure the health of nearby exurban wetland forests that receive excessive anthropogenic N inputs.

Introduction

Nitrogen (N) is a primary limiting nutrient that determines vegetation growth in most ecosystems. Over the last century, the balance of global N cycling has been severely altered due to anthropogenic factors such as fertilizer production and application, increased cultivation of N-fixing crops, fossil fuel combustion from vehicles and industries resulting in elevated emission as well as deposition of reactive inorganic N (Holland et al., 1999; Galloway et al., 2004; Fowler et al., 2013). Currently, global emissions of nitrogen oxides (NO_x) and ammonia (NH_3) are estimated to be about 100 Tg yr^{-1}, out of which, 60% are NH_3 emissions, while NO_x emissions contribute about 40% (Fowler et al., 2013). Global inorganic N deposition is currently 94 Tg N yr^{-1} (Ackerman et al., 2019), of which approximately 70 Tg yr^{-1}falls on the terrestrial surface (Fowler et

al., 2013), and 18 Tg yr^{-1} is deposited on forests (Hudson et al., 1994). While overall global N cycling rates are estimated to have doubled over the last century, deposition rates are believed to have tripled since the late 1800s (Vitousek et al., 1997; Galloway et al., 2004). In the US, major N deposition hotspots occur in the Midwest, California, urban areas in the northeast and in the southeast states along the Gulf coast (Zhang et al., 2012).

Deposition of N_r on ecosystems, especially on forests, is a matter of concern because N is a major driver of primary productivity and soil biogeochemistry (Aber et al., 1989; Vitousek and Howarth, 1991; De Vries et al., 2006). Large-scale additions of external N in these ecosystems can cause biogeochemical imbalance and alter forest structure and function (Campbell et al., 2009; Butterbach-Bahl et al., 2011). Through several studies in forests globally, it is well established that low N deposition levels can benefit forests by increasing primary productivity (Thomas et al., 2010; De Vries et al., 2014) and accelerating soil N cycling (Aber et al., 1998). However, excessive N deposition is known to decrease productivity (Aber et al., 1998; Bai et al., 2010), alter species composition (Stevens et al., 2004; Bobbink et al., 2010), reduce foliar N (Aber et al., 2003), aid invasive species (Siemann and Rogers, 2003b; Liu et al., 2018), slow down mineralization and nitrification (Aber et al., 1989; Aber and Federer, 1992; Aber et al., 1995; Lovett and Rueth, 1999; Carreiro et al., 2000; Frey et al., 2004), increase leaching (Fang et al., 2009; Gundersen et al., 2011) and gaseous N emissions through denitrification (Gundersen et al., 1998; van Groenigen et al., 2015), eventually causing soil acidification (Wallace et al., 2007) followed by massive N losses from the system and also tree mortality in extreme cases (Aber et al., 1998; Magill et al., 2000; Lovett and Goodale,

2011). However, these impacts are mainly dependent on N limitation or saturation in an ecosystem. If a system is N limited, deposition of N_r results in positive effects such as increased growth as a result of faster transformation and production of available N. If the system is N saturated, further deposition leads to decline in growth, reduced decomposition and N transformation through microbial activity and rapid N losses (Aber et al., 1998; Lovett and Goodale, 2011; Tian et al., 2016).

A significant amount of N_r is deposited in wetland forests around the world (Morris, 1991). In the southeastern US, the already threatened wetland forests experience elevated N deposition due to increasing industrialization and urbanization (Pardo et al., 2011). A large number of petroleum refineries, which are major sources of ammonia emissions, are located along the coast of Gulf of Mexico, where many remnant wetland forests occur. In Texas, bottomland hardwood forests occur along the Gulf coast, where a number of rivers form their floodplains. The Columbia bottomlands, located southwest of Houston have also been affected by these disturbances and their geographic extent has declined by nearly 75% (USFWS, 1997; Barrow and Renne, 2001; Barrow et al., 2005).

Although forest ecosystems are substantially dependent on N availability, they are equally reliant on climatic conditions as sufficient precipitation and optimum temperatures are critical for forest growth. In wetland forests, adequate moisture inputs are critical because the vegetation is adapted to saturated conditions (Kozlowski, 1997), which makes it even more sensitive to climatic variation, especially drier conditions. Over the last few decades, precipitation patterns along the Gulf coast have been irregular. In regions along the coast of Texas, annual precipitation amounts have been highly variable with up to 61%

more rainfall than average during some years, while up to 53% deficit during others. These fluctuations have resulted in numerous droughts (1988, 1999, 2005, 2011) and floods (1994, 2015, 2016). Additionally, the region is also prone to frequent tropical storms and hurricanes (1983, 2001, 2005, 2008, 2017). Since 1895, annual rainfall in the region has increased by approximately 130-200 mm and mean annual temperatures have increased by approximately 1.4 ^{o}C. Climate models have predicted a rise in temperature in this region over the next century, while precipitation is expected to be more erratic with increased storm events (IPCC, 2013). These changes pose a major threat to wetland forests in this region, considering their dependence on climate.

Effects of N deposition and climate change on forests are often studied separately. However, both of these factors are closely intertwined and occur simultaneously (Bytnerowicz et al., 2007; Serengil et al., 2011). A majority of N_r is deposited on forests through wet deposition (Fowler et al., 2013), which is directly related to the amount of precipitation. Moreover, atmospheric transformations of N prior to deposition are highly dependent on atmospheric moisture (Hertel et al., 2011). For example, NH_3 dissolves in atmospheric water vapor to form particulate NH_4^+. Hence, it is critical to study the combined effects of climate change and N deposition. Although several studies have explored this interactive effect, most studies have considered temperature effects along with deposition (Gaudio et al., 2015; Dirnböck et al., 2017; Tharammal et al., 2019; Van Houtven et al., 2019), but rarely precipitation (Hole and Engardt, 2008). Precipitation directly affects soil moisture, which drives microbial activity, thus controlling rates of mineralization (Sierra, 1997), nitrification (Stark and Firestone, 1995), denitrification

(Klemedtsson et al., 1988) and plant N uptake (Kulmatiski et al., 2017). Although higher wet deposition can accelerate mineralization and nitrification rates, excessive amounts of N_r in soils are known to inhibit microbial activity beyond a threshold and eventually slow down N cycling rates (Aber et al., 1998; Frey et al., 2004). In wetland forests, these processes become even more complex because excessive moisture can lead to leaching and run-off losses of N (Bowden, 1987; Gunnar et al., 1994). Furthermore, anaerobic conditions, which commonly occur in wetland forests, reduce mineralization and nitrification rates, and accelerate denitrification (Bernhard, 2010). Hence, N deposition and hydroclimatic changes can cause significantly different cascading effects in wetlands as compared to drier, upland ecosystems.

Biogeochemical models informed by field measurements are an efficient tool for simulating and assessing ecosystem-scale fluxes of C, N and water. A number of models have been developed and used over the last 20 years to model biogeochemical fluxes. Some of the most widely used models include Biome-BGC (Thornton et al., 2002), the PnET family (Aber and Federer, 1992), DNDC models (Li et al., 1992), NCAR CSEM (Gent et al., 2011), ForSAFE (Wallman et al., 2005), etc. To improve modeling quality, several of these models have been combined or developed for specific ecosystems and regions. The Forest-DNDC model (Li et al., 2005) is specifically applicable for studying biogeochemical interactions with N deposition and hydroclimate as primary drivers in wetland forests. The model was created by integrating the PnET-N-DNDC model (Li et al., 2000; Stange et al., 2000) with Wetland-DNDC (Zhang et al., 2002), with the former improving estimates of aboveground processes and the latter improving soil

biogeochemical and hydrological estimates. Additionally, Forest-DNDC can be used in upland or wetland mode, which increases its specific applicability. Although the model has mainly been used to simulate C or N fluxes separately and not their interactions, it can reliably replicate field measurements. The model has been validated and applied across a variety of ecosystems across the globe such as cypress swamps, slash pine, spruce forests (Kurbatova et al., 2008), broad-leaf pine (Shu et al., 2019), fir (Lu et al., 2008), *Eucalyptus* plantation (Miehle et al., 2006), wetland forests (Cui et al., 2005), boreal forests (Kim et al., 2014; Kim et al., 2016), subtropical forests (Wang et al., 2011b), tropical dry forests (Dai et al., 2014), etc.

In this study, we used the Forest-DNDC model to simulate and analyze forest productivity and soil N transformations in a bottomland hardwood in different hydroclimatic and elevated N deposition scenarios near a petrochemical refinery. Our objectives were to (i) validate the Forest-DNDC model for this ecosystem by comparing a set of modeled above- and belowground parameters to field measurements, (ii) model and determine the major controls over forest productivity and heterotrophic respiration amid a range of hydroclimatic and N deposition scenarios, and (iii) simulate soil N transformations under these scenarios to understand how precipitation and anthropogenic N deposition affects soil N cycling and its resultant impact on forest productivity. We hypothesized that modeled forest productivity and heterotrophic respiration will increase linearly with precipitation and N deposition as a result of increasing N mineralization and nitrification rates. Soil N transformation rates were also hypothesized to increase linearly under wetter and high N deposition conditions, while N losses were expected to increase

exponentially at very high N deposition levels and under extreme wetness as these are favorable conditions for leaching and denitrification.

Methods

Site description

The study was conducted at the Big Pond unit (29°9'56.66"N 95°49'43.34"W), of the San Bernard National Wildlife Refuge, Texas, USA. The refuge spans over Brazoria, Matagorda and Fort Bend counties on the Gulf coast of Texas, about 40 km southwest of the Houston Metropolitan Area. The 54,000-acre refuge extends 150 km from the coast to inland as the habitat transitions from salt water marshes to freshwater marshes and eventually into mixed bottomland hardwood forests known as the Columbia bottomlands. This floodplain ecosystem is formed as the Colorado, San Bernard and Brazos Rivers flow into the Gulf of Mexico. The bottomland hardwood forests mainly occur along these rivers and their smaller streams and bayous. The Big Pond unit is located in the Linnville Bayou subwatershed of the San Bernard River Basin and is dominated by hardwood forests with the main species being *Quercus nigra*, *Quercus virginiana*, *Celtis laevigata* and *Triadica sebifera* which account for 32%, 15%, 15% and 12% of the basal area, respectively (Cross et al., in preparation). The climate is humid subtropical (Koppen, 1900) and the area receives a mean annual rainfall of 1143 mm, with an average relative humidity of ~70% and the mean temperature is approximately 20 °C (NOAA, 2018a). Soils are mainly vertisols and alfisols dominated by clay, loam and sandy loam texture. The soils series include Aris fine sandy loam, Bacliff clay, Edna loam, Leton loam, Pledger Clay and Churnabog clay (NRCS, 2020).

The Big Pond unit is located 13 km in the downwind direction (northwest) from the Phillips 66 Sweeny Refinery, which is the 18th largest petroleum refinery in the US. The refinery, established in 1942, processes about 256,000 barrels of crude oil per day and emits about 16,300 kg of ammonia annually (USEPA, 2020).

Micrometeorological and eddy covariance measurements

The study site was equipped with a diverse set of eddy covariance (EC) and micrometeorological sensors installed on a 110 ft tower, covering an approximately 0.46 km^2 footprint encompassing about 90% drier, upland area and 10% intermittently flooded zones. Three sets of soil sensors at five different depths were also installed in different parts of the site. Precipitation was recorded using a TE525 Tipping Bucket Rain Gage (Campbell Scientific, Logan, UT) installed on top of the tower and gap-filled using measurements from the nearest NOAA weather station in Bay City, Texas (NOAA, 2018a). Ambient air temperature, relative humidity and vapor pressure deficit was measured using an EC100 module coupled with a CO_2/H_2O Gas Analyzer (Campbell Scientific, Logan, UT). A CNR4 Net Radiometer (Campbell Scientific, Logan, UT) was used to measure average incoming and outgoing shortwave and longwave radiation along with average net radiation.

CO_2 and water vapor fluxes were measured using an IRGASON eddy covariance system, which has an integrated infrared gas analyzer and a 3D sonic anemometer (Campbell Scientific, Logan, UT). Along with CO_2 and H_2O density, wind direction in three dimensions was also recorded by the IRGASON. All measurements were recorded every 30 seconds and averaged over 30 minutes for flux calculation. The EC system was

connected to a CR6 datalogger coupled with EasyFlux Web software tool to calculate fully corrected 30-minute fluxes (Campbell Scientific, Logan, UT). EasyFlux Web calculated raw and corrected CO_2 flux (Foken et al., 2012), evapotranspiration (ET) and friction velocity (u*) using recorded climatic and gas exchange measurements. The 30-minute CO_2 flux data was additionally processed using REddyProcWeb online tool (Wutzler et al., 2018). REddyProcWeb uses a 3-step processing, which includes u* filtering, gap-filling and flux partitioning. In the first step, measurements recorded during conditions with insufficient turbulence (low u*) are removed using the moving point test (Papale et al., 2006). Secondly, gaps in recorded data due to instrument failure and u* filtering are filled using available meteorological data such as net radiation, air temperature and vapor pressure deficit (Reichstein et al., 2005). The procedure is repeated with increased window sizes until the value can be filled. Lastly, CO_2 flux (net ecosystem exchange) is partitioned into gross primary productivity (GPP) and ecosystem respiration (R_{eco}) using the day-time based flux partitioning algorithm which utilizes the common rectangular hyperbolic light–response curve for a moving window of time (Falge et al., 2001; Lasslop et al., 2010). Daily and monthly CO_2 flux and ET were calculated from 30-minute averages for Forest-DNDC model validation. All micrometeorological and EC measurements were recorded from February 21-December 31, 2019 with gaps from March 24-29 and June 30-July 11 due to power failure.

Soil volumetric water content (θ_v) and temperature were recorded at five different depths (5, 15, 30, 76, 100 cm) and at 30-minute intervals continuously from February 21-

December 31, 2019 using CS655 multiparameter sensors are three different locations within the study site.

Nitrogen deposition

We measured total concentration of nitrate (NO_3^-) and ammonium (NH_4^+) deposition using ion exchange resin (IER) columns (Fenn and Poth, 2004). IER columns were prepared by filling a 36 cm long and 1.27 cm diameter PVC tube with 35 g Amberlite IRN150 mixed-bed IER, which is a mixture of Amberlite IRN77 cation exchange resin and IRN78 anion exchange resin. Every PVC tube was sealed with polyester fiber on both ends, a drain cap was fitted at the bottom as an outlet for rainwater and a 10 cm diameter funnel was attached at the top to capture precipitation. Four IER columns were installed at different locations within the study site to capture spatial variability. The columns were exposed for six months and replaced once over a one-year period (September 2018-2019). After the exposure, the columns were transported back to Texas A&M University and the captured NH_4^+ and NO_3^- ions were extracted using 400 ml 2N KCl solution. NO_3^- concentrations were estimated using the Cd reduction method at 543 nm (American Society for Testing Materials, 1987) and NH_4^+ concentrations were estimated using the phenate method at 640 nm (Parsons et al., 1984). NH_4^+ and NO_3^- concentrations from each column were added and total concentration from all four columns was averaged to determine site-level concentration of wet N deposition.

Forest-DNDC model description and validation

Forest-DNDC is a process-based biogeochemical model that simulates C and N fluxes as well as stocks (Li et al., 2005). The model is not only capable of simulating forest

growth in different levels of the canopy, but also C and N stored in the vegetation, litter and soils. Net ecosystem exchange (NEE) is simulated as the sum of GPP and R_{eco}, with leaf, wood, root and soil respiration simulated separately. The model can also simulate soil C dynamics such as CO_2 efflux and N dynamics such as trace gas emissions. Forest-DNDC tracks the entire N cycle and dynamic N processes such as fixation, mineralization, nitrification, plant uptake, leaching loss and gaseous loss due to denitrification. Forest-DNDC is a part of a long hierarchy of biogeochemical models based on the PnET and DNDC model family (Gilhespy et al., 2014). It was created by integrating PnET-N-DNDC model (Li et al., 2000; Stange et al., 2000) with Wetland-DNDC (Zhang et al., 2002), which gives the model the ability to run in both upland and wetland modes by simulating aerobic as well as anaerobic processes (Kurbatova et al., 2008; Kim et al., 2014). It simulates aboveground processes based on the functions of PnET (Aber and Federer, 1992) and soil biogeochemical and hydrologic processes based on the functions of DNDC (Li et al., 1992). Forest-DNDC is able to simulate this vast variety of fluxes and stocks using six sub-models that make up the skeleton of the main model. These sub-models include soil environment, vegetation growth, decomposition, nitrification, denitrification and fermentation. The first three components form the first component of the model, while the latter three form the second component (Li et al., 2005). Biogeochemical processes are partitioned between the sub-models through the concept of an ‘anaerobic balloon’ (Li et al., 2005; Miehle et al., 2006). The expansion and contraction of this anaerobic balloon is controlled by soil oxygen concentration and redox potential, which eventually determines the rates of decomposition, nitrification and denitrification (Li et al., 2005).

Forest-DNDC requires a variety of climatic, hydrologic, vegetation and soil input parameters. Most vegetation and soil parameters have default values set in the model depending on the forest and soil type, respectively, with the option to change default values based on user requirement. Climatic and hydrologic variables, however, need to be set by the user. Climatic input parameters include latitude, concentration of wet N deposition, concentration of atmospheric CO_2, daily minimum and maximum temperature and precipitation. Groundwater table depth is the only required hydrologic parameter (only for wetland mode). Vegetation parameters are age and type of overstory and shrub layer. Using this information, the model generates default values for parameters like plant biomass, plant N, leaf N content, coefficients of photosynthesis curve, respiration fractions, plant C:N, water-use efficiency, leaf geometry, etc. Required soil parameters include soil type, thickness, number of layers and pH, on the basis of which the model generates default values for bulk density, clay %, hydraulic conductivity, porosity, field capacity and wilting point.

To validate the Forest-DNDC model for our site, we used climatic measurements from the EC tower and rates of N deposition from the installed IER columns. Although our site is located within a forested wetland ecosystem, more than 90% of the site area has drier, upland conditions, while the remaining 10% area is intermittently flooded. Therefore, we ran the model in upland mode. Most vegetation parameters were set to default values with a few changes based on field measurements (Table 11).

Table 11. Description of input parameters for model validation.

Parameter	Definition	Value	Source
Atmospheric CO_2	Concentration of ambient CO_2	413 ppm	La Jolla Pier, CA, USA (Keeling and Keeling, 2017)
N deposition	Concentration of wet N deposition	1.15 mg/l	Field measurement
Forest type	Type of dominant vegetation	Hardwoods	Field observations
Initial leaf N content	Initial N concentration in foliage	1.8 %	Field measurement
AmaxA	Coefficient for photosynthesis curve	-46 mole CO_2 g^{-1} s^{-1}	Aber et al., 1996
AmaxB	Slope of relationship between foliar N and AmaxA	71.9 %	Aber et al., 1996
Optimum Psn temperature	Optimum temperature for photosynthesis	24 ^oC	Aber et al., 1996
Minimum Psn temperature	Minimum temperature for photosynthesis	4 ^oC	Aber et al., 1996
Amax fraction	Daily Amax as a fraction of instantaneous Amax	0.76	Aber et al., 1996
Growth respiration fraction	Growth respiration as a fraction of gross photosynthesis	0.25	Forest-DNDC default
Light half satur constant	Half saturation light intensity	200 µ mole m^{-2} s^{-1}	Aber et al., 1996
Respiration Q10	Effect of temperature on respiration	2	Aber et al., 1996
Canopy light attenuation k	Light attenuation constant *k*	0.58	Forest-DNDC default
Water use efficiency	Water demand for producing a unit of biomass	13.9	Forest-DNDC default
DVPD1 and DVPD2	Coefficients for calculating vapor pressure deficit	0.05, 2	Aber et al., 1996
Leaf N retranslocation	Fraction of leaf N transferred to plant N storage during senescence	0.5	Forest-DNDC default
Senescence start day	Starting Julian day for senescence	329	Field observations (Phenocam)
Leaf C/N	C/N ratio in foliage	28	Field measurement
Leaf retention	Time span of leaf retention (years)	1	Forest-DNDC default

Table 11. Continued.

Parameter	Definition	Value	Source
Leaf geometry	Leaf geometry index	2	Forest-DNDC default
SLWdel	Change in specific leaf weight with foliage biomass	0.2 g dry matter/(m^2 leaf * g foliage mass)	Forest-DNDC default
Mineral soil type	Soil type based on proportions of sand, silt and clay	Clay	Field observation/NRCS WSS
Thickness	Soil thickness	2.03 m	NRCS WSS
Layers	Number of soil layers	4	NRCS WSS
pH	Soil acidity	7.1	NRCS WSS
Bulk density	Soil bulk density	0.91 g/cm^3	NRCS WSS
Clay fraction	Clay fraction by weight	0.71	NRCS WSS
Hydraulic conductivity	Soil saturated hydraulic conductivity	0.0012 cm/min	NRCS WSS
Porosity	Pore volumetric fraction of the soil	0.65	Calculated from bulk density
Field capacity	Maximum water-filled fraction of total porosity in a freely drained soil	0.55	NRCS WSS
Wilting point	Maximum water-filled fraction of total porosity at which the plant starts wilting permanently	0.15	NRCS WSS

Model performance was evaluated by comparing modeled and observed measurements of GPP, R_{eco}, NEE and ET at a monthly timescale and soil θ_v and soil temperature at a daily timescale using statistical analyses and criteria described by Miehle et al. (2006) and Shu et al. (2019). The statistical tests include calculation of model accuracy (MA) (Eq. 6), relative mean error of prediction ($\bar{e}$) (Eq. 7), relative mean absolute error (MAE) (Eq. 8), relative root mean square error of prediction (RMSEP) (Eq. 9),

coefficient of determination (r^2) (Eq. 10) and the Nash–Sutcliffe index of model efficiency (ME) (Eq. 11).

$$MA = \frac{\bar{P}}{\bar{O}} \times 100 \tag{6}$$

where $\bar{P}$ is the mean of modeled values and $\bar{O}$ is the mean of observed values.

$$\bar{e} = \left(\frac{\sum_{i=1}^{n} O_i - P_i}{n}\right) / \bar{O} \times 100 \tag{7}$$

where O_i and P_i are the observed and modeled values.

$$MAE = \left(\frac{\sum_{i=1}^{n} |O_i - P_i|}{n}\right) / \bar{O} \times 100 \tag{8}$$

$$RMSEP = \left(\sqrt{\frac{\sum_{i=1}^{n} (P_i - O_i)^2}{n}}\right) / \bar{O} \times 100 \tag{9}$$

$$r^2 = \left(\frac{\sum (O_i - \bar{O})(P_i - \bar{P})}{\sqrt{\sum (O_i - \bar{O})^2 \times \sum (P_i - \bar{P})^2}}\right)^2 \tag{10}$$

$$ME = 1 - \frac{\sum_{i=1}^{n} (P_i - O_i)^2}{\sum_{i=1}^{n} (P_i - \bar{P})^2} \tag{11}$$

These tests provide a comprehensive assessment of the model performance. While MA provides a direct estimate of prediction accuracy, $\bar{e}$ and MAE assess the prediction bias. Unlike $\bar{e}$, MAE does not account for positive or negative errors while estimating the prediction bias. RMSEP estimates errors in a quadratic form, which makes it more responsive to outliers and large errors as compared to MAE. Therefore, the difference between RMSEP and MAE indicates the significance of prediction errors. r^2, the correlation between the modeled and simulated values indicates the capability of the

model to predict temporal variation. The Nash–Sutcliffe index of model efficiency is the most comprehensive parameter that provides a robust and overarching estimate of the model performance. It indicates the accuracy of model prediction with the field measurements as a standard. The values for ME can vary from -∞ to +1, with values between 0-1 (closer to 1) indicating high model efficiency.

Model application

To apply the Forest-DNDC model to our study site and simulate biogeochemical fluxes under a range of hydroclimatic and N deposition conditions, we ran the model in 20 different scenarios. These scenarios included combinations of annual precipitation ranging from extreme drought to very wet years and wet N deposition levels from nearly no deposition to about 6 times the average levels in the US. We increased the annual precipitation levels from 600 mm/year (extreme drought) to 1000 mm/year (moderate) to 1500 mm/year (wet) and 2000 mm/year (extremely wet). To simulate these conditions, we used climate data from the years 2011 (extreme drought), 2013 (moderate), 2007 (wet) and 2004 (extremely wet). Climate data was obtained from the NOAA NCEI database for the Bay City Waterworks, TX, USA weather station USC00410569 (NOAA, 2018a). Simultaneously, we increased concentration of wet N deposition in five increments (1, 5, 10, 15, 20 kg/ha/yr). Output parameters such as GPP, heterotrophic respiration, NO, N_2, N_2O emissions, mineralization, nitrification and N leaching from each simulation were used for further analyses.

Statistical analyses

Apart from the statistical tests used to assess model performance, we used multiple regression to understand the combined effect of precipitation and N deposition on GPP, heterotrophic respiration, mineralization, nitrification and total N loss. As not all relationships were strictly linear, we ran polynomial regressions (quadratic and cubic) and used the best fitted relationships. We also investigated the combined and individual effects of precipitation and N deposition on soil N transformation processes using multiple regression.

Results

Model validation

Comparing modeled fluxes with observed values indicates that Forest-DNDC can be applied to this ecosystem to simulate CO_2 fluxes. The model simulated monthly average GPP with a much higher accuracy as compared to R_{eco} and NEE (Table 12). Annual estimates of modeled CO_2 fluxes were also in good agreement with observed values, with only a 13% underestimation of GPP (Figure 24). Observed GPP and R_{eco} peaked in June and July, respectively, while NEE peaked relatively earlier in May. Although Forest-DNDC modeled large fluxes during these months, it modeled GPP, R_{eco} and NEE peaks in May, August and April, respectively. Observed GPP, modeled GPP and R_{eco} had similar monthly trends but observed R_{eco} was more variable early in the growing season, consequently resulting in differences in modeled and observed NEE during this period (Figure 25).

Forest-DNDC slightly underestimated monthly average GPP (9%) but the modeled values were highly correlated with the observed values (r^2 = 0.90) with sufficient model efficiency (0.74) (Table 12, Figure 25a). The model simulated R_{eco} with moderate accuracy (MA ~72%) with a high correlation with observed values (r^2 = 0.84) and an acceptable model efficiency (0.11) (Table 12, Figure 25b). The magnitude, bias and significance of prediction errors was also much lower in modeled GPP and R_{eco} (Table 12). For GPP, high model efficiency (>0.5) indicates the applicability of Forest-DNDC to accurately simulate C capture in this ecosystem. The error in NEE is higher because it accumulates individual errors from GPP and R_{eco}. When NEE gets closer to zero (no net C exchange), these relative errors increase exponentially (Kim et al., 2014). Consequently, Forest-DNDC overestimated NEE by 31.5% (Table 12). The correlation between modeled and observed values were lower (<0.5) and the model efficiency was less than zero. Large ē, MAE and RMSEP indicate significant prediction bias and large magnitude of errors (Table 12). However, modeling of C capture/release by the ecosystem as indicated by NEE mainly contradicted observed values only during two months at the onset of the growing season (February and March) (Figure 25c).

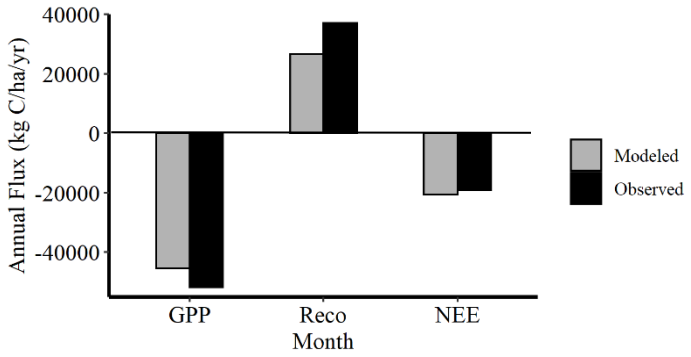

Figure 24. Comparison between total annual modeled (grey bars) and observed (black bars) NEP (kg C ha^{-1} $year^{-1}$).

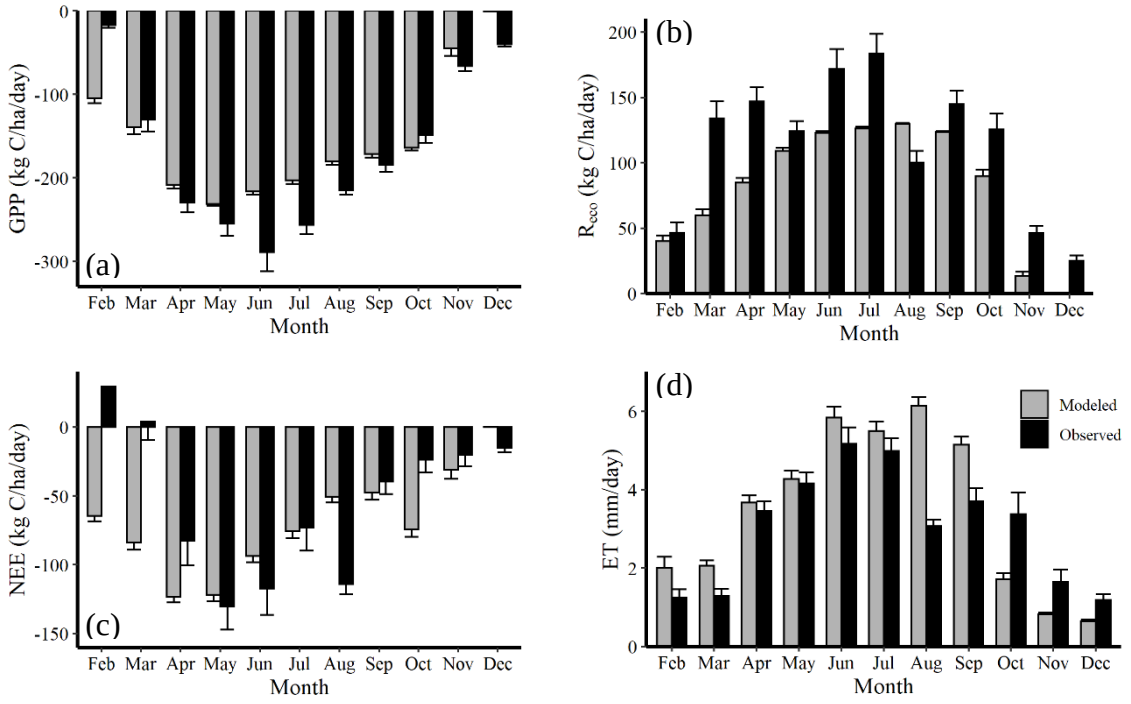

Figure 25. Comparison between mean monthly modeled (grey bars) and observed (black bars) a) GPP (kg C ha^{-1} day^{-1}), b) R_{eco} (kg C ha^{-1} day^{-1}), c) NEE (kg C ha^{-1} day^{-1}), and d) ET (mm day^{-1}). Error bars represent standard error.

Modeled monthly average ET estimates were also accurate with only about 14% overestimation, high correlation with observed values (r^2=0.80) and sufficient model efficiency (0.59) (Table 12, Figure 25d). Observed ET peaked in June, while Forest-DNDC modeled a peak in August, accounting for most of the overestimation. Although model accuracy was high for daily soil θ_v (~99%), correlation with observed values was low (<0.5) model efficiency was out of the acceptable range (Table 12). Although Forest-DNDC was able to predict peaks in soil θ_v, it was unable to simulate dry-downs, especially a long dry-down period in August-September (Figure 26a). Daily soil temperature was modeled with extremely high model accuracy (99%) and efficiency (0.95) with correlation to observed values close to 1 (Table 12, Figure 26b).

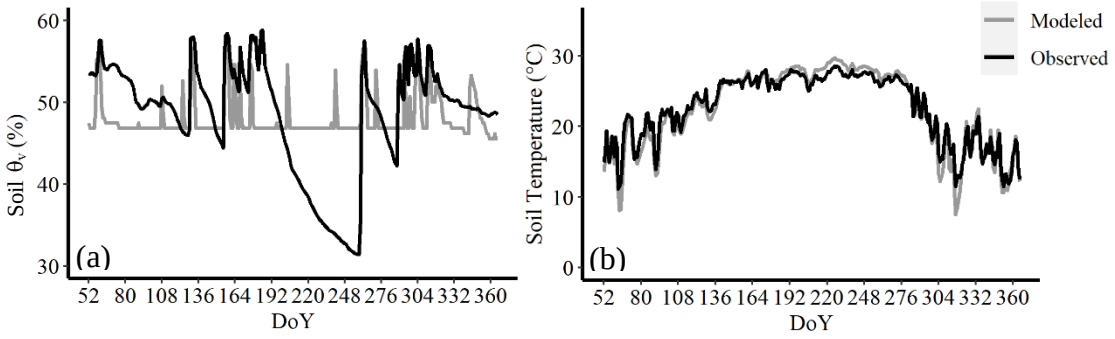

Figure 26. Comparison between mean daily modeled (grey line) and observed (black line) a) soil θ_v (%) and b) soil temperature (ºC).

Table 12. Performance parameters for Forest-DNDC model validation.

	Time-scale	n	MA %	$\bar{e}$ %	MAE %	RMSEP %	RMSEP% - MAE%	r^2	ME
GPP	Monthly	11	90.8	9.2	21.4	25.9	4.5	0.90	0.74
R_{eco}	Monthly	11	72.1	27.9	32.7	37.1	4.4	0.84	0.11
NEE	Monthly	11	131.5	31.5	69.5	91.4	21.9	0.49	-0.88
ET	Monthly	11	113.6	13.6	31.8	41.3	9.5	0.80	0.59
θ_v	Daily	314	97.9	1.03	10.3	13.02	2.7	0.35	-4.86
Soil temp.	Daily	314	99.1	0.9	4.3	5.5	1.2	0.98	0.95

Modeled C fluxes under a range of hydroclimatic and deposition scenarios

Despite the highest amount of precipitation in the 'extremely wet' scenario, annual modeled GPP was ~532 kg ha^{-1} $year^{-1}$ lower than in the 'wet' scenario, while 'drought' and 'moderate' hydroclimatic scenarios resulted in even lower annual GPP (Figure 27a). Modeled GPP did not increase as annual hydroclimate transitioned from drought to moderate. Under all four scenarios, GPP continued to increase with N deposition and indicated a fertilizing effect and active N retention even at extremely high deposition rates. N deposition had a stronger effect over GPP ($p < 0.0001$) as compared to precipitation (p

< 0.001) (Model $p < 0.0001$; $R^2 = 0.74$). Precipitation had a weaker effect on total annual CO_2 efflux from heterotrophic respiration ($p < 0.05$), for which N deposition was a stronger driver ($p < 0.0001$) (Model $p < 0.0001$; $R^2 = 0.96$). Heterotrophic respiration increased at a slower rate until deposition levels of 10 kg/ha/yr, beyond which further N inputs had a much stronger positive effect, suggesting a strong simulation of microbial activity after a threshold of N deposition (Figure 27b). CO_2 efflux from heterotrophic respiration was more sensitive to N deposition with sharper variations.

Applying N deposition and annual precipitation values from 2019 to the equation generated from the multiple regression model (Figure 27a), the annual GPP estimated for 2019 was 44,014 kg ha^{-1}, only a 15% error as compared to GPP measured in the field.

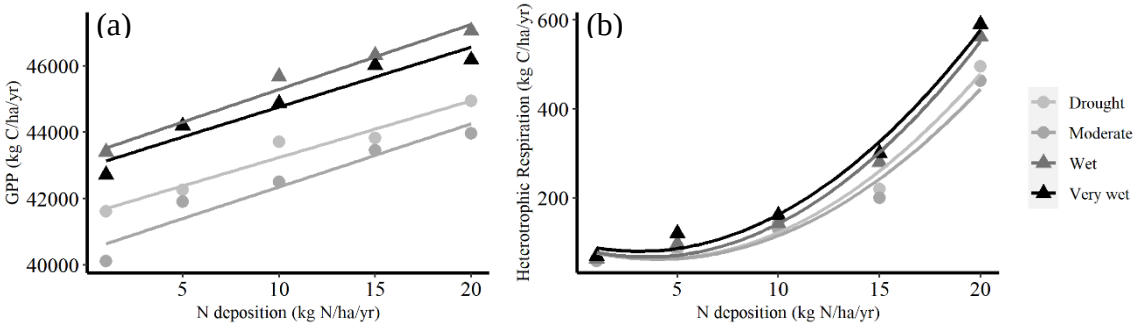

Figure 27. Relationship between N deposition and modeled a) total annual GPP (kg C ha^{-1} $year^{-1}$) and b) soil CO_2 efflux from heterotrophic respiration (kg C ha^{-1} $year^{-1}$) under dry to wet hydroclimatic scenarios.

Modeled N transformations under a range of hydroclimatic and deposition scenarios

Total annual nitrification rates averaged about one-third of mineralization rates. Overall, mineralization rates were higher for the 'very wet' hydroclimatic scenario. Mineralization and nitrification rates increased steadily until N deposition levels of ~10 kg/ha/yr, beyond which a more rapid increase was modeled ($p < 0.0001$), a trend similar

to that of heterotrophic respiration (Figure 28a,b). Hydroclimatic conditions had a slightly stronger effect on mineralization ($p < 0.001$) as compared to nitrification ($p < 0.01$). Total N loss, which includes nitrate leaching and gaseous emissions from nitrification as well as denitrification increased with both N deposition ($p < 0.0001$) and precipitation ($p < 0.0001$) (Figure 28c). Forest-DNDC modeled overall lower total annual N loss rates across deposition and hydroclimatic scenarios, which were on an average 19% of mineralization rates but 65% of nitrification rates.

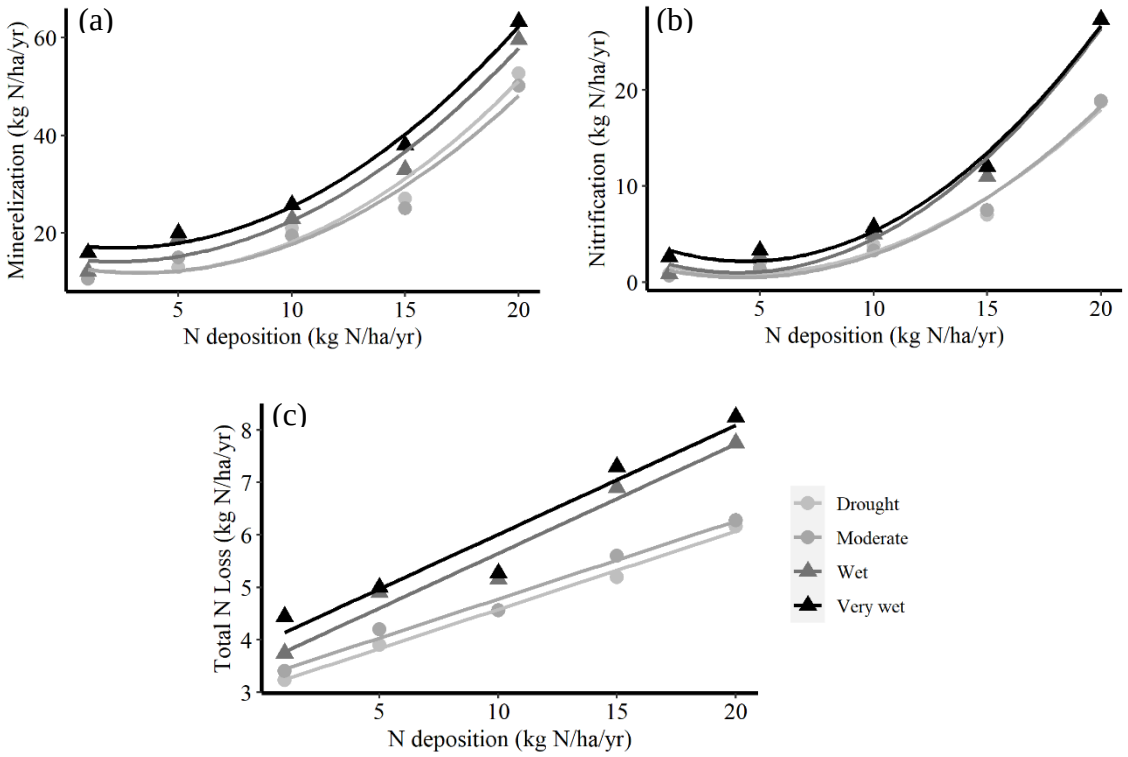

Figure 28. Relationship between N deposition and modeled a) total annual mineralization (kg N ha^{-1} $year^{-1}$), b) nitrification (kg N ha^{-1} $year^{-1}$), and c) N loss (kg N ha^{-1} $year^{-1}$) under dry to wet hydroclimatic scenarios.

Modeled GPP increased at moderate mineralization ($p < 0.0001$; $R^2 = 0.67$) and nitrification rates ($p < 0.001$; $R^2 = 0.59$), but at excessive mineralization and nitrification

rates, the rate of increase in GPP slowed down, indicating higher dependence of productivity on inorganic N availability at low and moderate N conditions (Figure 29).

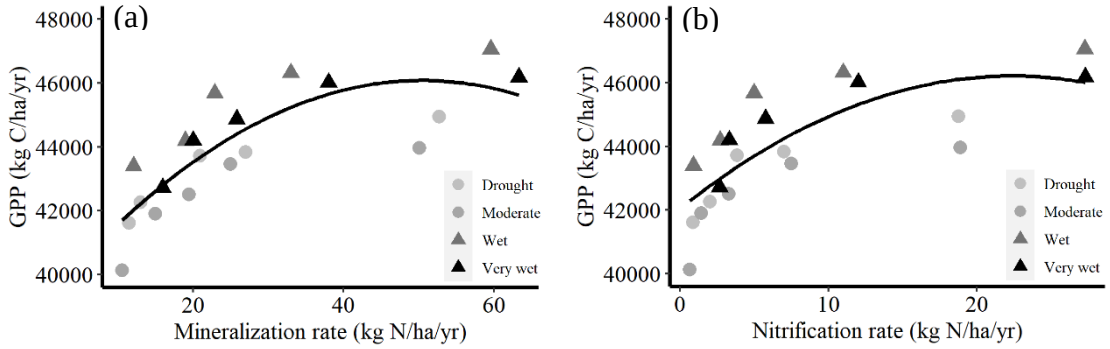

Figure 29. Relationship of modeled total annual GPP (kg C ha^{-1} $year^{-1}$) with a) total annual mineralization rate (kg N ha^{-1} $year^{-1}$) and b) total annual nitrification rate (kg N ha^{-1} $year^{-1}$).

Discussion

We applied Forest-DNDC to the Columbia bottomlands to study the integrated effect of a changing hydroclimate and elevated N deposition on productivity and N cycling. Our results indicated that N deposition was a stronger driver of productivity than hydroclimate in this system. A weaker response of productivity to precipitation in this intermittently flooded wetland forest can be explained by generally occurring higher soil water content, which renders the vegetation less sensitive to drier periods. In a previous study conducted in the same landscape, a weak response of forest growth to precipitation has been observed with a substantial unexplained variance in the relationship (Deshpande et al., 2020). A substantial proportion of this unexplained variance can be explained by adding N deposition to the growth-hydroclimate relationship. We observed a positive effect of N deposition on modeled productivity across low to high deposition levels with

no signs of N saturation. Considering the elevated N emissions from the local petrochemical refinery, our model suggests that even if current N deposition rates double, GPP will continue to respond positively to N inputs, indicating a continuing fertilizing effect and N retention within the plant N pool.

Productivity has been observed to decrease under excessive N inputs across various forest ecosystems (Aber et al., 1998; Lovett and Goodale, 2011; Tian et al., 2016) and this relationship has been explained by a common concept of *N saturation*, which occurs when the inputs of reactive N in an ecosystem exceed the plant and microbial demand, resulting in detrimental effects on the ecosystem along with accelerated N loss (Ågren and Bosatta, 1988; Aber et al., 1989). On the contrary, the constant increase in modeled productivity with N inputs in the Columbia Bottomlands indicates the high N demand in the plant and microbial N pools and the absence of N saturation. This large N retention capacity suggests that these bottomland hardwood ecosystems have the ability to remove and store excessive anthropogenic N from the atmosphere, a critical ecosystem service that has not yet been highlighted in this landscape. One of the major implications of this study is to ascertain the state of Columbia bottomlands with respect to a changing climate and increasing N deposition from anthropogenic sources. We placed this ecosystem on the deposition-hydroclimate-productivity model created using a spectrum of simulated deposition and hydroclimatic scenarios. By using measured precipitation and N deposition and observed as well as modeled GPP from the study site for 2019, we determined that the forest has been actively retaining large amounts of atmospheric N and

that it may have the capacity to store even more N if deposition rates continue to increase in the future.

Under elevated N deposition, as fixation becomes less important, mineralization becomes the primary limiting process in soil N cycling and N availability (Galloway et al., 2008). Under low N deposition scenarios, NH_4^+ is a major source of plant N uptake and results in increased productivity (Boudsocq et al., 2012). As deposition of NH_4^+ increases to intermediate concentrations, not only does more NH_4^+ become readily available for plant uptake, but it also further reduces the C:N ratio of organic matter (Aber et al., 2003). This accelerates the mineralization rates and subsequently productivity, which is evident from our results. Additionally, this is reinforced by a similar increasing trend in CO_2 efflux from heterotrophic respiration, which includes the activity of N transforming microbes.

NO_3^- is another source of inorganic N for plant uptake. Nitrification, the rate at which NO_3^- is produced by the oxidation of NH_4^+ by nitrifying bacteria, is directly related to the availability of residual NH_4^+ in the soil after plant uptake (Chapin et al., 2002). Therefore, in a trend similar to mineralization, our simulations show an exponential increase in nitrification rates under elevated N deposition as a result of higher NH_4^+ availability. This is in line with Aber et al.'s hypothesis of constantly increasing nitrification with N addition (Aber et al., 1998).

Along with declining mineralization and nitrification rates, increasing N losses from the system through NO_3^- leaching and denitrification-induced gaseous emission are considered as major mechanisms of nutrient imbalance under high N deposition (Aber et

al., 1998; Fenn et al., 1998; Driscoll et al., 2003). However, deciduous forests like subtropical forested wetlands are known to have high N retention rates and low N losses even at high deposition levels (Jacks et al., 1994; Aber et al., 1998; Magill et al., 2000). Our results support this understanding as total N losses simulated by the model were very low (average 5.3 kg ha^{-1} $year^{-1}$) under all hydroclimatic and N deposition scenarios, out of which leaching and denitrification made up ~3.7 kg ha^{-1}, while ~1.6 kg ha^{-1} resulted from NO emission, which is mainly released during nitrification. These low amount of N losses through leaching and denitrification could possibly be a result of high N retention in the plant and soil microbial pools.

Forest-DNDC has been successfully validated for several ecosystems across the globe (Cui et al., 2005; Miehle et al., 2006; Kurbatova et al., 2008; Wang et al., 2011b; Shu et al., 2019). Our results indicate that it can also be used in subtropical wetland forests such as bottomland hardwoods, where it accurately simulated CO_2 fluxes at monthly and annual scales. Our results reinforce the fact that Forest-DNDC simulates CO_2 flux more accurately in landscapes with a mosaic of upland-wetland patches as compared to other models (Kurbatova et al., 2008). To our knowledge, no other study has validated Forest-DNDC for evapotranspiration. Our results indicated high accuracy of ET modeling by Forest-DNDC. We observed that Forest-DNDC overestimated ET during a storm event in late-August, which was the result of the model being unable to simulate suppressed transpiration during the storm event, which suggests that transpiration estimated by Forest-DNDC in upland mode during periods with prolonged saturated soil conditions and low VPD needs improvement and should be used cautiously. As soil temperature is directly

related to air temperature, Forest-DNDC was able to simulate soil temperature with extremely high accuracy. However, modeled soil moisture lacked substantial accuracy. Although the model was able to reproduce peaks in soil moisture after rain events, it failed to simulate drydowns during drier conditions as modeled soil moisture remained constant until the next rain event. We assessed the sensitivity of modeled soil moisture by varying bulk density, hydraulic conductivity, porosity, field capacity and wilting point. Although this had an effect on the absolute values of modeled soil moisture, the patterns remained constant and drydowns could not be simulated. This indicates that soil type could be the primary constraint in Forest-DNDC to simulate soil moisture.

Although we acknowledge that results from modeling studies need to be inferred with caution, it needs to be noted that our field measurements are in good agreement with modeled values. One of the major drawbacks of applying the Forest-DNDC model in a high N deposition region is that it only considers the total N concentration in wet deposition but not its chemical composition. Therefore, it does not account for differences in NH_x or NO_y concentration in deposition, which can drive N cycling in very different directions. Secondly, the legacy of N deposition rates in this region is unknown, therefore, modeling an incremental N deposition trend over time may not reflect the actual *in situ* conditions accurately. However, this is a baseline study that provides initial insights of the effect of excessive N inputs to these forests and these observations need to be backed by continuous long-term field measurements of productivity and N deposition. A detailed soil study to estimate rates of *in situ* N soil transformation rates over a longer period is also highly recommended to reinforce our model. Lastly, most of the studies undertaken to

understand the impacts of N addition on forest ecosystems are conducted under controlled conditions in experimental settings where known constant or incremental amounts of N are added. However, in forests which receive ambient N deposition, rates of N addition can vary over time and progression to N saturation may not be a linear process as the system may recover from N saturation if deposition loads decrease over a certain period before increasing again. Therefore, we recommend more studies to understand the effect of ambient N deposition, especially in areas which receive elevated deposition loads.

Conclusion

Our study shows that the Forest-DNDC biogeochemical model can be applied in intermittently flooded bottomland hardwood forests, in the sense that it captured the range of ecosystem GPP, R_{eco}, NEE and ET. Post validation, the application of this model under a range of hydroclimatic and N deposition scenarios suggests that forest productivity is more strongly affected by N deposition than precipitation. The simulations indicate that elevated N deposition can accelerate mineralization and nitrification in these forests, positively affecting productivity. Applying the hydroclimate-N deposition-productivity model to the site using field observations suggests that productivity will continue to increase and atmospheric N will be rapidly transformed and stored in the plant and soil N pools even if N deposition rates continue to increase. N deposition loads from sources like refineries occurring in the proximity of these forests need to be regulated as the thresholds of N retention in these forests are unknown, rendering the projection of N saturation uncertain beyond deposition rates used in this modeling study.

CHAPTER VI

SUMMARY AND CONCLUSIONS

Wetland forests across the globe are ecologically unique and invaluable as they provide habitat for biodiversity that is not adapted to thrive in drier conditions. Wetland forests are also economically critical as they provide indispensable ecosystem services such as mitigating flooding risk, purifying drinking water sources, recharging groundwater levels, removing air and water pollutants, providing recreational opportunities, preventing soil erosion, providing timber and non-timber forest products for human consumption, etc. Bottomland hardwood forests (BHFs) of the southeastern United States are sub-tropical deciduous wetland forests that provide vital ecosystem services to this rapidly commercializing and urbanizing region. However, human-induced disturbances from urbanization, in combination with transitioning climatic conditions have biogeographically and ecologically damaged BHFs in the region, which has not only led to a decline in their distribution but also their ecosystem functioning through changes in species composition, community structure and invasion by non-native species.

Climate in this region is expected to warm over the next century and precipitation patterns are projected to become more non-uniform, with growing seasons expected to get drier and winters predicted to get wetter. BHFs in the southeastern US mainly occur close to the Gulf and Atlantic coasts, where warming has led to an increase in the frequency and intensity of storm events such as tropical storms and hurricanes. Although BHF vegetation is tolerant to moderate flooding, most species may not be able to sustain prolonged

waterlogging caused by these storm events. However, the knowledge of possible physiological responses of BHFs to excessively wet conditions remains sparse. The overall wetter conditions in BHFs prevent droughts from being as detrimental as compared to other drier forest ecosystems. However, droughts in the southern US, such as the 2011 one, cause extremely dry conditions in patches of this landscape that have already been rendered drier by draining and diverting water away from these forested wetlands. In addition to climate change, release of air and water pollutants from a range of sources such as agriculture, petroleum refineries, vehicles, power plants, etc. threaten these forests. Reactive nitrogen (N_r) deposition is one of the foremost concerns as balanced N availability is a major factor that drives productivity, physiology and biogeochemistry of forest ecosystems. Also, N_r deposition is closely intertwined with climatic conditions, such as precipitation, temperature and humidity, that determine its transformation and fate in ecosystems. However, these interactions are not fully understood, mainly because of evolving climatic conditions and chemical nature of N_r emissions. This dissertation aimed to understand the integrated effects of these disturbances on BHFs in southeast Texas and to address the following overarching questions: How have these forests been responding to physiological stress caused by hydroclimatic variation and has it affected annual growth patterns? How do water-use strategies in bottomland trees growing under flooded and non-flooded conditions differ in response to seasonal wetting and drying? Can the invasive Chinese tallow alter stand transpiration and outcompete native oaks for soil water? Do these forests receive excessive N deposition and what is its chemical nature? Has persistent elevated N deposition led to N saturation, affecting primary productivity, N

transformations in the soil and accelerated N loss? What is the relative importance of precipitation and N deposition in driving primary productivity in this ecosystem?

Trees growing in hydrologically wetter patches of the Columbia BHFs experienced less stress during growing seasons when hydroclimatic conditions were extreme. In these patches where flooding is more frequent, trees were expected to exhibit stressful response to prolonged flooding caused by root hypoxia and decreased root hydraulic conductivity. On the contrary, no such negative physiological response was observed. Also, during periods of drought or drought-like conditions, soil water reserves from erstwhile waterlogging events prevented trees in these patches from undergoing drought stress. These findings clearly indicated better adaptation of bottomland vegetation to intermittently flooded conditions, which seem to provide a hydrological buffer against drought and flood stress to the vegetation. On the other hand, vegetation at drier sites experienced growth inhibition and showed signals of stress during drought periods, and was more sensitive to wetter hydroclimatic conditions. Another important finding was the differing response of BHFs to seasonal climatic variation. While drier and harsher climatic conditions during the mid-growing season were the most detrimental to tree growth, similarly stressful conditions early in the growing season induced the most physiological stress. When drier early-growing seasons were followed by wetter mid-growing seasons, physiological stress subsided rapidly and growth rates were restored, a plastic response which is a unique characteristic of wetland trees. However, unlike the intermittently flooded trees, trees at the drier sites could not recover from stress induced during harsh mid-growing seasons, eventually resulting in stunted annual growth. This dissertation

provides evidence that vegetation in the hydrologically drier patches of these BHFs may not be able to sustain increasingly drier and warmer climatic conditions that are predicted for this region. Moreover, BHFs in the southeastern United States are rapidly being drained. In addition to a shrinking distribution range due to human encroachment, the remaining BHF patches are expected to experience drier conditions exacerbated by a warming climate, to which the vegetation is observed to be responding negatively. This may induce changes in the community structure, promote encroachment by invasive species, cause decline in productivity of native vegetation and possibly induce mortality if unfavorable conditions persist.

Plants within the same community can have varying water-use strategies in response to spatial heterogeneity in soil water conditions. While soil drying usually suppresses water-use, flooding may either suppress or stimulate water uptake. In wetland forests, few studies have been conducted to understand this response, which have yielded very contrasting results depending on topography, soil type, climate and species. Sharply fluctuating soil water conditions can thus affect transpiration, which can be a major component in the regional hydrologic cycle in ecosystems like wetland forests. This dissertation aimed at understanding how bottomland trees differ in their seasonal water-use strategies when growing under contrasting soil water conditions. Since Chinese tallow invasion is a major concern in this region, especially invading the intermittently flooded patches (sloughs), this dissertation also aimed at assessing if this invasive species has the potential to outcompete native bottomland oaks for soil water. Although trees growing in flooded conditions had lower water-use as compared to the upland trees, the flooded trees

were less sensitive to seasonal climatic variation and sustained their water uptake during the driest phases in the summer. These trees had suppressed water-use during early growing season flooding, but as the flooding receded, they reopened their stomata and water-use recovered. This stomatal reopening suggests that suppressed water-use in response to flooding might be an adaptive trait rather than an indication of hydraulic or physiological stress. Upland trees, on the other hand, experienced drought stress in the summer as their water-use declined sharply, reinforcing the findings from the first part of the dissertation. The results suggest that vegetation in BHF ecosystems can experience drought stress on a range of temporal and spatial scales, for which it might not be adapted. Vegetation in drier portions of BHFs can thus be sensitive to even slight reductions in soil moisture. Most Chinese tallows sampled in this study were younger individuals with smaller basal areas. Tallows were observed to have invaded sloughs, indicating their preference to wetter soil conditions, encroaching the habitat of native oaks in the already shrinking wet patches. They had higher relative sapwood area-to-basal area ratios than the mature oaks, which, despite their younger age and smaller size, enabled the tallows to have sap flux rates as much as 77% as compared to the oaks. These results suggest that in the near future, with the tallows growing to maturity, they may equate oak water-use in the flooded patches. Currently, Chinese tallows constitute more than 20% of stand individuals and their numbers are expected to rise, especially in unmanaged parts of these forests. If unchecked, a future scenario is very likely where the tallows (that are also more shade-tolerant) may outcompete native oaks in the sloughs and modify the regional hydrologic cycle with their water uptake. Moreover, tallows invade areas with high N

availability and are known to proliferate copiously in regions with elevated anthropogenic N inputs.

Excessive deposition of N is a major environmental concern emanating from anthropogenic emissions of different forms of N through air and water. In the southeastern United States, it aggravates environmental degradation caused by other factors such as climate change. Although BHFs in the southeastern United States are located in close proximity of reactive N sources, very little is known about the quantities, chemical nature and impacts of N deposition in these forests and its impact on soil and plant N status. The National Atmospheric Deposition Program (NADP) monitors N deposition across the United States through a network of sites, however, the distribution of NADP sites across the central US and the Great Plains is sparse. This dissertation aimed at understanding the effects of elevated N inputs on soil biogeochemistry and primary productivity using a combination of biogeochemical modeling and field-based techniques. In the Columbia Bottomlands, which occur in close proximity of N emission sources such as petroleum refineries and croplands, wet deposition of NH_4^+-N and NO_3^--N was measured to be about 3.5 times higher than the national average.

N deposition across the globe was dominated by oxidized N compounds throughout the 20th century. Subsequently, the current knowledge of N deposition effects on forest ecosystems is largely based on the understanding of how oxidized N is cycled through forest soils and vegetation. However, with changing technologies and evolving emission policies, the chemical nature of N emissions and deposition is transitioning from oxidized N-dominated to reduced N-dominated. In the Columbia Bottomlands,

isotopically lighter NH_4^+-N constituted 87-95% of bulk wet N deposition, which is mainly attributed to NH_3 emissions from a petroleum refinery located in the upwind direction and from the mosaic of croplands interspersed with BHFs. Primary productivity generally increases with N inputs, especially with NH_4^+-N, which is preferentially absorbed by plants. However, excessive N_r inputs over a longer time period in areas such as in the Columbia Bottomlands, where N emission sources across the landscape have been present for more than six decades, the possibility of N saturation remains.

Contrary to the general understanding based on several studies (most of which have been conducted in temperate forests), that have shown forest ecosystems to experience N saturation after years of excessive N inputs, these BHFs were found to be actively retaining and cycling deposited N despite exposure to excessive deposition for decades. Generally, in N saturated forests, growth as well as tree-ring N concentration either remains constant or declines over time. However, in the Columbia Bottomlands, increases in basal area increments and the concentration of N absorbed by trees over time indicated active absorption and a fertilizing effect of N deposition on plants. Also, the average tree-ring $\delta^{15}N$ signature at the site closest to the refinery was distinctly lower, suggesting active incorporation of emitted and deposited N in the plant N pool. Other common indications of N saturation are soil acidification and N losses through leaching and denitrification, all of which require high concentrations of soil NO_3^--N. However, results from this dissertation indicated extremely low concentrations of NO_3^--N in the soil N pools, further disproving the possibility of N saturation in these forests.

The Forest-DNDC biogeochemical model, which was successfully validated for the Columbia Bottomlands in this dissertation, provided insights on the relationship between primary productivity and N mineralization at high N deposition levels. In contrast to the N saturation concept, the model indicated that forest productivity in these BHFs continues to respond positively to N mineralization even at high deposition rates. This reinforces findings from tree-ring measurements, where radial growth and N absorption increased rapidly with deposition. The model also simulated low N losses through leaching and gaseous emissions, supporting the low NO_3^--N estimates from field measurements. These findings from field-based methods as well as a modeling approach provide compelling evidence that these BHFs are strong sinks of anthropogenic N that can retain and cycle deposited N without incurring detrimental impacts on plants and soils. The evidence of minimal N losses from this ecosystem through leaching and gaseous emissions even under high deposition levels suggests that these forests are effective filters of pollutant N that can otherwise pollute streams, rivers, groundwater and the atmosphere.

Significant knowledge gaps pertaining to plant physiology, soil biogeochemistry, hydrology and air quality were observed over the course of this study. Despite their ecological value, environmental research in BHFs has remained limited and several processes have remained unexplored, resulting in a striking lack of literature and data availability. However, two Texas Water Observatory sites in the region are rapidly filling some of these gaps and are continuously providing valuable ecosystem-level information. Despite this progress, future research activities focusing on flood dynamics and monitoring, continual deposition measurement, atmospheric transport and chemical

transformation of pollutants, pollutant-climate relationships, N gas and methane emissions, groundwater chemistry, seasonal soil analyses and a sociological understanding of private landowners' perceptions about BHFs will effectively strengthen our position to preserve and beneficially manage these ecosystems.

Results from this dissertation suggest that productivity in the Columbia Bottomlands is weakly affected by moisture inputs from precipitation because of the sufficient moisture availability in these floodplain forests from frequent flooding of streams and rivers and clayey soils that retain moisture, thus causing the vegetation to be less dependent on precipitation. Although this suggests that these forests might able to sustain extreme hydroclimatic conditions, this sustenance is contingent upon the frequent flooding and optimum wetting of these forests over a large spatial extent. Drying of these wetland forests, which is already underway, may induce stressful conditions and reduce productivity, while rendering the vegetation to be more sensitive to and dependent on precipitation inputs. Therefore, in addition to forest conservation and protection efforts, maintaining hydrologic connectivity within this patchy landscape through river regulation is of utmost importance. Moreover, through the findings from this dissertation, deposition of inorganic N has emerged as an important factor driving productivity and soil biogeochemistry in these forests. Columbia Bottomlands and other BHFs that occur in exurban or peri-urban locations have rarely been perceived as sinks and filters for air and water pollutants. While most wetland forests are protected as wildlife habitats, floodwater reservoirs, wetland mitigation banks, barriers to soil erosion, this lesser known ecosystem service of pollutant retention has not yet been fully highlighted and realized. This

dissertation provides vital baseline ecological, hydrological and biogeochemical information about this understudied ecosystem that can aid cohesive conservation action between agencies, inform pollutant emission standards and lead to an effective use of these ecosystems to sequester and filter pollutants along with flood risk mitigation. The study also integrates knowledge of distinct processes within the water, carbon and nitrogen cycles, that are strongly interconnected but usually studied and applied disjointedly.

REFERENCES

Abbott, B. W., Bishop, K., Zarnetske, J. P., Minaudo, C., Chapin, F. S., Krause, S., Hannah, D. M., Conner, L., Ellison, D., Godsey, S. E., Plont, S., Marçais, J., Kolbe, T., Huebner, A., Frei, R. J., Hampton, T., Gu, S., Buhman, M., Sara Sayedi, S., Ursache, O., Chapin, M., Henderson, K. D., and Pinay, G.: Human Domination of the Global Water Cycle Absent from Depictions and Perceptions, Nature Geoscience, 12, 533-540, 10.1038/s41561-019-0374-y, 2019.

Aber, J., McDowell, W., Nadelhoffer, K., Magill, A., Berntson, G., Kamakea, M., McNulty, S., Currie, W., Rustad, L., and Fernandez, I.: Nitrogen Saturation in Temperate Forest Ecosystems: Hypotheses Revisited, BioScience, 48, 921-934, 10.2307/1313296, 1998.

Aber, J. D., Nadelhoffer, K. J., Steudler, P., and Melillo, J. M.: Nitrogen Saturation in Northern Forest Ecosystems: Excess Nitrogen from Fossil Fuel Combustion May Stress the Biosphere, BioScience, 39, 378-386, 10.2307/1311067, 1989.

Aber, J. D., and Federer, C. A.: A Generalized, Lumped-Parameter Model of Photosynthesis, Evapotranspiration and Net Primary Production in Temperate and Boreal Forest Ecosystems, Oecologia, 92, 463-474, 10.1007/BF00317837, 1992.

Aber, J. D., Magill, A., McNulty, S. G., Boone, R. D., Nadelhoffer, K. J., Downs, M., and Hallett, R.: Forest Biogeochemistry and Primary Production Altered by Nitrogen Saturation, Water, Air, and Soil Pollution, 85, 1665-1670, 10.1007/BF00477219, 1995.

Aber, J. D., Goodale, C. L., Ollinger, S. V., Smith, M.-L., Magill, A. H., Martin, M. E., Hallett, R. A., and Stoddard, J. L.: Is Nitrogen Deposition Altering the Nitrogen Status of Northeastern Forests?, BioScience, 53, 375-389, 10.1641/0006-3568(2003)053[0375:Indatn]2.0.Co;2, 2003.

Ackerman, D., Millet, D. B., and Chen, X.: Global Estimates of Inorganic Nitrogen Deposition across Four Decades, Global Biogeochemical Cycles, 33, 100-107, 10.1029/2018gb005990, 2019.

Adelman, J. D., Ewers, B. E., and MacKay, D. S.: Use of Temporal Patterns in Vapor Pressure Deficit to Explain Spatial Autocorrelation Dynamics in Tree Transpiration, Tree Physiology, 28, 647-658, 10.1093/treephys/28.4.647, 2008.

Ågren, G. I., and Bosatta, E.: Nitrogen Saturation of Terrestrial Ecosystems, Environmental Pollution, 54, 185-197, https://doi.org/10.1016/0269-7491(88)90111-X, 1988.

Allen, S. T., Krauss, K. W., Cochran, J. W., King, S. L., and Keim, R. F.: Wetland Tree Transpiration Modified by River-Floodplain Connectivity, Journal of Geophysical Research G: Biogeosciences, 121, 753-766, https://doi.org/10.1002/2015JG003208, 2016.

American Society for Testing Materials: Annual Book of Astm Standards, Section 11 : Water and Environmental Technology, Committee, D. On Water, The Society, Philadelphia, Pa, 1987.

Amundson, R., Austin, A. T., Schuur, E. A. G., Yoo, K., Matzek, V., Kendall, C., Uebersax, A., Brenner, D., and Baisden, W. T.: Global Patterns of the Isotopic Composition of Soil and Plant Nitrogen, Global Biogeochemical Cycles, 17, 10.1029/2002gb001903, 2003.

Andersen, P. C., Lombard, P. B., and Westwood, M. N.: Leaf Conductance, Growth, and Survival of Willow and Deciduous Fruit Tree Species under Flooded Soil Conditions [Waterlogging Tolerance, Quince, Apple, Peach, and Pyrus Species], Journal American Society for Horticultural Science, 109, 132-138, 1984.

Anderson, W. T., Sternberg, L. S. L., Pinzon, M. C., Gann-Troxler, T., Childers, D. L., and Duever, M.: Carbon Isotopic Composition of Cypress Trees from South Florida and Changing Hydrologic Conditions, Dendrochronologia, 23, 1-10, https://doi.org/10.1016/j.dendro.2005.07.006, 2005.

Astrade, L., and Bégin, Y.: Tree-Ring Response of *Populus Tremula* L. And *Quercus Robur* L. To Recent Spring Floods of the Saône River, France, Écoscience, 4, 232-239, https://doi.org/10.1080/11956860.1997.11682400, 1997.

Au, R., and Tardif, J. C.: Drought Signals Inferred from Ring-Width and Stable Carbon Isotope Chronologies from *Thuja Occidentalis* Trees Growing at Their Northwestern

Distribution Limit, Central Canada, Canadian Journal of Forest Research, 42, 517-531, https://doi.org/10.1139/x2012-012, 2012.

Awal, Bayabil, K. H., and Fares, A.: Analysis of Potential Future Climate and Climate Extremes in the Brazos Headwaters Basin, Texas, Water, 8, https://doi.org/10.3390/w8120603, 2016.

Babst, F., Poulter, B., Trouet, V., Tan, K., Neuwirth, B., Wilson, R., Carrer, M., Grabner, M., Tegel, W., Levanic, T., Panayotov, M., Urbinati, C., Bouriaud, O., Ciais, P., and Frank, D.: Site- and Species-Specific Responses of Forest Growth to Climate across the European Continent, Global Ecology and Biogeography, 22, 706-717, https://doi.org/10.1111/geb.12023, 2013.

Bai, E., Houlton, B. Z., and Wang, Y. P.: Isotopic Identification of Nitrogen Hotspots across Natural Terrestrial Ecosystems, Biogeosciences, 9, 3287-3304, 10.5194/bg-9-3287-2012, 2012.

Bai, Y., Wu, J., Clark, C., Naeem, S., Pan, Q., Huang, J., Zhang, L., and Guohan, X.: Tradeoffs and Thresholds in the Effects of Nitrogen Addition on Biodiversity and Ecosystem Functioning: Evidence from Inner Mongolia Grasslands, Global Change Biology, 16, 889-889, 10.1111/j.1365-2486.2009.02142.x, 2010.

Bailey-Serres, J., and Colmer, T. D.: Plant Tolerance of Flooding Stress – Recent Advances, Plant, Cell & Environment, 37, 2211-2215, 10.1111/pce.12420, 2014.

Baker, T. T., Conner, W., Lockaby, H. B. G., and Stanturf, J. A.: Fine Root Productivity and Dynamics on a Forested Floodplain in South Carolina, Soil Science Society of America Journal, 65, 545-556, https://www.fs.usda.gov/treesearch/pubs/2287, 2001.

Ballesteros-Canovas, J., Stoffel, M., St. George, S., and Katie, H.: A Review of Flood Records from Tree Rings, Progress in Physical Geography, 1-23, https://doi.org/10.1177/0309133315608758, 2015.

Barrow, W. C., and Renne, I.: Interactions between Migrant Landbirds and an Invasive Exotic Plant: The Chinese Tallow Tree, Flyway, 8:11, 2001.

Barrow, W. C., Johnson Randall, L. A., Woodrey, M. S., Cox, J., Ruelas Inzunza, E., Riley, C. M., Hamilton, R. B., and Eberly, C.: Coastal Forests of the Gulf of Mexico: A Description and Some Thoughts on Their Conservation, General Technical Report PSWGTR-191, U.S. Department of Agriculture, Forest Service, Washington, D.C. , 2005.

Batson, J. A., Mander, U., and Mitsch, W. J.: Denitrification and a Nitrogen Budget of Created Riparian Wetlands, J Environ Qual, 41, 2024-2032, 10.2134/jeq2011.0449, 2012.

Battipaglia, G., Marzaioli, F., Lubritto, C., Altieri, S., Strumia, S., Cherubini, P., and Cotrufo, M. F.: Traffic Pollution Affects Tree-Ring Width and Isotopic Composition of *Pinus Pinea*, The Science of the Total Environment, 408, 586-593, 10.1016/j.scitotenv.2009.09.036, 2009.

Beckett, K. P., Freer-Smith, P. H., and Taylor, G.: Urban Woodlands: Their Role in Reducing the Effects of Particulate Pollution, Environmental Pollution, 99, 347-360, https://doi.org/10.1016/S0269-7491(98)00016-5, 1998.

Bernhard, A.: The Nitrogen Cycle: Processes, Players, and Human Impact, Nature Education Knowledge, 3, 25, https://www.nature.com/scitable/knowledge/library/the-nitrogen-cycle-processes-players-and-human-15644632/, 2010.

Biondi, F.: Comparing Tree-Ring Chronologies and Repeated Timber Inventories as Forest Monitoring Tools, Ecological Applications, 9, 216-227, 10.1890/1051-0761(1999)009[0216:Ctrcar]2.0.Co;2, 1999.

Biondi, F., and Qeadan, F.: A Theory-Driven Approach to Tree-Ring Standardization: Defining the Biological Trend from Expected Basal Area Increment, Tree-Ring Research, 64, 81-96, 16, https://doi.org/10.3959/2008-6.1, 2008.

Blann, K., Anderson, J., Sands, G., and Vondracek, B.: Effects of Agricultural Drainage on Aquatic Ecosystems: A Review, Critical Reviews in Environmental Science and Technology, 39, 909-1001, https://doi.org/10.1080/10643380801977966, 2009.

Bobbink, R., Hicks, K., Galloway, J., Spranger, T., Alkemade, R., Ashmore, M., Bustamante, M., Cinderby, S., Davidson, E., Dentener, F., Emmett, B., Erisman, J.-W., Fenn, M., Gilliam, F., Nordin, A., Pardo, L., and De Vries, W.: Global Assessment of

Nitrogen Deposition Effects on Terrestrial Plant Diversity: A Synthesis, Ecological Applications, 20, 30-59, 10.1890/08-1140.1, 2010.

Boisvenue, C., and Running, S. W.: Impacts of Climate Change on Natural Forest Productivity – Evidence since the Middle of the 20th Century, Global Change Biology, 12, 862-882, 10.1111/j.1365-2486.2006.01134.x, 2006.

Boudsocq, S., Niboyet, A., Lata, J. C., Raynaud, X., Loeuille, N., Mathieu, J., Blouin, M., Abbadie, L., Barot, S., Associate Editor: James, J. E., and Editor: Mark, A. M.: Plant Preference for Ammonium Versus Nitrate: A Neglected Determinant of Ecosystem Functioning?, The American Naturalist, 180, 60-69, 10.1086/665997, 2012.

Bouwman, A. F., Van Vuuren, D. P., Derwent, R. G., and Posch, M.: A Global Analysis of Acidification and Eutrophication of Terrestrial Ecosystems, Water, Air, and Soil Pollution, 141, 349-382, 10.1023/A:1021398008726, 2002.

Bovard, B. D., Curtis, P. S., Vogel, C. S., Su, H. B., and Schmid, H. P.: Environmental Controls on Sap Flow in a Northern Hardwood Forest, Tree Physiology, 25, 31-38, 10.1093/treephys/25.1.31, 2005.

Bowden, W. B.: The Biogeochemistry of Nitrogen in Freshwater Wetlands, Biogeochemistry, 4, 313-348, www.jstor.org/stable/1468671, 1987.

Bray, W. L.: Distribution and Adaptation of the Vegetation of Texas, Bulletin 82. no. 10. University of Texas. Austin, 1906.

Briffa, K. R., Jones, P. D., Bartholin, T. S., Eckstein, D., Schweingruber, F. H., Karlén, W., Zetterberg, P., and Eronen, M.: Fennoscandian Summers from Ad 500: Temperature Changes on Short and Long Timescales, Climate Dynamics, 7, 111-119, 10.1007/BF00211153, 1992.

Briffa, K. R., and Melvin, T. M.: A Closer Look at Regional Curve Standardization of Tree-Ring Records: Justification of the Need, a Warning of Some Pitfalls, and Suggested Improvements in Its Application, in: Dendroclimatology: Progress and Prospects, edited by: Hughes, M. K., Swetnam, T. W., and Diaz, H. F., Springer Netherlands, Dordrecht, 113-145, 2011.

Britto, D. T., and Kronzucker, H. J.: Nh4+ Toxicity in Higher Plants: A Critical Review, Journal of Plant Physiology, 159, 567-584, https://doi.org/10.1078/0176-1617-0774, 2002.

Broadfoot, W. M., and Williston, H. L.: Flooding Effects on Southern Forests, Journal of Forestry, 71, 584-587, 10.1093/jof/71.9.584, 1973.

Brooks, J. R., Flanagan, L. B., and Ehleringer, J. R.: Responses of Boreal Conifers to Climate Fluctuations: Indications from Tree-Ring Widths and Carbon Isotope Analyses, Canadian Journal of Forest Research, 28, 524-533, https://doi.org/10.1139/x98-018, 1998.

Bruce, K. A., Cameron, G. N., and Harcombe, P. A.: Initiation of a New Woodland Type on the Texas Coastal Prairie by the Chinese Tallow Tree *(Sapium Sebiferum* (L.) Roxb.), Bulletin of the Torrey Botanical Club, 122, 215-225, 10.2307/2996086, 1995.

Bruce, K. A., Cameron, G. N., Harcombe, P. A., and Jubinsky, G.: Introduction, Impact on Native Habitats, and Management of a Woody Invader, the Chinese Tallow Tree, *Sapium Sebiferum* (L.) Roxb, Natural Areas Journal, 17, 255-260, www.jstor.org/stable/43911684, 1997.

Bruland, G., and Richardson, C.: Spatial Variability of Soil Properties in Created, Restored and Paired Natural Wetlands, Soil Science Society of America Journal, 69, 273-284, 2005.

Buhay, W. M., Timsic, S., Blair, D., Reynolds, J., Jarvis, S., Petrash, D., Rempel, M., and Bailey, D.: Riparian Influences on Carbon Isotopic Composition of Tree Rings in the Slave River Delta, Northwest Territories, Canada, Chemical Geology, 252, 9-20, https://doi.org/10.1016/j.chemgeo.2008.01.012, 2008.

Burke, M. K., and Chambers, J. L.: Root Dynamics in Bottomland Hardwood Forests of the Southeastern United States Coastal Plain, Plant and Soil, 250, 141-153, 10.1023/A:1022848303010, 2003.

Bustamante, M. M. C., Martinelli, L. A., Silva, D. A., Camargo, P. B., Klink, C. A., Domingues, T. F., and Santos, R. V.: ^{15}n Natural Abundance in Woody Plants and Soils of Central Brazilian Savannas (Cerrado), Ecological Applications, 14, 200-213, 10.1890/01-6013, 2004.

Butterbach-Bahl, K., Gundersen, P., Ambus, P., Augustin, J., Beier, C., Boeckx, P., Dannenmann, M., Gimeno, B. S., Ibrom, A., Kiese, R., Kitzler, B., Rees, R. M., Smith, K. A., Stevens, C., Vesala, T., and Zechmeister-Boltenstern, S.: Nitrogen Processes in Terrestrial Ecosystems, in: The European Nitrogen Assessment: Sources, Effects and Policy Perspectives, edited by: Bleeker, A., Grizzetti, B., Howard, C. M., Billen, G., van Grinsven, H., Erisman, J. W., Sutton, M. A., and Grennfelt, P., Cambridge University Press, Cambridge, 99-125, 2011.

Bytnerowicz, A., Omasa, K., and Paoletti, E.: Integrated Effects of Air Pollution and Climate Change on Forests: A Northern Hemisphere Perspective, Environ Pollut, 147, 438-445, 10.1016/j.envpol.2006.08.028, 2007.

Cameron, G. N., and Spencer, S. R.: Rapid Leaf Decay and Nutrient Release in a Chinese Tallow Forest, Oecologia, 80, 222-228, 10.1007/BF00380155, 1989.

Campbell, J. L., Rustad, L. E., Boyer, E. W., Christopher, S. F., Driscoll, C. T., Fernandez, I. J., Groffman, P. M., Houle, D., Kiekbusch, J., Magill, A. H., Mitchell, M. J., and Ollinger, S. V.: Consequences of Climate Change for Biogeochemical Cycling in Forests of Northeastern North Americathis Article Is One of a Selection of Papers from Ne Forests 2100: A Synthesis of Climate Change Impacts on Forests of the Northeastern Us and Eastern Canada, Canadian Journal of Forest Research, 39, 264-284, 10.1139/X08-104, 2009.

Capon, S. J., Chambers, L. E., Mac Nally, R., Naiman, R. J., Davies, P., Marshall, N., Pittock, J., Reid, M., Capon, T., Douglas, M., Catford, J., Baldwin, D. S., Stewardson, M., Roberts, J., Parsons, M., and Williams, S. E.: Riparian Ecosystems in the 21st Century: Hotspots for Climate Change Adaptation?, Ecosystems, 16, 359-381, 10.1007/s10021-013-9656-1, 2013.

Carreiro, M. M., Sinsabaugh, R., Repert, D., and Parkhurst, D.: Microbial Enzyme Shifts Explain Litter Decay Responses to Simulated Nitrogen Deposition, Ecology, 81, 2359-2365, 10.1890/0012-9658(2000)081[2359:MESELD]2.0.CO;2, 2000.

Cavaleri, M. A., and Sack, L.: Comparative Water Use of Native and Invasive Plants at Multiple Scales: A Global Meta-Analysis, Ecology, 91, 2705-2715, 10.1890/09-0582.1, 2010.

Chaillou, S., and Lamaze, T.: Ammonical Nutrition of Plants, in: Nitrogen Assimilation by Plants, edited by: Morot-Gaudry, J.-F., Science Publishers Inc., New Hampshire, USA, 53–69, 2001.

Chalk, P., Inácio, C., and Chen, D.: An Overview of Contemporary Advances in the Usage of ^{15}n Natural Abundance (Δ^{15}n) as a Tracer of Agro-Ecosystem N Cycle Processes That Impact the Environment, Agriculture, Ecosystems & Environment, 283, 106570, 10.1016/j.agee.2019.106570, 2019.

Chapin, E. S., Matson, P. A., and Mooney, H. A.: Terrestrial Nutrient Cycling, in: Principles of Terrestrial Ecosystem Ecology, Springer, New York, NY, 197-215, 2002.

Chapin, F. S., Vitousek, P. M., and Matson, P. A.: Principles of Terrestrial Ecosystem Ecology, Springer New York : Imprint : Springer, New York, NY, 2012.

Charney, N. D., Babst, F., Poulter, B., Record, S., Trouet, V. M., Frank, D., Enquist, B. J., and Evans, M. E. K.: Observed Forest Sensitivity to Climate Implies Large Changes in 21st Century North American Forest Growth, Ecology Letters, 19, 1119-1128, https://doi.org/10.1111/ele.12650, 2016.

Clawson, R. G., Lockaby, B. G., and Rummer, B.: Changes in Production and Nutrient Cycling across a Wetness Gradient within a Floodplain Forest, Ecosystems, 4, 126-138, https://doi.org/10.1007/s100210000063, 2001.

Colmer, T. D., and Greenway, H.: Oxygen Transport, Respiration, and Anaerobic Carbohydrate Catabolism in Roots in Flooded Soils, in: Plant Respiration: From Cell to Ecosystem, edited by: Lambers, H., and Ribas-Carbo, M., Springer Netherlands, Dordrecht, 137-158, 2005.

Cook, E. R., and Holmes, R. L.: Program Arstan Users Manual, Laboratory of Tree-Ring Research, University of Arizona, Tucson, 15, 1984.

Coplen, T. B.: Reporting of Stable Hydrogen, Carbon, and Oxygen Isotopic Abundances, Geothermics, 24, 707-712, https://doi.org/10.1016/0375-6505(95)00024-0, 1995.

Craine, J. M., Elmore, A. J., Aidar, M. P. M., Bustamante, M., Dawson, T. E., Hobbie, E. A., Kahmen, A., Mack, M. C., McLauchlan, K. K., Michelsen, A., Nardoto, G. B., Pardo, L. H., Peñuelas, J., Reich, P. B., Schuur, E. A. G., Stock, W. D., Templer, P. H., Virginia, R. A., Welker, J. M., and Wright, I. J.: Global Patterns of Foliar Nitrogen Isotopes and Their Relationships with Climate, Mycorrhizal Fungi, Foliar Nutrient Concentrations, and Nitrogen Availability, New Phytologist, 183, 980-992, 10.1111/j.1469-8137.2009.02917.x, 2009.

Craine, J. M., Brookshire, E. N. J., Cramer, M. D., Hasselquist, N. J., Koba, K., Marin-Spiotta, E., and Wang, L.: Ecological Interpretations of Nitrogen Isotope Ratios of Terrestrial Plants and Soils, Plant and Soil, 396, 1-26, 10.1007/s11104-015-2542-1, 2015.

Crawford, R. M. M.: Physiological Responses to Flooding, in: Physiological Plant Ecology Ii. Encyclopedia of Plant Physiology (New Series), edited by: Lange, O. L., Nobel, P. S., Osmond, C. B., and Ziegler, H. e., Springer, Berlin, Heidelberg, 453-477, 1982.

Cui, J., Li, C., and Trettin, C.: Analyzing the Ecosystem Carbon and Hydrologic Characteristics of Forested Wetland Using a Biogeochemical Process Model, Global Change Biology, 11, 278-289, 10.1111/j.1365-2486.2005.00900.x, 2005.

Cullen, L., and Macfarlane, C.: Comparison of Cellulose Extraction Methods for Analysis of Stable Isotope Ratios of Carbon and Oxygen in Plant Material, Tree Physiology, 25, 563-569, https://doi.org/10.1093/treephys/25.5.563, 2005.

Dahl, T. E., and Allford, G. J.: History of Wetlands in the Conterminous United States, Https://Www.Fws.Gov/Wetlands/Documents/History-of-Wetlands-in-the-Conterminous-United-States.Pdf, 1996.

Dahl, T. E.: Status and Trends of Wetlands in the Conterminous United States 2004 to 2009, U.S. Fish and Wildlife Service, https://www.fws.gov/wetlands/Documents/Status-and-Trends-of-Wetlands-in-the-Conterminous-United-States-2004-to-2009.pdf, 2011.

Dai, Z., Birdsey, R. A., Johnson, K. D., Dupuy, J. M., Hernandez-Stefanoni, J. L., and Richardson, K.: Modeling Carbon Stocks in a Secondary Tropical Dry Forest in the Yucatan Peninsula, Mexico, Water, Air, & Soil Pollution, 225, 1925, 10.1007/s11270-014-1925-x, 2014.

Daryadel, E., and Talaie, F.: Analytical Study on Threats to Wetland Ecosystems and Their Solutions in the Framework of the Ramsar Convention, International Journal of Environmental and Ecological Engineering, 91, https://publications.waset.org/pdf/9998721, 2014.

Davies, F. S., and Flore, J. A.: Flooding, Gas Exchange and Hydraulic Root Conductivity of Highbush Blueberry, Physiologia Plantarum, 67, 545-551, https://doi.org/10.1111/j.1399-3054.1986.tb05053.x, 1986.

De Vries, W., Reinds, G. J., Gundersen, P., and Sterba, H.: The Impact of Nitrogen Deposition on Carbon Sequestration in European Forests and Forest Soils, Global Change Biology, 12, 1151-1173, 10.1111/j.1365-2486.2006.01151.x, 2006.

De Vries, W., Du, E., and Butterbach-Bahl, K.: Short and Long-Term Impacts of Nitrogen Deposition on Carbon Sequestration by Forest Ecosystems, Current Opinion in Environmental Sustainability, 9-10, 90-104, 10.1016/j.cosust.2014.09.001, 2014.

Decina, S. M., Hutyra, L. R., and Templer, P. H.: Hotspots of Nitrogen Deposition in the World's Urban Areas: A Global Data Synthesis, Frontiers in Ecology and the Environment, 18, 92-100, 10.1002/fee.2143, 2020.

Denk, T. R. A., Mohn, J., Decock, C., Lewicka-Szczebak, D., Harris, E., Butterbach-Bahl, K., Kiese, R., and Wolf, B.: The Nitrogen Cycle: A Review of Isotope Effects and Isotope Modeling Approaches, Soil Biology and Biochemistry, 105, 121-137, https://doi.org/10.1016/j.soilbio.2016.11.015, 2017.

Deshpande, A. G., Boutton, T. W., Lafon, C. W., and Moore, G. W.: Bottomland Hardwood Forest Growth and Stress Response to Hydroclimatic Variation: Evidence from Dendrochronology and Tree-Ring Δ13c Values, Biogeosciences Discuss., 2020, 1-28, 10.5194/bg-2020-131, 2020.

Dewey, J. C., Schoenholtz, S. H., Shepard, J. P., and Messina, M. G.: Issues Related to Wetland Delineation of a Texas, USA Bottomland Hardwood Forest, Wetlands, 26, 410-429, 10.1672/0277-5212(2006)26[410:IRTWDO]2.0.CO;2, 2006.

Dirnböck, T., Foldal, C., Djukic, I., Kobler, J., Haas, E., Kiese, R., and Kitzler, B.: Historic Nitrogen Deposition Determines Future Climate Change Effects on Nitrogen Retention in Temperate Forests, Climatic Change, 10.1007/s10584-017-2024-y, 2017.

Driscoll, C. T., Whitall, D., Aber, J., Boyer, E., Castro, M., Cronan, C., Goodale, C. L., Groffman, P., Hopkinson, C., Lambert, K., Lawrence, G., and Ollinger, S.: Nitrogen Pollution in the Northeastern United States: Sources, Effects, and Management Options, BioScience, 53, 357-374, 10.1641/0006-3568(2003)053[0357:Npitnu]2.0.Co;2, 2003.

Du, E., de Vries, W., Galloway, J. N., Hu, X., and Fang, J.: Changes in Wet Nitrogen Deposition in the United States between 1985 and 2012, Environmental Research Letters, 9, 095004, 10.1088/1748-9326/9/9/095004, 2014.

Ehleringer, J. R., Hall, A. E., and Farquhar, G. D.: Stable Isotopes and Plant Carbon/Water Relations, Academic Press, San Diego, 555 pp., 1993.

Elliott, E. M., Kendall, C., Boyer, E. W., Burns, D. A., Lear, G. G., Golden, H. E., Harlin, K., Bytnerowicz, A., Butler, T. J., and Glatz, R.: Dual Nitrate Isotopes in Dry Deposition: Utility for Partitioning Nox Source Contributions to Landscape Nitrogen Deposition, Journal of Geophysical Research: Biogeosciences, 114, 10.1029/2008jg000889, 2009.

Else, M. A., Janowiak, F., Atkinson, C. J., and Jackson, M. B.: Root Signals and Stomatal Closure in Relation to Photosynthesis, Chlorophyll a Fluorescence and Adventitious Rooting of Flooded Tomato Plants, Annals of botany, 103, 313-323, 10.1093/aob/mcn208, 2009.

Emmett, B. A., Kjønaas, O. J., Gundersen, P., Koopmans, C., Tietema, A., and Sleep, D.: Natural Abundance of ^{15}n in Forests across a Nitrogen Deposition Gradient, Forest Ecology and Management, 101, 9-18, https://doi.org/10.1016/S0378-1127(97)00121-7, 1998.

Erickson, N. E.: Survival of Plant Materials Established on a Floodplain in Central Oklahoma, Wildlife Society Bulletin (1973-2006), 17, 63-65, http://www.jstor.org/stable/3782040, 1989.

Erlandsson, S.: Dendrochronological Studies, *Geochronology Institute Report* 23, University of Upsala, 1-119, 1936.

Erwin, K. L.: Wetlands and Global Climate Change: The Role of Wetland Restoration in a Changing World, Wetlands Ecology and Management, 17, 71, https://doi.org/10.1007/s11273-008-9119-1, 2008.

Evans, J.: Photosynthesis and Nitrogen Relationships in Leaves of C3 Plants, Oecologia, 78, 9-19, 10.1007/BF00377192, 1989.

Evans, J., and Seemann, J. R.: The Allocation of Protein Nitrogen in the Photosynthetic Apparatus: Costs, Consequences, and Control, in: Photosynthesis, edited by: Brigs, W. R., Alan R. Liss, New York, USA, 183-205, 1989.

Ewe, S. M., and Sternberg, D. L.: Seasonal Water-Use by the Invasive Exotic, *Schinus Terebinthifolius*, in Native and Disturbed Communities, Oecologia, 133, 441-448, https://doi.org/10.1007/s00442-002-1047-9, 2002.

Ewe, S. M. L., and Sternberg, L.: Seasonal Gas Exchange Characteristics of *Schinus Terebinthifolius* in a Native and Disturbed Upland Community in Everglades National Park, Florida, Forest Ecology and Management, 179, 27-36, https://doi.org/10.1016/S0378-1127(02)00531-5, 2003.

Ewers, B. E., Mackay, D. S., Gower, S. T., Ahl, D. E., Burrows, S. N., and Samanta, S. S.: Tree Species Effects on Stand Transpiration in Northern Wisconsin, Water Resources Research, 38, 8-1-8-11, doi:10.1029/2001WR000830, 2002.

Ewers, B. E., Gower, S. T., Bond-Lamberty, B., and Wang, C. K.: Effects of Stand Age and Tree Species on Canopy Transpiration and Average Stomatal Conductance of Boreal Forests, Plant, Cell & Environment, 28, 660-678, 10.1111/j.1365-3040.2005.01312.x, 2005.

Falge, E., Baldocchi, D., Olson, R., Anthoni, P., Aubinet, M., Bernhofer, C., Burba, G., Ceulemans, R., Clement, R., Dolman, H., Granier, A., Gross, P., Grünwald, T., Hollinger, D., Jensen, N.-O., Katul, G., Keronen, P., Kowalski, A., Lai, C. T., Law, B. E., Meyers, T., Moncrieff, J., Moors, E., Munger, J. W., Pilegaard, K., Rannik, Ü., Rebmann, C., Suyker, A., Tenhunen, J., Tu, K., Verma, S., Vesala, T., Wilson, K., and Wofsy, S.: Gap Filling Strategies for Defensible Annual Sums of Net Ecosystem Exchange, Agricultural and Forest Meteorology, 107, 43-69, https://doi.org/10.1016/S0168-1923(00)00225-2, 2001.

Fang, K., Gou, X., Chen, F., Cook, E., Li, J., Buckley, B., and D'Arrigo, R.: Large-Scale Precipitation Variability over Northwest China Inferred from Tree Rings, Journal of Climate, 24, 3457-3468, https://doi.org/10.1175/2011JCLI3911.1, 2011.

Fang, Y.-T., Yoh, M., Mo, J.-M., Gundersen, P., and Zhou, G.-Y.: Response of Nitrogen Leaching to Nitrogen Deposition in Disturbed and Mature Forests of Southern China, Pedosphere, 19, 111-120, https://doi.org/10.1016/S1002-0160(08)60090-9, 2009.

Farquhar, G., O'Leary, M. H. O., and Berry, J.: On the Relationship between Carbon Isotope Discrimination and the Intercellular Carbon Dioxide Concentration in Leaves, 121-137 pp., 1982.

Farquhar, G.: On the Nature of Carbon Isotope Discrimination in C_4 Species, Functional Plant Biology, 10, 205-226, https://doi.org/10.1071/PP9830205, 1983.

Farquhar, G. D., and Sharkey, T. D.: Stomatal Conductance and Photosynthesis, Annual Review of Plant Physiology, 33, 317-345, 10.1146/annurev.pp.33.060182.001533, 1982.

Farquhar, G. D., Hubick, K. T., Condon, A. G., and Richards, R. A.: Carbon Isotope Fractionation and Plant Water-Use Efficiency, in: Stable Isotopes in Ecological Research, edited by: Rundel, P. W., Ehleringer, J. R., and Nagy, K. A., Ecological Studies (Analysis and Synthesis), Springer, New York, NY, 21-40, 1989.

Fenn, M. E., Poth, M. A., Aber, J. D., Baron, J. S., Bormann, B. T., Johnson, D. W., Lemly, A. D., McNulty, S. G., Ryan, D. F., and Stottlemyer, R.: Nitrogen Excess in North American Ecosystems: Predisposing Factors, Ecosystem Responses, and Management Strategies, Ecological Applications, 8, 706-733, 1998.

Fenn, M. E., Baron, J. S., Allen, E. B., Rueth, H. M., Nydick, K. R., Geiser, L., Bowman, W. D., Sickman, J. O., Meixner, T., Johnson, D. W., and Neitlich, P.: Ecological Effects of Nitrogen Deposition in the Western United States, BioScience, 53, 404-420, 10.1641/0006-3568(2003)053[0404:Eeondi]2.0.Co;2, 2003a.

Fenn, M. E., Haeuber, R., Tonnesen, G. S., Baron, J. S., Grossman-Clarke, S., Hope, D., Jaffe, D. A., Copeland, S., Geiser, L., Rueth, H. M., and Sickman, J. O.: Nitrogen Emissions, Deposition, and Monitoring in the Western United States, BioScience, 53, 391-403, 10.1641/0006-3568(2003)053[0391:Nedami]2.0.Co;2, 2003b.

Fenn, M. E., and Poth, M. A.: Monitoring Nitrogen Deposition in Throughfall Using Ion Exchange Resin Columns, Journal of Environmental Quality, 33, 2007-2014, 10.2134/jeq2004.2007, 2004.

Ferrati, R., Ana Canziani, G., and Ruiz Moreno, D.: Esteros Del Ibera: Hydrometeorological and Hydrological Characterization, Ecological Modelling, 186, 3-15, https://doi.org/10.1016/j.ecolmodel.2005.01.021, 2005.

Filer, T.: Mycorrhizae and Soil Microflora in a Green-Tree Reservoir, Forest Science, 21, 36-39, 1975.

Fisher, R. E., France, J. L., Lowry, D., Lanoisellé, M., Brownlow, R., Pyle, J. A., Cain, M., Warwick, N., Skiba, U. M., Drewer, J., Dinsmore, K. J., Leeson, S. R., Bauguitte, S. J.-B., Wellpott, A., O'Shea, S. J., Allen, G., Gallagher, M. W., Pitt, J., Percival, C. J., Bower, K., George, C., Hayman, G. D., Aalto, T., Lohila, A., Aurela, M., Laurila, T., Crill, P. M., McCalley, C. K., and Nisbet, E. G.: Measurement of the ^{13}c Isotopic Signature of Methane Emissions from Northern European Wetlands, Global Biogeochemical Cycles, 31, 605-623, 10.1002/2016gb005504, 2017.

Fowler, D., Coyle, M., Skiba, U., Sutton, M. A., Cape, J. N., Reis, S., Sheppard, L. J., Jenkins, A., Grizzetti, B., Galloway, J. N., Vitousek, P., Leach, A., Bouwman, A. F., Butterbach-Bahl, K., Dentener, F., Stevenson, D., Amann, M., and Voss, M.: The Global Nitrogen Cycle in the Twenty-First Century, Philosophical Transactions of the Royal Society B: Biological Sciences, 368, http://rstb.royalsocietypublishing.org/content/368/1621/20130164.abstract, 2013.

Frey, S. D., Knorr, M., Parrent, J. L., and Simpson, R. T.: Chronic Nitrogen Enrichment Affects the Structure and Function of the Soil Microbial Community in Temperate Hardwood and Pine Forests, Forest Ecology and Management, 196, 159-171, https://doi.org/10.1016/j.foreco.2004.03.018, 2004.

Gabler, C. A., and Siemann, E.: Rapid Ontogenetic Niche Expansions in Invasive Chinese Tallow Tree Permit Establishment in Unfavourable but Variable Environments and Can Be Exploited to Streamline Restoration, Journal of Applied Ecology, 50, 748-756, 10.1111/1365-2664.12071, 2013.

Galloway, J. N., Dentener, F. J., Capone, D. G., Boyer, E. W., Howarth, R. W., Seitzinger, S. P., Asner, G. P., Cleveland, C. C., Green, P. A., Holland, E. A., Karl, D. M., Michaels, A. F., Porter, J. H., Townsend, A. R., and Vöosmarty, C. J.: Nitrogen Cycles: Past, Present, and Future, Biogeochemistry, 70, 153-226, 10.1007/s10533-004-0370-0, 2004.

Galloway, J. N., Townsend, A. R., Erisman, J. W., Bekunda, M., Cai, Z., Freney, J. R., Martinelli, L. A., Seitzinger, S. P., and Sutton, M. A.: Transformation of the Nitrogen Cycle: Recent Trends, Questions, and Potential Solutions, Science, 320, 889, 10.1126/science.1136674, 2008.

Gao, S., Liu, R., Zhou, T., Fang, W., Yi, C., Lu, R., Zhao, X., and Luo, H.: Dynamic Responses of Tree-Ring Growth to Multiple Dimensions of Drought, Global Change Biology, 24, 5380-5390, https://doi.org/10.1111/gcb.14367, 2018.

García-Gómez, H., Aguillaume, L., Izquieta-Rojano, S., Valiño, F., Àvila, A., Elustondo, D., Santamaría, J. M., Alastuey, A., Calvete-Sogo, H., González-Fernández, I., and Alonso, R.: Atmospheric Pollutants in Peri-Urban Forests of *Quercus Ilex*: Evidence of Pollution Abatement and Threats for Vegetation, Environmental Science and Pollution Research, 23, 6400-6413, 10.1007/s11356-015-5862-z, 2016.

Gardiner, E. S.: Ecology of Bottomland Oaks in the Southeastern United States, Proceedings of the third International Oak Conference, Asheville, North Carolina, USA, 2001,

Garten, C. T.: Variation in Foliar ^{15}n Abundance and the Availability of Soil Nitrogen on Walker Branch Watershed, Ecology, 74, 2098-2113, 10.2307/1940855, 1993.

Gasson, P.: Some Implications of Anatomical Variations in the Wood of Pedunculate Oak (*Quercus Robur* L.), Including Comparisons with Common Beech (*Fagus Sylvatica* L.), 8, 149-166, 10.1163/22941932-90001042, 1987.

Gaudio, N., Belyazid, S., Gendre, X., Mansat, A., Nicolas, M., Rizzetto, S., Sverdrup, H., and Probst, A.: Combined Effect of Atmospheric Nitrogen Deposition and Climate Change on Temperate Forest Soil Biogeochemistry: A Modeling Approach, Ecological Modelling, 306, 24-34, https://doi.org/10.1016/j.ecolmodel.2014.10.002, 2015.

Gee, H. K. W., King, S. L., and Keim, R. F.: Tree Growth and Recruitment in a Leveed Floodplain Forest in the Mississippi River Alluvial Valley, USA, Forest Ecology and Management, 334, 85-95, https://doi.org/10.1016/j.foreco.2014.08.024, 2014.

Gent, P., Danabasoglu, G., Donner, L., Holland, M., Hunke, E., Jayne, S., Lawrence, D., Neale, R., Rasch, P., Vertenstein, M., Worley, P., Yang, Z.-L., and Zhang, M.: The

Community Climate System Model Version 4, Journal of Climate, 24, 4973-4991, 10.1175/2011JCLI4083.1, 2011.

Gerhart, L. M., and McLauchlan, K. K.: Reconstructing Terrestrial Nutrient Cycling Using Stable Nitrogen Isotopes in Wood, Biogeochemistry, 120, 1-21, 10.1007/s10533-014-9988-8, 2014.

Gessler, A., Brandes, E., Buchmann, N., Helle, G., Rennenberg, H., and Barnard Romain, L.: Tracing Carbon and Oxygen Isotope Signals from Newly Assimilated Sugars in the Leaves to the Tree-Ring Archive, Plant, Cell & Environment, 32, 780-795, https://doi.org/10.1111/j.1365-3040.2009.01957.x, 2009.

Gessler, A., Ferrio, J. P., Hommel, R., Treydte, K., Werner, R. A., and Monson, R. K.: Stable Isotopes in Tree Rings: Towards a Mechanistic Understanding of Isotope Fractionation and Mixing Processes from the Leaves to the Wood, Tree Physiology, 34, 796-818, https://doi.org/10.1093/treephys/tpu040, 2014.

Gilhespy, S. L., Anthony, S., Cardenas, L., Chadwick, D., del Prado, A., Li, C., Misselbrook, T., Rees, R. M., Salas, W., Sanz-Cobena, A., Smith, P., Tilston, E. L., Topp, C. F. E., Vetter, S., and Yeluripati, J. B.: First 20 Years of Dndc (Denitrification Decomposition): Model Evolution, Ecological Modelling, 292, 51-62, https://doi.org/10.1016/j.ecolmodel.2014.09.004, 2014.

Gilman, E. F., Watson, D. G., Klein, R. W., Koeser, A. K., Hilbert, D. R., and McLean, D. C.: *Quercus Nigra*: Water Oak, 1994.

Giothiomi, J. K., and Dougal, E.: Analysis of Heartwood-Sapwood Demarcation Methods and Variation of Sapwood and Heartwood within and between 15 Year Old Plantation Grown *Eucalyptus Regnans*, International Journal of Applied Science and Technology, 2, 63-70, 2002.

Granier, A.: Evaluation of Transpiration in a Douglas-Fir Stand by Means of Sap Flow Measurements, Tree Physiology, 3, 309-320, 10.1093/treephys/3.4.309, 1987.

Granier, A., Anfodillo, T., Sabatti, M., Cochard, H., Dreyer, E., Tomasi, M., Valentini, R., and Bréda, N.: Axial and Radial Water Flow in the Trunks of Oak Trees: A Quantitative and Qualitative Analysis, Tree Physiology, 14, 1383-1396, 10.1093/treephys/14.12.1383, 1994.

Graven, H., Allison, C. E., Etheridge, D. M., Hammer, S., Keeling, R. F., Levin, I., Meijer, H. A. J., Rubino, M., Tans, P. P., Trudinger, C. M., Vaughn, B. H., and White, J. W. C.: Compiled Records of Carbon Isotopes in Atmospheric Co_2 for Historical Simulations in Cmip6, Geosci. Model Dev., 10, 4405-4417, https://doi.org/10.5194/gmd-10-4405-2017, 2017.

Green, J. W.: Wood Cellulose, in: Methods in Carbohydrate Chemistry, edited by: Whistler, R. L., Academic Press, New York, 9-21, 1963.

Griffith, B., Omernik, Comstock, Rogers, Harrison, Hatch, Bezanson: Ecoregions of Texas, U.S., Environmental Protection Agency, Corvallis, OR, 2004.

Grissino-Mayer, H.: Evaluating Crossdating Accuracy: A Manual and Tutorial for the Computer Program Cofecha, Tree-Ring Research, 57, 205-221, 2001.

Guerra, K. A.: Ecohydrological Analysis in a Forest Ecosystem of Seasonal Variations in the Moisture Content of Clay-Rich Soil, Master of Science Dissertation, Department of Geology & Geophysics, Texas A&M University, College Station, TX, 2020.

Guerrieri, M. R., Siegwolf, R. T. W., Saurer, M., Jäggi, M., Cherubini, P., Ripullone, F., and Borghetti, M.: Impact of Different Nitrogen Emission Sources on Tree Physiology as Assessed by a Triple Stable Isotope Approach, Atmospheric Environment, 43, 410-418, https://doi.org/10.1016/j.atmosenv.2008.08.042, 2009.

Gundersen, P., Emmett, B. A., Kjønaas, O. J., Koopmans, C. J., and Tietema, A.: Impact of Nitrogen Deposition on Nitrogen Cycling in Forests: A Synthesis of Nitrex Data, Forest Ecology and Management, 101, 37-55, https://doi.org/10.1016/S0378-1127(97)00124-2, 1998.

Gundersen, P., Schmidt, I., and Raulund-Rasmussen, K.: Leaching of Nitrate from Temperate Forests - Effects of Air Pollution and Forest Management, Environmental Reviews, 14, 1-57, 10.1139/a05-015, 2011.

Gunnar, J., Arne, J., and Siegfried, F.: Nitrogen Retention in Forest Wetlands, Ambio, 23, 358-362, www.jstor.org/stable/4314236, 1994.

Gutschick, and Hormoz, B.: Extreme Events as Shaping Physiology, Ecology, and Evolution of Plants: Toward a Unified Definition and Evaluation of Their Consequences, New Phytologist, 160, 21-42, https://doi.org/10.1046/j.1469-8137.2003.00866.x, 2003.

Handley, L. L., and Raven, J. A.: The Use of Natural Abundance of Nitrogen Isotopes in Plant Physiology and Ecology, Plant, Cell & Environment, 15, 965-985, 10.1111/j.1365-3040.1992.tb01650.x, 1992.

Handley, L. L., Austin, A. T., Stewart, G. R., Robinson, D., Scrimgeour, C. M., Raven, J. A., Heaton, T. H. E., and Schmidt, S.: The ^{15}n Natural Abundance (Δ^{15}n) of Ecosystem Samples Reflects Measures of Water Availability, Functional Plant Biology, 26, 185-199, https://doi.org/10.1071/PP98146, 1999.

Harrison, J. L., Reinmann, A. B., Maloney, A. S., Phillips, N., Juice, S. M., Webster, A. J., and Templer, P. H.: Transpiration of Dominant Tree Species Varies in Response to Projected Changes in Climate: Implications for Composition and Water Balance of Temperate Forest Ecosystems, Ecosystems, 10.1007/s10021-020-00490-y, 2020.

Haycock, N. E., and Burt, T. P.: Role of Floodplain Sediments in Reducing the Nitrate Concentration of Subsurface Run-Off: A Case Study in the Cotswolds, Uk, Hydrological Processes, 7, 287-295, 10.1002/hyp.3360070306, 1993.

Heaton, T. H. E., Spiro, B., and Robertson, S. M. C.: Potential Canopy Influences on the Isotopic Composition of Nitrogen and Sulphur in Atmospheric Deposition, Oecologia, 109, 600-607, 10.1007/s004420050122, 1997.

Helle, G., and Schleser, G. H.: Beyond Co_2-Fixation by Rubisco – an Interpretation of ^{13}c/^{12}c Variations in Tree Rings from Novel Intra-Seasonal Studies on Broad-Leaf Trees, Plant, Cell & Environment, 27, 367-380, https://doi.org/10.1111/j.0016-8025.2003.01159.x, 2004.

Hertel, O., Reis, S., Skjøth, C. A., Bleeker, A., Harrison, R., Cape, J. N., Fowler, D., Skiba, U., Simpson, D., Jickells, T., Baker, A., Kulmala, M., Gyldenkærne, S., Sørensen, L. L., and Erisman, J. W.: Nitrogen Processes in the Atmosphere, in: The European Nitrogen Assessment: Sources, Effects and Policy Perspectives, edited by: Bleeker, A., Grizzetti, B., Howard, C. M., Billen, G., van Grinsven, H., Erisman, J. W., Sutton, M. A., and Grennfelt, P., Cambridge University Press, Cambridge, 177-208, 2011.

Hobbie, E. A., Macko, S. A., and Williams, M.: Correlations between Foliar Δ^{15}n and Nitrogen Concentrations May Indicate Plant-Mycorrhizal Interactions, Oecologia, 122, 273-283, 10.1007/pl00008856, 2000.

Hobbie, E. A., and Ouimette, A. P.: Controls of Nitrogen Isotope Patterns in Soil Profiles, Biogeochemistry, 95, 355-371, 10.1007/s10533-009-9328-6, 2009.

Hobbie, E. A., and Högberg, P.: Nitrogen Isotopes Link Mycorrhizal Fungi and Plants to Nitrogen Dynamics, New Phytologist, 196, 367-382, 10.1111/j.1469-8137.2012.04300.x, 2012.

Hoerling, M., Kumar, A., Dole, R., Nielsen-Gammon, J. W., Eischeid, J., Perlwitz, J., Quan, X.-W., Zhang, T., Pegion, P., and Chen, M.: Anatomy of an Extreme Event, Journal of Climate, 26, 2811-2832, https://doi.org/10.1175/jcli-d-12-00270.1, 2013.

Högberg, P., Högbom, L., Schinkel, H., Högberg, M., Johannisson, C., and Wallmark, H.: ^{15}n Abundance of Surface Soils, Roots and Mycorrhizas in Profiles of European Forest Soils, Oecologia, 108, 207-214, 10.1007/BF00334643, 1996.

Högberg, P.: Tansley Review No. 95 ^{15}n Natural Abundance in Soil-Plant Systems, New Phytologist, 137, 179-203, 10.1046/j.1469-8137.1997.00808.x, 1997.

Hole, L., and Engardt, M.: Climate Change Impact on Atmospheric Nitrogen Deposition in Northwestern Europe: A Model Study, AMBIO: A Journal of the Human Environment, 37, 9-17, 19, https://doi.org/10.1579/0044-7447(2008)37[9:CCIOAN]2.0.CO;2, 2008.

Holland, E. A., Dentener, F. J., Braswell, B. H., and Sulzman, J. M.: Contemporary and Pre-Industrial Global Reactive Nitrogen Budgets, Biogeochemistry, 46, 7-43, 10.1007/BF01007572, 1999.

Holland, E. A., Braswell, B. H., Sulzman, J., and Lamarque, J.-F.: Nitrogen Deposition onto the United States and Western Europe: Synthesis of Observations and Models, Ecological Applications, 15, 38-57, 10.1890/03-5162, 2005.

Hölscher, D., Koch, O., Korn, S., and Leuschner, C.: Sap Flux of Five Co-Occurring Tree Species in a Temperate Broad-Leaved Forest During Seasonal Soil Drought, Trees, 19, 628-637, 10.1007/s00468-005-0426-3, 2005.

Hook, D. D., and Scholtens, J. R.: Adaptations and Flood Tolerance of Tree Species, in: Plant Life in Anaerobic Envrionments, edited by: Hook, D. D., and Crawford, R. M. M., Ann Arbor Science Publishers, Ann Arbor, MI, 299-331, 1978.

Houlton, B. Z., Sigman, D. M., and Hedin, L. O.: Isotopic Evidence for Large Gaseous Nitrogen Losses from Tropical Rainforests, Proceedings of the National Academy of Sciences, 103, 8745-8750, 10.1073/pnas.0510185103, 2006.

Houston Wilderness: Houston Wilderness, Houston Atlas of Biodiversity, Columbia Bottomlands Map, Texas a&M Press. Url: Http://Houstonwilderness.Org/Colombia-Bottomlands, 2007.

Hudson, R. J. M., Gherini, S. A., and Goldstein, R. A.: Modeling the Global Carbon Cycle: Nitrogen Fertilization of the Terrestrial Biosphere and the "Missing" Co2 Sink, Global Biogeochemical Cycles, 8, 307-333, doi:10.1029/94GB01044, 1994.

IPCC: Climate Change 2013: The Physical Science Basis. Contribution of Working Group I to the Fifth Assessment Report of the Intergovernmental Panel on Climate Change, Cambridge University Press, Cambridge, United Kingdom and New York, NY, USA, 1535 pp., 2013.

Jacks, G., Joelsson, A., and Fleischer, S.: Nitrogen Retention in Forest Wetlands, Ambio, 23, 358-362, www.jstor.org/stable/4314236, 1994.

Jackson, M. B., and Drew, M. C.: Effects of Flooding on Growth and Metabolism of Herbaceous Plants in: Flooding and Plant Growth, edited by: Kozlowski, T. T., Academic Press, San Diego, 47-128, 1984.

Jasechko, S., Sharp, Z. D., Gibson, J. J., Birks, S. J., Yi, Y., and Fawcett, P. J.: Terrestrial Water Fluxes Dominated by Transpiration, Nature, 496, 347-350, 10.1038/nature11983, 2013.

Jenkins, W. A., Murray, B. C., Kramer, R. A., and Faulkner, S. P.: Valuing Ecosystem Services from Wetlands Restoration in the Mississippi Alluvial Valley, Ecological Economics, 69, 1051-1061, https://doi.org/10.1016/j.ecolecon.2009.11.022, 2010.

Jiang, X., and Yang, Z. L.: Projected Changes of Temperature and Precipitation in Texas from Downscaled Global Climate Models, Clim Res, 53, 229-244, https://doi.org/10.3354/cr01093, 2012.

Jones, H. G.: Plants and Microclimate: A Quantitative Approach to Environmental Plant Physiology. 2nd Edition., 2nd Edn. Cambridge University Press, Cambridge. 428 P., 1992.

Jones, R. H., and Sharitz, R. R.: Effects of Root Competition and Flooding on Growth of Chinese Tallow Tree Seedlings, Canadian Journal of Forest Research, 20, 573-578, 10.1139/x90-074, 1990.

Jubinsky, G.: Chinese Tallow *(Sapium Sebiferum*). Report No. Tss-93-03, Florida Department of Environmental Protection, Bureau of Aquatic Plant Management, Tallahassee, FL, 12, 1995.

Jung, K., Choi, W.-J., Chang, S. X., and Arshad, M. A.: Soil and Tree Ring Chemistry of *Pinus Banksiana* and *Populus Tremuloides* Stands as Indicators of Changes in Atmospheric Environments in the Oil Sands Region of Alberta, Canada, Ecological Indicators, 25, 256-265, https://doi.org/10.1016/j.ecolind.2012.10.006, 2013.

Jurgensen, M. F., Richter, D. L., Davis, M. M., McKevlin, M. R., and Craft, M. H.: Mycorrhizal Relationships in Bottomland Hardwood Forests of the Southern United States, Wetlands Ecology and Management, 4, 223-233, 10.1007/BF02150536, 1996.

Kanakidou, M., Myriokefalitakis, S., Daskalakis, N., Fanourgakis, G., Nenes, A., Baker, A. R., Tsigaridis, K., and Mihalopoulos, N.: Past, Present, and Future Atmospheric Nitrogen Deposition, Journal of the Atmospheric Sciences, 73, 2039-2047, 10.1175/jas-d-15-0278.1, 2016.

Kearns, T., Wang, G., Bao, Y., Jiang, J., and Lee, D.: Current Land Subsidence and Groundwater Level Changes in the Houston Metropolitan Area (2005–2012), Journal of Surveying Engineering, 141, 05015002, https://doi.org/10.1061/(ASCE)SU.1943-5428.0000147, 2015.

Keeling, R. F., and Keeling, C. D.: Atmospheric in Situ Co_2 Data - La Jolla Pier, California and Mauna Loa Observatory, Hawaii. In Scripps Co_2 Program Data, UC San Diego Library Digital Collections, https://doi.org/10.6075/J0QJ7F7N, 2017.

Kim, Y., Roulet, N., Peng, C., Li, C., Frolking, S., Strachan, I., and Tremblay, A.: Multi-Year Carbon Dioxide Flux Simulations for Mature Canadian Black Spruce Forests and Ombrotrophic Bogs Using Forest-Dndc, Boreal Environment Research, 19, 417–440, 2014.

Kim, Y., Roulet, N. T., Li, C., Frolking, S., Strachan, I. B., Peng, C., Teodoru, C. R., Prairie, Y. T., and Tremblay, A.: Simulating Carbon Dioxide Exchange in Boreal Ecosystems Flooded by Reservoirs, Ecological Modelling, 327, 1-17, https://doi.org/10.1016/j.ecolmodel.2016.01.006, 2016.

King, S. L., and Keim, R. F.: Hydrologic Modifications Challenge Bottomland Hardwood Forest Management, Journal of Forestry, 117, 504-514, 10.1093/jofore/fvz025, 2019.

Kirschbaum, M. U. F., and McMillan, A. M. S.: Warming and Elevated Co_2 Have Opposing Influences on Transpiration. Which Is More Important?, Current Forestry Reports, 4, 51-71, 10.1007/s40725-018-0073-8, 2018.

Klemedtsson, L., Svensson, B. H., and Rosswall, T.: Relationships between Soil Moisture Content and Nitrous Oxide Production During Nitrification and Denitrification, Biology and Fertility of Soils, 6, 106-111, 10.1007/BF00257658, 1988.

Kolb, K. J., and Evans, R. D.: Implications of Leaf Nitrogen Recycling on the Nitrogen Isotope Composition of Deciduous Plant Tissues, New Phytologist, 156, 57-64, 10.1046/j.1469-8137.2002.00490.x, 2002.

Koppen, W.: Versuch Einer Klassifikation Der Klimate, Vorzugsweise Nach Ihren Beziehungen Zur Pflanzenwelt, Geographische Zeitschrift, 6, 593-611, http://www.jstor.org/stable/27803924, 1900.

Kozlowski, T.: Physiological-Ecological Impacts of Flooding on Riparian Forest Ecosystems, Wetlands, 22, 550-561, https://doi.org/10.1672/0277-5212(2002)022[0550:PEIOFO]2.0.CO;2, 2002.

Kozlowski, T. T., and Pallardy, S. G.: Stomatal Responses of *Fraxinus Pennsylvanica* Seedlings During and after Flooding, Physiologia Plantarum, 46, 155-158, doi:10.1111/j.1399-3054.1979.tb06549.x, 1979.

Kozlowski, T. T., and Pallardy, S. G.: Effect of Flooding on Water, Carbohydrate, and Mineral Relations, in: Flooding and Plant Growth, edited by: Kozlowski, T. T., Academic Press, San Diego, 165-193, 1984.

Kozlowski, T. T.: Responses of Woody Plants to Flooding and Salinity, Tree Physiology, 17, 490-490, https://doi.org/10.1093/treephys/17.7.490, 1997.

Krauss, K. W., Duberstein, J. A., and Conner, W. H.: Assessing Stand Water Use in Four Coastal Wetland Forests Using Sapflow Techniques: Annual Estimates, Errors and Associated Uncertainties, Hydrological Processes, 29, 112-127, 10.1002/hyp.10130, 2015.

Kreuzwieser, J., and Rennenberg, H.: Molecular and Physiological Response of Trees to Waterlogging Stress, Plant, cell & environment, 37, 10.1111/pce.12310, 2014.

Kulmatiski, A., Adler, P. B., Stark, J. M., and Tredennick, A. T.: Water and Nitrogen Uptake Are Better Associated with Resource Availability Than Root Biomass, Ecosphere, 8, e01738, 10.1002/ecs2.1738, 2017.

Kurbatova, J., Li, C., Varlagin, A., Xiao, X., and Vygodskaya, N.: Modeling Carbon Dynamics in Two Adjacent Spruce Forests with Different Soil Conditions in Russia, Biogeosciences, 5, 969-980, 10.5194/bg-5-969-2008, 2008.

Laanisto, L., and Niinemets, Ü.: Polytolerance to Abiotic Stresses: How Universal Is the Shade-Drought Tolerance Trade-Off in Woody Species?, Glob Ecol Biogeogr, 24, 571-580, 10.1111/geb.12288, 2015.

Lande, R.: Adaptation to an Extraordinary Environment by Evolution of Phenotypic Plasticity and Genetic Assimilation, Journal of Evolutionary Biology, 22, 1435-1446, doi:10.1111/j.1420-9101.2009.01754.x, 2009.

Lasslop, G., Reichstein, M., Papale, D., Richardson, A. D., Arneth, A., Barr, A., Stoy, P., and Wohlfahrt, G.: Separation of Net Ecosystem Exchange into Assimilation and

Respiration Using a Light Response Curve Approach: Critical Issues and Global Evaluation, Global Change Biology, 16, 187-208, 10.1111/j.1365-2486.2009.02041.x, 2010.

Leavitt, S., Wright, W., and Long, A.: Spatial Expression of Enso, Drought, and Summer Monsoon in Seasonal Δ^{13}c of Ponderosa Pine Tree Rings in Southern Arizona and New Mexico, Journal of Geophysical Research Atmospheres, 107, ACL 3-1-ACL 3-10, https://doi.org/10.1029/2001JD001312, 2002.

Leavitt, S. W., and Danzer, S. R.: Method for Batch Processing Small Wood Samples to Holocellulose for Stable-Carbon Isotope Analysis, Analytical Chemistry, 65, 87-89, https://doi.org/10.1021/ac00049a017, 1993.

LeBlanc, D. C., and Stahle, D. W.: Radial Growth Responses of Four Oak Species to Climate in Eastern and Central North America, Canadian Journal of Forest Research, 45, 793-804, https://doi.org/10.1139/cjfr-2015-0020, 2015.

Lei, H., Milota, M. R., and Gartner, B. L.: Between- and within-Tree Variation in the Anatomy and Specific Gravity of Wood in Oregon White Oak (*Quercus Garryana* Dougl.), lAWA Journal, 17, 445-461, https://doi.org/10.1163/22941932-90000642, 1996.

Leonelli, G., Battipaglia, G., Siegwolf, R. T. W., Saurer, M., Morra di Cella, U., Cherubini, P., and Pelfini, M.: Climatic Isotope Signals in Tree Rings Masked by Air Pollution: A Case Study Conducted Along the Mont Blanc Tunnel Access Road (Western Alps, Italy), Atmospheric Environment, 61, 169-179, https://doi.org/10.1016/j.atmosenv.2012.07.023, 2012.

Li, C., Frolking, S., and Frolking, T. A.: A Model of Nitrous Oxide Evolution from Soil Driven by Rainfall Events: 1. Model Structure and Sensitivity, Journal of Geophysical Research: Atmospheres, 97, 9759-9776, 10.1029/92jd00509, 1992.

Li, C., Aber, J., Stange, F., Butterbach-Bahl, K., and Papen, H.: A Process-Oriented Model of N2o and No Emissions from Forest Soils: 1. Model Development, Journal of Geophysical Research: Atmospheres, 105, 4369-4384, 10.1029/1999jd900949, 2000.

Li, C., Trettin, C., Sun, G., McNulty, S., and Butterbach-Bahl, K.: Modeling Carbon and Nitrogen Biogeochemistry in Forest Ecosystems, 3rd International Nitrogen Conference, Nanjing, China, 2005.

Li, Y., Schichtel, B. A., Walker, J. T., Schwede, D. B., Chen, X., Lehmann, C. M. B., Puchalski, M. A., Gay, D. A., and Collett, J. L.: Increasing Importance of Deposition of Reduced Nitrogen in the United States, Proceedings of the National Academy of Sciences, 113, 5874-5879, 10.1073/pnas.1525736113, 2016.

Lipp, J., Trimborn, P., Edwards, T., Waisel, Y., and Yakir, D.: Climatic Effects on the Δ^{18}o and Δ^{13}c of Cellulose in the Desert Tree *Tamarix Jordanis*, Geochimica et Cosmochimica Acta, 60, 3305-3309, https://doi.org/10.1016/0016-7037(96)00166-4, 1996.

Liu, G., Yang, Y.-B., and Zhu, Z.-H.: Elevated Nitrogen Allows the Weak Invasive Plant *Galinsoga Quadriradiata* to Become More Vigorous with Respect to Inter-Specific Competition, Scientific Reports, 8, 3136, 10.1038/s41598-018-21546-z, 2018.

Liu, X., Shao, X., Wang, L., Liang, E., Qin, D., and Ren, J.: Response and Dendroclimatic Implications of Δ^{13}c in Tree Rings to Increasing Drought on the Northeastern Tibetan Plateau, Journal of Geophysical Research, 113, 10.1029/2007JG000610, 2008.

Lovett, G. M., and Rueth, H.: Soil Nitrogen Transformations in Beech and Maple Stands Along a Nitrogen Deposition Gradient, Ecological Applications, 9, 1330-1344, 10.1890/1051-0761(1999)009[1330:Sntiba]2.0.Co;2, 1999.

Lovett, G. M., and Goodale, C. L.: A New Conceptual Model of Nitrogen Saturation Based on Experimental Nitrogen Addition to an Oak Forest, Ecosystems, 14, 615-631, 10.1007/s10021-011-9432-z, 2011.

Lowrance, R.: Groundwater Nitrate and Denitrification in a Doastal Plain Riparian Forest, Journal of Environmental Quality, 21, 401-405, 10.2134/jeq1992.00472425002100030017x, 1992.

Lowrance, R., Altier, L. S., Newbold, J. D., Schnabel, R. R., Groffman, P. M., Denver, J. M., Correll, D. L., Gilliam, J. W., Robinson, J. L., Brinsfield, R. B., Staver, K. W., Lucas, W., and Todd, A. H.: Water Quality Functions of Riparian Forest Buffers in

Chesapeake Bay Watersheds, Environmental Management, 21, 687-712, 10.1007/s002679900060, 1997.

Lowrance, R., Hubbard, R. K., and Williams, R. G.: Effects of a Managed Three Zone Riparian Buffer System on Shallow Groundwater Quality in the Southeastern Coastal Plain, Journal of Soil and Water Conservation, 55, 212-220, https://www.jswconline.org/content/jswc/55/2/212.full.pdf, 2000.

Lowrance, R., and Sheridan, J. M.: Surface Runoff Water Quality in a Managed Three Zone Riparian Buffer, Journal of Environmental Quality, 34, 1851-1859, 10.2134/jeq2004.0291, 2005.

Lu, X., Cheng, G., Xiao, F., and Huo, C.: Simulating Carbon Sequestration and Ghgs Emissions in Abies Fabric Forest on the Gongga Mountains Using a Biogeochemical Process Model Forest-Dndc, Journal of Mountain Science, 5, 249-256, 10.1007/s11629-008-0157-1, 2008.

Luo, W., Song, F., and Xie, Y.: Trade-Off between Tolerance to Drought and Tolerance to Flooding in Three Wetland Plants, Wetlands, 28, 866, 10.1672/07-225.1, 2008.

Magill, A. H., Aber, J. D., Berntson, G. M., McDowell, W. H., Nadelhoffer, K. J., Melillo, J. M., and Steudler, P.: Long-Term Nitrogen Additions and Nitrogen Saturation in Two Temperate Forests, Ecosystems, 3, 238-253, 10.1007/s100210000023, 2000.

Mara, P., Mihalopoulos, N., Gogou, A., Dähnke, K., Schlarbaum, T., Emeis, K., and Krom, M.: Isotopic Composition of Nitrate in Wet and Dry Atmospheric Deposition on Crete in the Eastern Mediterranean Sea Global Biogeochemical Cycles, 23, 10.1029/2008GB003395, 2009.

Mariotti, A.: Atmospheric Nitrogen Is a Reliable Standard for Natural 15n Abundance Measurements, Nature, 303, 685-687, 10.1038/303685a0, 1983.

Martin, A. R., Gezahegn, S., and Thomas, S. C.: Variation in Carbon and Nitrogen Concentration among Major Woody Tissue Types in Temperate Trees, Canadian Journal of Forest Research, 45, 744-757, 10.1139/cjfr-2015-0024, 2015.

Martinelli, L. A., Piccolo, M. C., Townsend, A. R., Vitousek, P. M., Cuevas, E., McDowell, W., Robertson, G. P., Santos, O. C., and Treseder, K.: Nitrogen Stable Isotopic Composition of Leaves and Soil: Tropical Versus Temperate Forests, Biogeochemistry, 46, 45-65, www.jstor.org/stable/1469636, 1999.

Martius, C.: Density, Humidity, and Nitrogen Content of Dominant Wood Species of Floodplain Forests (Várzea) in Amazonia, Holz als Roh- und Werkstoff, 50, 300-303, 10.1007/BF02615357, 1992.

Mayer, P. M., Reynolds Jr., S. K., McCutchen, M. D., and Canfield, T. J.: Meta-Analysis of Nitrogen Removal in Riparian Buffers, Journal of Environmental Quality, 36, 1172-1180, 10.2134/jeq2006.0462, 2007.

McCarroll, D., and Loader, N. J.: Stable Isotopes in Tree Rings, Quaternary Science Reviews, 23, 771-801, https://doi.org/10.1016/j.quascirev.2003.06.017, 2004.

McKnight, J. S., Hook, D. D., Langdon, O. G., and Johnson, R. L.: Flood Tolerance and Related Characteristics of Trees of the Bottomland Forests of the Southern United States, Bottomland hardwood forest wetlands of the Southeast United States, Lake Lanier, GA, USA, 1980,

McLauchlan, K. K., and Craine, J. M.: Species-Specific Trajectories of Nitrogen Isotopes in Indiana Hardwood Forests, USA, Biogeosciences, 9, 867-874, 10.5194/bg-9-867-2012, 2012.

Megonigal, J. P., H., C. W., Steven, K., and R., S. R.: Aboveground Production in Southeastern Floodplain Forests: A Test of the Subsidy-Stress Hypothesis, Ecology, 78, 370-384, doi:10.1890/0012-9658(1997)078[0370:APISFF]2.0.CO;2, 1997.

Meko, M. D., and Therrell, M. D.: A Record of Flooding on the White River, Arkansas Derived from Tree-Ring Anatomical Variability and Vessel Width, Physical Geography, 41, 83-98, https://doi.org/10.1080/02723646.2019.1677411, 2020.

Miao, S., Zou, C., and Breshears, D.: Vegetation Responses to Extreme Hydrological Events: Sequence Matters, The American Naturalist, 173, 113-118, https://doi.org/10.1086/593307, 2009.

Middleton, B., and Kleinebecker, T.: The Effects of Climate-Change-Induced Drought and Freshwater Wetlands, in: Global Change and the Function and Distribution of Wetlands, 117-147, 2012.

Miehle, P., Livesley, S. J., Feikema, P. M., Li, C., and Arndt, S. K.: Assessing Productivity and Carbon Sequestration Capacity of Eucalyptus Globulus Plantations Using the Process Model Forest-Dndc: Calibration and Validation, Ecological Modelling, 192, 83-94, https://doi.org/10.1016/j.ecolmodel.2005.07.021, 2006.

Mikac, S., Žmegač, A., Trlin, D., Paulić, V., Oršanić, M., and Anić, I.: Drought-Induced Shift in Tree Response to Climate in Floodplain Forests of Southeastern Europe, Scientific Reports, 8, 16495, https://doi.org/10.1038/s41598-018-34875-w, 2018.

Miller, A. J., and Cramer, M. D.: Root Nitrogen Acquisition and Assimilation, Plant and Soil, 274, 1-36, 10.1007/s11104-004-0965-1, 2005.

Mitsch, W. J., Taylor, J. R., and Benson, K. B.: Estimating Primary Productivity of Forested Wetland Communities in Different Hydrologic Landscapes, Landscape Ecology, 5, 75-92, 10.1007/BF00124662, 1991.

Moore, G., Edgar, C. B., Vogel, J., Washington-Allen, R., March, R., and Zehnder, R.: Tree Mortality from an Exceptional Drought Spanning Mesic to Semiarid Ecoregions, Ecological Applications, 26, https://doi.org/10.1890/15-0330.1, 2015.

Morris, J. T.: Effects of Nitrogen Loading on Wetland Ecosystems with Particular Reference to Atmospheric Deposition, Annual Review of Ecology and Systematics, 22, 257-279, www.jstor.org/stable/2097262, 1991.

Naiman, R. J., Décamps, H., and McClain, M. E.: Riparia: Ecology, Conservation and Management of Streamside Communities, Academic Press, New York, USA, 2005.

National Inventory of Dams, U.S. Army Corps of Engineers: https://nid.sec.usace.army.mil/ords/f?p=105:113:891673838449::NO:::, access: 3/26/2020, 2020.

NOAA: National Centers for Environmental Information, National Oceanic and Atmospheric Administration, United States Department of Commerce. Available Online

at Https://Www.Ncdc.Noaa.Gov/Data-Access/Land-Based-Station-Data. Accessed [07/18/2018], 2018a.

NOAA: National Centers for Environmental Information, National Environmental Satellite, Data, and Information Service, United States Department of Commerce. Available Online at Https://Www7.Ncdc.Noaa.Gov/Cdo/Cdodivisionalselect.Jsp. Accessed [07/18/2018], 2018b.

Nowak, D.: Air Pollution Removal by Chicago's Urban Forest, Chicago's Urban Forest Ecosystem: Results of the Chicago Urban Forest Climate Project, 63-81, 1994.

Nowak, D. J., Smith, P. D., Merritt, M., Giedraitis, J., Walton, J. T., Hoehn, R. E., Stevens, J. C., Crane, D. E., Estes, M., Stetson, S., Burditt, C., Hitchcock, D., and Holtcamp, W.: Houston's Regional Forest, Texas Forest Service Communication/Urban and Community Forestry 9/05-5000. 24p., https://www.nrs.fs.fed.us/pubs/jrnl/2005/ne_2005_nowak_001.pdf, 2005.

Nowak, D. J., Crane, D. E., and Stevens, J. C.: Air Pollution Removal by Urban Trees and Shrubs in the United States, Urban Forestry & Urban Greening, 4, 115-123, https://doi.org/10.1016/j.ufug.2006.01.007, 2006.

NRCS: Soil Survey Staff, Natural Resources Conservation Service, United States Department of Agriculture. Web Soil Survey. Available Online at the Following Link: Https://Websoilsurvey.Sc.Egov.Usda.Gov/. Accessed [02/09/2020], 2020.

Ober, H. K.: The Importance of Bottomland Hardwood Forests for Wildlife, University of Florida, Gainesville, FL, USA, 2019.

Odum, E. P., Finn, J. T., and Franz, E. H.: Perturbation Theory and the Subsidy-Stress Gradient, BioScience, 29, 349-352, 10.2307/1307690, 1979.

Oki, T., and Kanae, S.: Global Hydrological Cycles and World Water Resources, Science, 313, 1068, 10.1126/science.1128845, 2006.

Oren, R., and Pataki, D. E.: Transpiration in Response to Variation in Microclimate and Soil Moisture in Southeastern Deciduous Forests, Oecologia, 127, 549-559, 10.1007/s004420000622, 2001.

Oren, R., Sperry, J. S., Ewers, B. E., Pataki, D. E., Phillips, N., and Megonigal, J. P.: Sensitivity of Mean Canopy Stomatal Conductance to Vapor Pressure Deficit in a Flooded *Taxodium Distichum* L. Forest: Hydraulic and Non-Hydraulic Effects, Oecologia, 126, 21-29, 10.1007/s004420000497, 2001.

Papale, D., Reichstein, M., Aubinet, M., Canfora, E., Bernhofer, C., Kutsch, W., Longdoz, B., Rambal, S., Valentini, R., Vesala, T., and Yakir, D.: Towards a Standardized Processing of Net Ecosystem Exchange Measured with Eddy Covariance Technique: Algorithms and Uncertainty Estimation, Biogeosciences, 3, 571-583, 10.5194/bg-3-571-2006, 2006.

Pardo, L. H., Robin-Abbott, M. J., and Driscoll, C. T., eds.: Assessment of Nitrogen Deposition Effects and Empirical Critical Loads of Nitrogen for Ecoregions of the United States. Gen. Tech. Rep. Nrs-80. Newtown Square, Pa: U.S. Department of Agriculture, Forest Service, Northern Research Station. 291 P., 2011.

Pardo, L. H., Semaoune, P., Schaberg, P. G., Eagar, C., and Sebilo, M.: Patterns in Δ15n in Roots, Stems, and Leaves of Sugar Maple and American Beech Seedlings, Saplings, and Mature Trees, Biogeochemistry, 112, 275-291, 10.1007/s10533-012-9724-1, 2013.

Parolin, P.: Morphological and Physiological Adjustments to Waterlogging and Drought in Seedlings of Amazonian Floodplain Trees, Oecologia, 128, 326-335, 10.1007/s004420100660, 2001.

Parolin, P., and Wittmann, F.: Struggle in the Flood: Tree Responses to Flooding Stress in Four Tropical Floodplain Systems, plq003 pp., 2010.

Parsons, T. R., Maita, Y., and Lalli, C. M.: A Manual of Chemical and Biological Methods for Seawater Analysis, Pergamon Press, Oxford [Oxfordshire]; New York, 1984.

Paulot, F., Jacob, D. J., and Henze, D. K.: Sources and Processes Contributing to Nitrogen Deposition: An Adjoint Model Analysis Applied to Biodiversity Hotspots Worldwide, Environmental Science & Technology, 47, 3226-3233, 10.1021/es3027727, 2013.

Pennock, J. R., Velinsky, D. J., Ludlam, J. M., Sharp, J. H., and Fogel, M. L.: Isotopic Fractionation of Ammonium and Nitrate During Uptake by *Skeletonema Costatum*:

Implications for Δ^{15}n Dynamics under Bloom Conditions, Limnology and Oceanography, 41, 451-459, 10.4319/lo.1996.41.3.0451, 1996.

Peralta, A. L., Matthews, J. W., and Kent, A. D.: Microbial Community Structure and Denitrification in a Wetland Mitigation Bank, Applied and Environmental Microbiology, 76, 4207-4215, 10.1128/aem.02977-09, 2010.

Pezeshki, S. R., and Chambers, J. L.: Stomatal and Photosynthetic Response of Sweet Gum (*Liquidambar Styraciflua*) to Flooding, Canadian Journal of Forest Research, 15, 371-375, 10.1139/x85-059, 1985.

Pezeshki, S. R.: Differences in Patterns of Photosynthetic Responses to Hypoxia in Flood-Tolerant and Flood-Sensitive Tree Species, Photosynthetica, 28, 423-430, https://ci.nii.ac.jp/naid/10025360117/en/, 1993.

Porter, T. J., Pisaric, M. F. J., Kokelj, S. V., and Edwards, T. W. D.: Climatic Signals in Δ^{13}c and Δ^{18}o of Tree-Rings from White Spruce in the Mackenzie Delta Region, Northern Canada, Arctic, Antarctic, and Alpine Research, 41, 497-505, https://doi.org/10.1657/1938-4246-41.4.497, 2009.

Poulson, S. R., Chamberlain, C. P., and Friedland, A. J.: Nitrogen Isotope Variation of Tree Rings as a Potential Indicator of Environmental Change, Chemical Geology, 125, 307-315, https://doi.org/10.1016/0009-2541(95)00097-6, 1995.

Putnam, J. A., Furnival, G. M., and McKnight, J. S.: Management and Inventory of Southern Hardwoods. Agriculture Handbook 181. U.S. Department of Agriculture, Forest Service. Washington, D.C. , 1960.

R Core Team: R: A Language and Environment for Statistical Computing. R Foundation for Statistical Computing, Vienna, Austria. Isbn 3-900051-07-0, http://www.R-project.org/, 2012.

Rao, M., George, L. A., Rosenstiel, T. N., Shandas, V., and Dinno, A.: Assessing the Relationship among Urban Trees, Nitrogen Dioxide, and Respiratory Health, Environmental Pollution, 194, 96-104, https://doi.org/10.1016/j.envpol.2014.07.011, 2014.

Rao, R. V.: Latewood Density in Relation to Wood Fibre Diameter, Wall Thickness, and Fibre and Vessel Percentages in *Quercus Robur* L, 18, 127-138, 10.1163/22941932-90001474, 1997.

Raven, J. A., and Smith, F. A.: Nitrogen Assimilation and Transport in Vascular Land Plants in Relation to Intracellular Ph Regulation, New Phytologist, 76, 415-431, 10.1111/j.1469-8137.1976.tb01477.x, 1976.

Rehm, Paulo, O., James, S., and J., F. K.: Losing Your Edge: Climate Change and the Conservation Value of Range-Edge Populations, Ecology and Evolution, 5, 4315-4326, doi:10.1002/ece3.1645, 2015.

Reichstein, M., Falge, E., Baldocchi, D., Papale, D., Aubinet, M., Berbigier, P., Bernhofer, C., Buchmann, N., Gilmanov, T., Granier, A., Grünwald, T., Havránková, K., Ilvesniemi, H., Janous, D., Knohl, A., Laurila, T., Lohila, A., Loustau, D., Matteucci, G., Meyers, T., Miglietta, F., Ourcival, J.-M., Pumpanen, J., Rambal, S., Rotenberg, E., Sanz, M., Tenhunen, J., Seufert, G., Vaccari, F., Vesala, T., Yakir, D., and Valentini, R.: On the Separation of Net Ecosystem Exchange into Assimilation and Ecosystem Respiration: Review and Improved Algorithm, Global Change Biology, 11, 1424-1439, 10.1111/j.1365-2486.2005.001002.x, 2005.

Rhodes, C., Bingham, A., Heard, A. M., Hewitt, J., Lynch, J., Waite, R., and Bell, M. D.: Diatoms to Human Uses: Linking Nitrogen Deposition, Aquatic Eutrophication, and Ecosystem Services, Ecosphere, 8, e01858, 10.1002/ecs2.1858, 2017.

Robertson, I., Switsur, V. R., Carter, A. H. C., Barker, A. C., Waterhouse, J. S., Briffa, K. R., and Jones, P. D.: Signal Strength and Climate Relationships in $^{13}c/^{12}c$ Ratios of Tree Ring Cellulose from Oak in East England, Journal of Geophysical Research: Atmospheres, 102, 19507-19516, https://doi.org/10.1029/97JD01226, 1997.

Robinson, D.: $\Delta^{15}n$ as an Integrator of the Nitrogen Cycle, Trends Ecol Evol, 16, 153-162, 10.1016/s0169-5347(00)02098-x, 2001.

Rosen, D., Steven, D., and Lange, M.: Conservation Strategies and Vegetation Characterization in the Columbia Bottomlands, an under-Recognized Southern Floodplain Forest Formation, Natural Areas Journal, 28, 74-82, https://doi.org/10.3375/0885-8608(2008)28[74:CSAVCI]2.0.CO;2, 2008.

Saha, A., Sternberg, L., Ross, M., and Miralles-Wilhelm, F.: Water Source Utilization and Foliar Nutrient Status Differs between Upland and Flooded Plant Communities in Wetland Tree Islands, Wetlands Ecology and Management, 18, 343-355, 10.1007/s11273-010-9175-1, 2010.

Saurer, M., Siegenthaler, U., and Schweingruber, F.: The Climate-Carbon Isotope Relationship in Tree Rings and the Significance of Site Conditions, Tellus B: Chemical and Physical Meteorology, 47, 320-330, https://doi.org/10.3402/tellusb.v47i3.16051, 1995.

Saurer, M., Cherubini, P., Ammann, M., De Cinti, B., and Siegwolf, R.: First Detection of Nitrogen from Nox in Tree Rings: A 15n/14n Study near a Motorway, Atmospheric Environment, 38, 2779-2787, https://doi.org/10.1016/j.atmosenv.2004.02.037, 2004.

Savard, M., Cole, A., Smirnoff, A., and Vet, R.: Δ^{15}n Values of Atmospheric N Species Simultaneously Collected Using Sector-Based Samplers Distant from Sources – Isotopic Inheritance and Fractionation, Atmospheric Environment, 162, 10.1016/j.atmosenv.2017.05.010, 2017.

Savard, M. M., Bégin, C., Smirnoff, A., Marion, J., and Rioux-Paquette, E.: Tree-Ring Nitrogen Isotopes Reflect Anthropogenic No_x Emissions and Climatic Effects, Environmental Science & Technology, 43, 604-609, 10.1021/es802437k, 2009.

Schaffer, B., and Ploetz, R.: Net Gas-Exchange as a Damage Indicator for Phytophthora Root-Rot of Flooded and Nonflooded Avocado, 653-655 pp., 1989.

Schmidt, D. H., and Garland, K. A.: Bone Dry in Texas: Resilience to Drought on the Upper Texas Gulf Coast, Journal of Planning Literature, 27, 434-445, https://doi.org/10.1177/0885412212454013, 2012.

Schollaen, K., Heinrich, I., Neuwirth, B., Krusic, P. J., D'Arrigo, R. D., Karyanto, O., and Helle, G.: Multiple Tree-Ring Chronologies (Ring Width, Δ^{13}c and Δ^{18}o) Reveal Dry and Rainy Season Signals of Rainfall in Indonesia, Quaternary Science Reviews, 73, 170-181, https://doi.org/10.1016/j.quascirev.2013.05.018, 2013.

Schwede, D. B., and Lear, G. G.: A Novel Hybrid Approach for Estimating Total Deposition in the United States, Atmospheric Environment, 92, 207-220, https://doi.org/10.1016/j.atmosenv.2014.04.008, 2014.

Seager, Ting, M., Held, I., Kushnir, Y., Lu, J., Vecchi, G., Huang, H.-P., Harnik, N., Leetmaa, A., Lau, N.-C., Li, C., Velez, J., and Naik, N.: Model Projections of an Imminent Transition to a More Arid Climate in Southwestern North America, Science, 316, 1181, https://doi.org/10.1126/science.1139601, 2007.

Sebastian, A., Gori, A., Blessing, R. B., van der Wiel, K., and Bass, B.: Disentangling the Impacts of Human and Environmental Change on Catchment Response During Hurricane Harvey, Environmental Research Letters, 14, 124023, https://doi.org/10.1088/1748-9326/ab5234, 2019.

Sedaghatdoost, A., Mohanty, B., and Huang, Y.: The Effect of Heterogeneities in Soil Physical and Chemical Properties on Redox Biogeochemistry in Subsurface Soils, AGUFM, 2019, San Francisco, CA, USA, 2019.

Serengil, Y., Augustaitis, A., Bytnerowicz, A., Grulke, N., Kozovitz, A., Matyssek, R., Muller-Starck, G., Schaub, M., Wieser, G., Aydin Coskun, A., and Paoletti, E.: Adaptation of Forest Ecosystems to Air Pollution and Climate Change: A Global Assessment on Research Priorities, iForest - Biogeosciences and Forestry, 4, 44-48, 10.3832/ifor0566-004, 2011.

Shabala, S., Shabala, L., Barcelo, J., and Poschenrieder, C.: Membrane Transporters Mediating Root Signalling and Adaptive Responses to Oxygen Deprivation and Soil Flooding, Plant, Cell & Environment, 37, 2216-2233, 10.1111/pce.12339, 2014.

Shafroth, P., Stromberg, J., and Patten, D.: Riparian Vegetation Response to Altered Disturbance and Stress Regimes, Ecological Applications, 12, 107-123, 10.2307/3061140, 2002.

Shannon, J., Van Grinsven, M., Davis, J., Bolton, N., Noh, N., Pypker, T., and Kolka, R.: Water Level Controls on Sap Flux of Canopy Species in Black Ash Wetlands, Forests, 9, 147, http://www.mdpi.com/1999-4907/9/3/147, 2018.

Shu, Y., Chuying, G., Jiayin, H., Leiming, Z., Guanhua, D., Xuefa, W., and Guirui, Y.: Modelling Soil Greenhouse Gas Fluxes from a Broad-Leaved Korean Pine Forest in Changbai Mountain: Forest-Dndc Model Validation, Journal of Resources and Ecology, 10, 127-136, 110, https://doi.org/10.5814/j.issn.1674-764x.2019.02.003, 2019.

Siemann, E., and Rogers, W. E.: Herbivory, Disease, Recruitment Limitation, and Success of Alien and Native Tree Species, Ecology, 84, 1489-1505, 10.1890/0012-9658(2003)084[1489:Hdrlas]2.0.Co;2, 2003a.

Siemann, E., and Rogers, W. E.: Changes in Light and Nitrogen Availability under Pioneer Trees May Indirectly Facilitate Tree Invasions of Grasslands, Journal of Ecology, 91, 923-931, 10.1046/j.1365-2745.2003.00822.x, 2003b.

Siemann, E., Carrillo, J., Gabler, C., Zipp, R., and Rogers, W.: Experimental Test of the Impacts of Feral Hogs on Forest Dynamics and Processes in the Southeastern Us, Forest Ecology and Management, 258, 546-553, 10.1016/j.foreco.2009.03.056, 2009.

Sierra, J.: Temperature and Soil Moisture Dependence of N Mineralization in Intact Soil Cores, Soil Biology and Biochemistry, 29, 1557-1563, https://doi.org/10.1016/S0038-0717(96)00288-X, 1997.

Silvertown, J., Dodd, M. E., Gowing, D. J. G., and Mountford, J. O.: Hydrologically Defined Niches Reveal a Basis for Species Richness in Plant Communities, Nature, 400, 61-63, 10.1038/21877, 1999.

Simmons, M., Wu, X., and Whisenant, S. G.: Bottomland Hardwood Forest Species Responses to Flooding Regimes Along an Urbanization Gradient, Ecological Engineering, 29, 223-231, 10.1016/j.ecoleng.2006.07.005, 2007.

Smith, W. H.: Air Pollution and Forests, 2 ed., Springer Series on Environmental Management, Springer-Verlag New York, New York, USA, 618 pp., 1990.

Sorrell, B. K., Mendelssohn, I. A., McKee, K. L., and Woods, R. A.: Ecophysiology of Wetland Plant Roots: A Modelling Comparison of Aeration in Relation to Species Distribution, Annals of Botany, 86, 675-685, https://doi.org/10.1006/anbo.2000.1173, 2000.

Speer, J.: The Fundamentals of Tree-Ring Research, University of Arizona Press, Tucson, Arizona, 2012.

Spoelstra, J., Schiff, S. L., Hazlett, P. W., Jeffries, D. S., and Semkin, R. G.: The Isotopic Composition of Nitrate Produced from Nitrification in a Hardwood Forest

Floor, Geochimica et Cosmochimica Acta, 71, 3757-3771, https://doi.org/10.1016/j.gca.2007.05.021, 2007.

Sra, A. K., Hu, Y., Martin, G. E., Snow, D. D., Ribbe, M. W., and Kohen, A.: Competitive ^{15}n Kinetic Isotope Effects of Nitrogenase-Catalyzed Dinitrogen Reduction, Journal of the American Chemical Society, 126, 12768-12769, 10.1021/ja0458470, 2004.

St. George, S.: An Overview of Tree-Ring Width Records across the Northern Hemisphere, Quaternary Science Reviews, 95, 132-150, https://doi.org/10.1016/j.quascirev.2014.04.029, 2014.

Stange, F., Butterbach-Bahl, K., Papen, H., Zechmeister-Boltenstern, S., Li, C., and Aber, J.: A Process-Oriented Model of N2o and No Emissions from Forest Soils: 2. Sensitivity Analysis and Validation, Journal of Geophysical Research: Atmospheres, 105, 4385-4398, 10.1029/1999jd900948, 2000.

Stark, J. M., and Firestone, M. K.: Mechanisms for Soil Moisture Effects on Activity of Nitrifying Bacteria, Applied and Environmental Microbiology, 61, 218, http://aem.asm.org/content/61/1/218.abstract, 1995.

Stevens, C. J., Dise, N. B., Mountford, J. O., and Gowing, D. J.: Impact of Nitrogen Deposition on the Species Richness of Grasslands, Science, 303, 1876, 10.1126/science.1094678, 2004.

Stokes, M. A., and Smiley, T. L.: An Introduction to Tree-Ring Dating, The University of Arizona Press, Tucson, Arizona, 1968.

Stuiver, M., Burk, R. L., and Quay, P. D.: ^{13}c/^{12}c Ratios in Tree Rings and the Transfer of Biospheric Carbon to the Atmosphere, Journal of Geophysical Research: Atmospheres, 89, 11731-11748, https://doi.org/10.1029/JD089iD07p11731, 1984.

Sun, F., Kuang, Y., Wen, D., Xu, Z., Li, J., Zuo, W., and Hou, E.: Long-Term Tree Growth Rate, Water Use Efficiency, and Tree Ring Nitrogen Isotope Composition of Pinus Massoniana L. In Response to Global Climate Change and Local Nitrogen Deposition in Southern China, Journal of Soils and Sediments, 10, 1453-1465, 10.1007/s11368-010-0249-8, 2010.

Swift, B. L.: Status of Riparian Ecosystems in the United States, JAWRA Journal of the American Water Resources Association, 20, 223-228, 10.1111/j.1752-1688.1984.tb04675.x, 1984.

Szejner, P., Belmecheri, S., Ehleringer, J. R., and Monson, R. K.: Recent Increases in Drought Frequency Cause Observed Multi-Year Drought Legacies in the Tree Rings of Semi-Arid Forests, Oecologia, 192, 241-259, https://doi.org/10.1007/s00442-019-04550-6, 2020.

Takashima, T., Hikosaka, K., and Hirose, T.: Photosynthesis or Persistence: Nitrogen Allocation in Leaves of Evergreen and Deciduous Quercus Species, Plant, Cell & Environment, 27, 1047-1054, 10.1111/j.1365-3040.2004.01209.x, 2004.

Tang, Z., Xu, W., Zhou, G., Bai, Y., Li, J., Tang, X., Chen, D., Liu, Q., Ma, W., Xiong, G., He, H., He, N., Guo, Y., Guo, Q., Zhu, J., Han, W., Hu, H., Fang, J., and Xie, Z.: Patterns of Plant Carbon, Nitrogen, and Phosphorus Concentration in Relation to Productivity in China's Terrestrial Ecosystems, Proceedings of the National Academy of Sciences, 115, 4033-4038, 10.1073/pnas.1700295114, 2018.

Tei, S., Sugimoto, A., Yonenobu, H., Matsuura, Y., Osawa, A., Sato, H., Fujinuma, J., and Maximov, T.: Tree-Ring Analysis and Modeling Approaches Yield Contrary Response of Circumboreal Forest Productivity to Climate Change, Global Change Biology, 23, 5179-5188, https://doi.org/10.1111/gcb.13780, 2017.

Tharammal, T., Bala, G., Narayanappa, D., and Nemani, R.: Potential Roles of Co2 Fertilization, Nitrogen Deposition, Climate Change, and Land Use and Land Cover Change on the Global Terrestrial Carbon Uptake in the Twenty-First Century, Climate Dynamics, 52, 4393-4406, 10.1007/s00382-018-4388-8, 2019.

Therrell, M. D., and Bialecki, M. B.: A Multi-Century Tree-Ring Record of Spring Flooding on the Mississippi River, Journal of Hydrology, 529, 490-498, https://doi.org/10.1016/j.jhydrol.2014.11.005, 2015.

Thomas, Q. R., Canham, C. D., Weathers, K. C., and Goodale, C. L.: Increased Tree Carbon Storage in Response to Nitrogen Deposition in the Us, Nature Geoscience, 3, 13-17, 10.1038/ngeo721, 2010.

Thornton, P. E., Law, B. E., Gholz, H. L., Clark, K. L., Falge, E., Ellsworth, D. S., Goldstein, A. H., Monson, R. K., Hollinger, D., Falk, M., Chen, J., and Sparks, J. P.: Modeling and Measuring the Effects of Disturbance History and Climate on Carbon and Water Budgets in Evergreen Needleleaf Forests, Agricultural and Forest Meteorology, 113, 185-222, https://doi.org/10.1016/S0168-1923(02)00108-9, 2002.

Tian, D., Wang, H., Sun, J., and Niu, S.: Global Evidence on Nitrogen Saturation of Terrestrial Ecosystem Net Primary Productivity, Environmental Research Letters, 11, 024012, 10.1088/1748-9326/11/2/024012, 2016.

Timofeeva, G., Treydte, K., Bugmann, H., Rigling, A., Schaub, M., Siegwolf, R., and Saurer, M.: Long-Term Effects of Drought on Tree-Ring Growth and Carbon Isotope Variability in Scots Pine in a Dry Environment, Tree Physiology, 37, 1028-1041, 10.1093/treephys/tpx041, 2017.

Tockner, K., and Stanford, J. A.: Riverine Flood Plains: Present State and Future Trends, Environmental Conservation, 29, 308-330, 10.1017/S037689290200022X, 2002.

TWDB: 2017 Texas State Water Plan, Texas Water Development Board, http://www.twdb.texas.gov/waterplanning/swp/2017/doc/SWP17-Water-for-Texas.pdf, 2017.

Ullah, S., and Zinati, G. M.: Denitrification and Nitrous Oxide Emissions from Riparian Forests Soils Exposed to Prolonged Nitrogen Runoff, Biogeochemistry, 81, 253-267, 10.1007/s10533-006-9040-8, 2006.

USEPA: Bottomland Hardwoods, Wetlands, Https://Www.Epa.Gov/Wetlands/Bottomland-Hardwoods, 2016.

USFWS: Draft Land Protection Plan Austin's Woods San Bernard National Wildlife Refuge Brazoria, Fort Bend, Matagorda and Wharton Counties Texas Texas Mid-coast NWR Complex Draft Comprehensive Conservation Plan and Environmental Assessment, https://www.fws.gov/southwest/refuges/plan/PDFs/TMC%20CCP%20files/15_Appendix%20I.%20LPP_Austins_woods_08-10-12.pdf, 1997.

van Cleemput, O., Boeckx, P., Lindgren, P.-E., and Tonderski, K.: Denitrification in Wetlands, in: Biology of the Nitrogen Cycle, edited by: Bothe, H., Ferguson, S. J., and Newton, W. E., Elsevier, Amsterdam, The Netherlands, 359-367, 2007.

van Groenigen, J. W., Huygens, D., Boeckx, P., Kuyper, T. W., Lubbers, I. M., Rütting, T., and Groffman, P. M.: The Soil N Cycle: New Insights and Key Challenges, SOIL, 1, 235-256, 10.5194/soil-1-235-2015, 2015.

Van Houtven, G., Phelan, J., Clark, C., Sabo, R. D., Buckley, J., Thomas, R. Q., Horn, K., and LeDuc, S. D.: Nitrogen Deposition and Climate Change Effects on Tree Species Composition and Ecosystem Services for a Forest Cohort, Ecological Monographs, 89, e01345, 10.1002/ecm.1345, 2019.

van Oldenborgh, G. J., van der Wiel, K., Sebastian, A., Singh, R., Arrighi, J., Otto, F., Haustein, K., Li, S., Vecchi, G., and Cullen, H.: Attribution of Extreme Rainfall from Hurricane Harvey, August 2017, Environmental Research Letters, 12, 124009, https://doi.org/10.1088/1748-9326/aa9ef2, 2017.

Verhoeven, J. T. A., Arheimer, B., Yin, C., and Hefting, M. M.: Regional and Global Concerns over Wetlands and Water Quality, Trends in Ecology & Evolution, 21, 96-103, https://doi.org/10.1016/j.tree.2005.11.015, 2006.

Vitousek, P. M., and Howarth, R. W.: Nitrogen Limitation on Land and in the Sea: How Can It Occur?, Biogeochemistry, 13, 87-115, 10.1007/BF00002772, 1991.

Vitousek, P. M., Aber, J. D., Howarth, R. W., Likens, G. E., Matson, P. A., Schindler, D. W., Schlesinger, W. H., and Tilman, D. G.: Technical Report: Human Alteration of the Global Nitrogen Cycle: Sources and Consequences, Ecological Applications, 7, 737-750, 10.2307/2269431, 1997.

Vivian, L. M., Godfree, R. C., Colloff, M. J., Mayence, C. E., and Marshall, D. J.: Wetland Plant Growth under Contrasting Water Regimes Associated with River Regulation and Drought: Implications for Environmental Water Management, Plant Ecology, 215, 997-1011, https://doi.org/10.1007/s11258-014-0357-4, 2014.

Voelker, S., Meinzer, F., Lachenbruch, B., Brooks, J. R., and Guyette, R.: Drivers of Radial Growth and Carbon Isotope Discrimination of Bur Oak (*Quercus Macrocarpa*

Michx.) across Continental Gradients in Precipitation, Vapor Pressure Deficit and Irradiance, Plant, cell & environment, 37, 10.1111/pce.12196, 2014.

Voesenek, L. A. C. J., Rijnders, J. H. G. M., Peeters, A. J. M., van de Steeg, H. M., and de Kroon, H.: Plant Hormones Regulate Fast Shoot Elongation under Water: From Genes to Communities, Ecology, 85, 16-27, www.jstor.org/stable/3450462, 2004.

Vozzo, J. A.: *Quercus Nigra* L. Water Oak, in: Tech. Coords. Agric. Handb. 654. Silvics of North America. Vol. 2. Hardwoods., edited by: Burns, Russell, M., Honkala, and Barbara, H., Department of Agriculture, Forest Service, Washington, DC, 701-703, 1990.

Wallace, Z. P., Lovett, G. M., Hart, J. E., and Machona, B.: Effects of Nitrogen Saturation on Tree Growth and Death in a Mixed-Oak Forest, Forest Ecology and Management, 243, 210-218, https://doi.org/10.1016/j.foreco.2007.02.015, 2007.

Wallman, P., Svensson, M. G. E., Sverdrup, H., and Belyazid, S.: Forsafe—an Integrated Process-Oriented Forest Model for Long-Term Sustainability Assessments, Forest Ecology and Management, 207, 19-36, https://doi.org/10.1016/j.foreco.2004.10.016, 2005.

Wang, H.-H., Grant, W. E., Swannack, T. M., Gan, J., Rogers, W. E., Koralewski, T. E., Miller, J. H., and Taylor Jr, J. W.: Predicted Range Expansion of Chinese Tallow Tree (*Triadica Sebifera*) in Forestlands of the Southern United States, Diversity and Distributions, 17, 552-565, 10.1111/j.1472-4642.2011.00760.x, 2011a.

Wang, H.-Q., Chen, F., Ermenbaev, B., and Satylkanov, R.: Comparison of Drought-Sensitive Tree-Ring Records from the Tien Shan of Kyrgyzstan and Xinjiang (China) During the Last Six Centuries, Advances in Climate Change Research, 8, 18-25, https://doi.org/10.1016/j.accre.2017.03.004, 2017.

Wang, X., Zhu, B., Li, C., Gao, M., Wang, Y., Zhou, Z., and Yuan, H.: Dissecting Soil Co2 Fluxes from a Subtropical Forest in China by Integrating Field Measurements with a Modeling Approach, Geoderma, 161, 88-94, 10.1016/j.geoderma.2010.12.010, 2011b.

Wear, D. N., and Greis, J. G.: Southern Forest Resource Assessment, Final Report Technical SRS-53. U.S. Department of Agriculture, Forest Service, Southern Research Station. Asheville, NC. 635 p., 053, https://www.srs.fs.usda.gov/pubs/4833, 2002.

Williams, A. P., Michaelsen, J., Leavitt, S. W., and Still, C. J.: Using Tree Rings to Predict the Response of Tree Growth to Climate Change in the Continental United States During the Twenty-First Century, Earth Interactions, 14, 1-20, 10.1175/2010ei362.1, 2010.

Wutzler, T., Lucas-Moffat, A., Migliavacca, M., Knauer, J., Sickel, K., Šigut, L., Menzer, O., and Reichstein, M.: Basic and Extensible Post-Processing of Eddy Covariance Flux Data with Reddyproc, Biogeosciences, 15, 5015-5030, 10.5194/bg-15-5015-2018, 2018.

Yin, S., Shen, Z., Zhou, P., Zou, X., Che, S., and Wang, W.: Quantifying Air Pollution Attenuation within Urban Parks: An Experimental Approach in Shanghai, China, Environmental Pollution, 159, 2155-2163, https://doi.org/10.1016/j.envpol.2011.03.009, 2011.

Yoneyama, T., Omata, T., Nakata, S., and Yazaki, J.: Fractionation of Nitrogen Isotopes During the Uptake and Assimilation of Ammonial by Plants, Plant and Cell Physiology, 32, 1211-1217, 10.1093/oxfordjournals.pcp.a078199, 1991.

Yoneyama, T., Matsumaru, T., Usui, K., and Engelaar, W. M. H. G.: Discrimination of Nitrogen Isotopes During Absorption of Ammonium and Nitrate at Different Nitrogen Concentrations by Rice (*Oryza Sativa* L.) Plants, Plant, Cell & Environment, 24, 133-139, 10.1046/j.1365-3040.2001.00663.x, 2001.

Zaerr, J. B.: Short-Term Flooding and Net Photosynthesis in Seedlings of Three Conifers, Forest Science, 29, 71-78, 10.1093/forestscience/29.1.71, 1983.

Zedler, J., Kercher, S., Professor, R., and Schierenbeck, K.: Causes and Consequences of Invasive Plants in Wetlands: Opportunities, Opportunists, and Outcomes, Critical Reviews in Plant Sciences, 23, 431-452, 10.1080/07352680490514673, 2004.

Zhang, L., Jacob, D., Knipping, E., Kumar, N., Munger, J., Carouge, C., Donkelaar, A., Wang, Y., and Chen, D.: Nitrogen Deposition to the United States: Distribution, Sources, and Processes, Atmospheric Chemistry and Physics, 12, 4539-4554, 10.5194/acp-12-4539-2012, 2012.

Zhang, Y., Li, C., Trettin, C. C., Li, H., and Sun, G.: An Integrated Model of Soil, Hydrology, and Vegetation for Carbon Dynamics in Wetland Ecosystems, Global Biogeochem. Cycles, 16, 1-17, 2002.

APPENDIX A

SUPPLEMENTARY TABLES FOR CHAPTER II

Table 13. R^2 values obtained from linear regressions between climate variables (precipitation, maximum temperature and PDSI) from the corresponding months (predictor variables) and annual ring-width index of the same year (response variable). Values shown here are sums of R^2 values from linear regression models run separately for all four sites. R^2 values only from statistically significant regressions were used to calculate the sums.

Period	Precipitation	Maximum Temperature	PDSI
Feb	0.23	0.15	0.37
Mar	0.25	0.04	0.49
Apr	0.29	0.06	0.63
May	0.44	0.23	0.76
Jun	0.40	0.51	0.91
Jul	0.58	0.72	**1.39**
Aug	0.14	0.17	1.20
Sep	0.03	0.22	0.64
Feb-Mar	0.22	0.08	0.44
Feb-Apr	0.21	0.11	0.53
Feb-May	0.42	0.14	0.63
Feb-Jun	0.63	0.26	0.74
Feb-Jul	1.17	0.35	0.90
Feb-Aug	1.26	0.43	0.99
Feb-Sep	0.62	0.48	1.00
Mar-Apr	0.46	0.05	0.58
Mar-May	1.02	0.08	0.68
Mar-Jun	0.74	0.24	0.79
Mar-Jul	1.17	0.40	0.96
Mar-Aug	1.23	0.28	1.05
Mar-Sep	0.66	0.30	1.04
Apr-May	0.88	0.12	0.73
Apr-Jun	0.60	0.36	0.84
Apr-Jul	1.35	0.54	1.02
Apr-Aug	1.35	0.42	1.10
Apr-Sep	0.73	0.45	1.08
May-Jun	0.63	0.55	0.87

Table 13. Continued.

Period	Precipitation	Maximum Temperature	PDSI
May-Jul	**1.39**	**0.75**	1.08
May-Aug	1.26	0.64	1.16
May-Sep	0.65	0.67	1.11
Jun-Jul	1.05	0.70	1.17
Jun-Aug	0.85	0.68	1.23
Jun-Sep	0.45	0.66	1.15
Jul-Aug	0.51	0.58	1.35
Jul-Sep	0.21	0.55	1.17
Aug-Sep	0.05	0.27	0.96

Table 14. R^2 values obtained from linear regressions between climate variables (precipitation and maximum temperature) from the corresponding months (predictor variables) and annual tree-ring $\delta^{13}C$ values of the same year (response variable). Values shown here are sums of R^2 values from linear regression models run separately for all four sites. R^2 values only from statistically significant regressions were used to calculate the sums. PDSI had no correlation with tree-ring $\delta^{13}C$ values.

Period	Precipitation	Maximum Temperature
Feb	0.29	0.12
Mar	1.18	0.52
Apr	**1.88**	**1.86**
May	0.41	0.06
Jun	0.37	0.17
Jul	0.61	0.33
Aug	0.62	1.02
Sep	0.24	0.81
Feb-Mar	0.79	0.56
Feb-Apr	1.24	0.61
Feb-May	1.26	0.45
Feb-Jun	0.93	0.34
Feb-Jul	1.15	0.34
Feb-Aug	1.26	0.47
Feb-Sep	0.77	0.51
Mar-Apr	1.64	0.95
Mar-May	1.77	0.65
Mar-Jun	1.04	0.51

Table 14. Continued.

Period	Precipitation	Maximum Temperature
Mar-Jul	1.28	0.47
Mar-Aug	1.34	0.60
Mar-Sep	0.81	0.62
Apr-May	1.32	1.07
Apr-Jun	0.79	0.78
Apr-Jul	1.18	0.63
Apr-Aug	1.22	0.75
Apr-Sep	0.72	0.75
May-Jun	0.41	0.11
May-Jul	0.83	0.24
May-Aug	0.88	0.43
May-Sep	0.51	0.45
Jun-Jul	0.88	0.30
Jun-Aug	0.92	0.57
Jun-Sep	0.54	0.56
Jul-Aug	0.72	0.69
Jul-Sep	0.85	0.70
Aug-Sep	0.53	0.87